

UNIVERSITY OF WOLLONGONG

DOCTORAL THESIS

Thesis Title

Author:
Jesse GREENSLADE

Supervisor:
Dr. Jenny FISHER

*A thesis submitted in fulfillment of the requirements
for the degree of Doctor of Philosophy
in the*

Centre of Atmospheric Chemistry
Chemistry Department

March 29, 2018

Declaration of Authorship

I, Jesse GREENSLADE, declare that this thesis titled, "Thesis Title" and the work presented in it are my own. I confirm that:

- This work was done wholly or mainly while in candidature for a research degree at this University.
- Where any part of this thesis has previously been submitted for a degree or any other qualification at this University or any other institution, this has been clearly stated.
- Where I have consulted the published work of others, this is always clearly attributed.
- Where I have quoted from the work of others, the source is always given. With the exception of such quotations, this thesis is entirely my own work.
- I have acknowledged all main sources of help.
- Where the thesis is based on work done by myself jointly with others, I have made clear exactly what was done by others and what I have contributed myself.

Signed:

Date:

“Thanks to my solid academic training, today I can write hundreds of words on virtually any topic without possessing a shred of information, which is how I got a good job in journalism.”

Dave Barry

Contents

Declaration of Authorship	iii
1 Introduction and Literature Review	1
1.1 The atmosphere	1
1.1.1 Structure	2
1.1.2 Composition	3
Hydroxyl radicals	3
1.2 Ozone	3
NOx	4
1.2.1 Stratosphere to troposphere transport	6
1.2.2 Chemical production	7
1.3 VOCs	8
1.3.1 Emissions	10
1.3.2 Isoprene	10
1.3.3 The isoprene cascade	11
Oxidation	11
Low NOx scenario	12
Ozonolysis	13
Oxidation by NO ₃	14
1.3.4 Radiative Forcing	14
1.4 HCHO	17
1.4.1 Sources and sinks	17
1.4.2 Measurement techniques	18
Satellite measurements	20
1.5 Atmospheric Chemistry Modelling	21
1.5.1 Box models	22
1.5.2 Emissions	23
1.5.3 Uncertainties?	23
Emissions Inventories	24
Resolution	24
Chemistry mechanisms	24
Clouds	25
Soil Moisture	25
1.6 Australia and the southern hemisphere	26
1.6.1 Ozone	28
1.6.2 VOCs	28
1.6.3 Measurements	29
1.7 Aims	30

2 Data and Modelling	31
2.1 Introduction	31
2.2 List of runs and outputs used in my work TODO: good place for this?	31
2.2.1 GEOS-Chem	31
2.2.2 CAABA/MECCA	32
2.2.3 Reading Data	32
CAABA/MECCA outputs	32
GEOS-Chem Satellite output	32
HEMCO diagnostics	32
2.3 GEOS-Chem	32
2.3.1 GEOS-Chem isoprene modelling	33
Outline	33
Emissions from MEGAN	35
2.3.2 Chemical Mechanisms	37
2.3.3 Running GEOS-Chem (before isop?)	37
Installation and requirements	37
Outputs	37
Tropospheric chemistry run	38
UCX run	38
2.3.4 Run comparisons	38
2.4 Measurement Techniques	42
2.4.1 DOAS	42
2.4.2 Satellites	44
OMI	44
AMF	45
Uncertainties	46
2.4.3 OMI Satellite measurements	48
OMI HCHO	48
OMI NO ₂	48
2.5 Recalculation of OMI HCHO	48
2.6 Campaigns	50
2.6.1 Marine and Urban MBA ? (MUMBA)	50
2.6.2 Sydney Particle Studies (SPS1, SPS2)	50
2.7 Analysing output	52
2.7.1 Satellite HCHO recalculations	52
2.7.2 Circadian emissions cycle	54
2.7.3 HCHO: Simulated vs Measured	54
2.7.4 Accounting for Fires	54
2.7.5 Accounting for NO _x	58
2.7.6 HCHO Comparisons	60
2.8 Data Access	60
Bibliography	69

List of Figures

1.1	Pressure (red) logarithmically decreasing, shown with percentage of atmosphere below at several points. Temperature (green) changes throughout the atmosphere. Figure edited from https://climate.ncsu.edu/edu/Structure	2
1.2	Tropospheric ozone processes, Figure 1 in Young et al., 2017. DOI: https://doi.org/10.1525/elementa.265.f1	5
1.3	Ozone production rate dependent on NO _x and VOC concentrations (Mazzuca et al., 2016).	8
1.4	The overall radiative forcings and uncertainties of several atmospheric constituents This is an image taken from Forster et al., 2007, found at https://www.ipcc.ch/publications_and_data/ar4/wg1/en/faq-2-1.html	15
1.5	The overall radiative forcings and uncertainties of several atmospheric constituents This is an image taken from IPCC, 2013: <i>Climate Change 2013: The Physical Science Basis. Contribution of Working Group I to the Fifth Assessment Report of the Intergovernmental Panel on Climate Change</i> , chapter 8.	16
1.6	HCHO spectrum, with a typical band of wavelengths used for DOAS path measurements. This is a portion of an image from Davenport et al., 2015.	19
1.7	An example spectrum showing interferences used for species concentration measurements by GOME-2. Image by EUMETSAT and ESA (EUMETSAT, 2015).	20
1.8	Standard box model parameters, image taken from Jacob, 1999.	22
1.9	Forest types in Australia (http://www.agriculture.gov.au/abares/forestsaustralia/australias-forests)	27
1.10	Part of a figure from Guenther et al., 2006 showing global isoprene emission factors.	27
2.1	MEGAN schematic, copied from Guenther (2016)	35
2.2	Surface HCHO simulated by GEOS-Chem with UCX (top left), and without UCX (top right), along with their absolute and relative differences(bottom left, right respectively). Amounts simulated by GEOS-Chem for the 1st of January, 2005.	39
2.3	As figure 2.2, except looking at isoprene.	40
2.4	As figure 2.2, except looking at ozone.	41
2.5	Image from Lee et al., 2015.	43

2.6	Figure 1 and Table 1 from Schenkeveld et al., 2017, with the following caption “An impression of OMI flying over the Earth. The spectrum of a ground pixel is projected on the wavelength dimension of the charge-coupled device (CCD; the columns). The cross-track ground pixels are projected on the swath dimension of the CCD (the rows). The forward speed of 7 kms^{-1} and an exposure time of 2 s lead to a ground pixel size of 13 km in the flight direction. The viewing angle of 114° leads to a swath width on the ground of 2600 km.” The table shows the optical properties for OMIs three channels.	45
2.7	Depiction of processes and datasets used to recalculate OMI AMFs.	49
2.8	Locations of Australian campaigns which are analysed within this thesis	51
2.9	SPS 1 and 2 HCHO (yellow) and isoprene (green) time series, along with detection limits (dashed).	52
2.10	Comparison between GEOS-Chem HCHO concentrations in the grid-square containing Sydney for the duration of the SPS 1 and 2 campaigns	53
2.11	Top panel: surface temperature averaged over January 2005. Bottom panel: surface temperature correlated against temperature over January 2005, with different colours for each gridbox, and the combined correlation. A reduced major axis regression is used within each gridbox (shown in top panel) using daily overpass time surface temperature and HCHO amounts (ppbv). The distribution of slopes and regression corellation coefficients (one datapoint per gridbox) for the exponential regression is shown in the embedded plot.	55
2.12	As figure 2.11 but for northern Australia.	56
2.13	As figure 2.11 but for south-western Australia.	57
2.14	GEOS-Chem mid-day tropospheric column NO_2 vs OMNO2d columns (averaged to match GEOS-Chems lower resolution). Absolute and relative differences, along with corellation shown on bottom row.	59
2.15	Top row (left to right): GEOS-Chem NO_2 mid-day tropospheric columns, OMNO2d NO_2 columns, modelled anthropogenic NO emissions. Second row: absolute and relative difference between GEOS-Chem and OMI NO_2 data, and the corellation. Third row: corellation between GEOS-Chem tropospheric column NO_2 and emitted NO, then between the model-satellite bias and the emissions. All corellation plots are coloured by emission rates.	61
2.16	As figure 2.15, for Autumn 2005.	62
2.17	As figure 2.15, for Winter 2005.	63
2.18	As figure 2.15, for Spring 2005.	64
2.19	As figure 2.15, except anthropogenic NO emissions are replaced by soil NO emissions.	65
2.20	As figure 2.15, for Autumn 2005, with soil NO emissions replacing anthropogenic NO emissions.	66
2.21	As figure 2.15, for Winter 2005, with soil NO emissions replacing anthropogenic NO emissions.	67
2.22	As figure 2.15, for Spring 2005, with soil NO emissions replacing anthropogenic NO emissions.	68

List of Tables

Chapter 1

Introduction and Literature Review

1.1 The atmosphere

The atmosphere is made up of gases held to the earth's surface by gravity. These gases undergo transport on all scales, from barbecue smoke being blown about the garden, to smoke plumes from forest fires travelling across the world and depositing in the Antarctic snow. They take part in innumerable chemical reactions along the way, largely driven by solar input and interactions with each other. Many gases are lofted into the atmosphere by soil, trees, factories, cars, seas and oceans. They are also deposited back to the surface both directly and in rainfall.

The atmosphere is made up of nitrogen (N_2 : $\sim 78\%$), oxygen (O_2 : $\sim 21\%$), and argon (Ar : $\sim 1\%$), along with water (H_2O) and *trace gases* (those that make up less than 1% of the atmosphere). Water (H_2O) ranges from 0.001 to 1% depending on evaporation and precipitation. Beyond these major constituents the atmosphere has a vast number of *trace gases*, including carbon dioxide (CO_2 : $\sim 0.4\%$), Ozone (O_3 : .000001 to 0.001%), and methane (CH_4 : $\sim 0.4\%$) (Brasseur and Jacob, 2017, Ch. 2). Trace gases in the atmosphere can have a large impact on living conditions. They react in complex ways with other elements (anthropogenic and natural), affecting all surface ecosystems upon which life depends.

Ozone in the lower atmosphere is a serious hazard that causes health problems (Hsieh and Liao, 2013), damages agricultural crops worth billions of dollars (Avnery et al., 2013; Yue et al., 2017), and increases the rate of climate warming (Myhre and Shindell, 2013). Around 5 to 20 percent of all air pollution related deaths are due to ozone (Monks et al., 2015), roughly .8 million deaths per year (Lelieveld et al., 2013). In the short term, ozone concentrations of ~ 50 - 60 ppbv over eight hours or ~ 80 ppbv over one hour are agreed to constitute a human health hazard (Ayers and Simpson, 2006; Lelieveld et al., 2009). Long term exposure causes problems with crop loss and ecosystem damage (Ashmore, Emberson, and Murray Frank, 2003), and concentrations may get worse in the future (Lelieveld et al., 2009; Stevenson et al., 2013). Further tropospheric ozone enhancements are projected to drive reductions in global crop yields equivalent to losses of up to \$USD₂₀₀₀ 35 billion per year by 2030 (Avnery et al., 2013), along with detrimental health outcomes equivalent to \sim \$USD₂₀₀₀ 11.8 billion per year by 2050 (Selin et al., 2009). Recently Yue et al., 2017 showed that the net effect of near-surface ozone on is a $\sim 14\%$ decrease in net primary productivity (NPP) in China. They state that reducing this decrease by $\sim 70\%$ before 2030 would require drastic measures.

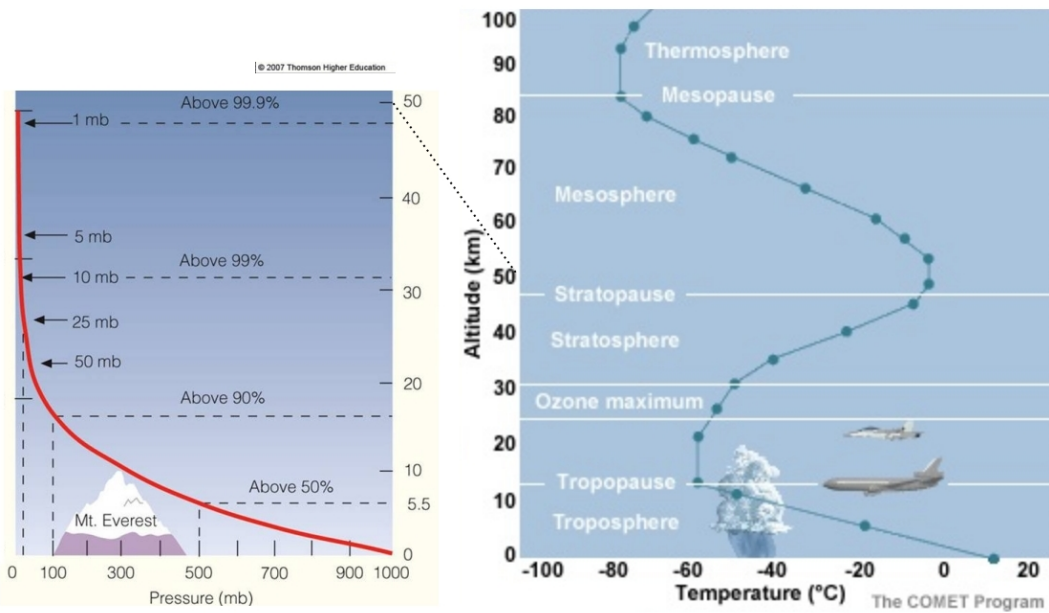


FIGURE 1.1: Pressure (red) logarithmically decreasing, shown with percentage of atmosphere below at several points. Temperature (green) changes throughout the atmosphere. Figure edited from <https://climate.ncsu.edu/Structure>.

1.1.1 Structure

Most of the atmosphere ($\sim 85\%$) is within 10 km of the earth's surface. This is due to air pressure, which decreases logarithmically with altitude. Any entity is subjected to the weight of all the air above it, and the density of the atmosphere is driven by this pressure.

The atmosphere extends above us to the edges of space. This is split into various layers, defined by the *lapse rate*: the decrease in temperature with increasing altitude, or $\frac{-dT}{dz}$. Figure 1.1 shows the pressure and temperature profiles against altitude through the atmosphere. The first layer is the troposphere, which extends to roughly 10 km and is characterised by positive lapse rate (or decreasing temperature with altitude). At the top of the troposphere (the tropopause) the temperature stops decreasing, and then the stratosphere is defined by a negative lapse rate. This is due to UV radiation being absorbed by ozone, and leads to a very vertically stable environment.

In addition to these atmospheric layers, the troposphere can be subset: into a *boundary layer*, and the *free troposphere*. The *boundary layer* is the lowest layer and involves increased atmospheric mixing due to ground heating and friction effects. It generally extends anywhere from 200 - 1000 m, above which the ground effects have fewer direct impacts. The *free troposphere* is the remainder of the troposphere and is more affected by transport, both horizontally and from the stratosphere.

1.1.2 Composition

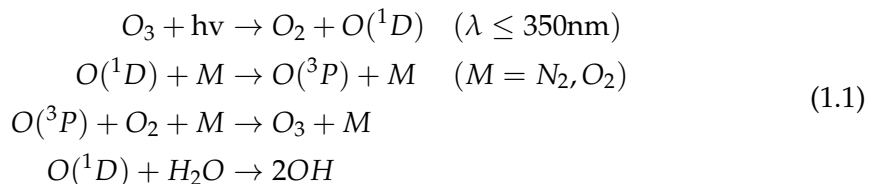
TODO overview here Oxidation and photolysis are the two main processes whereby compounds are broken down in the atmosphere.

Hydroxyl radicals

OH and HO₂ concentrations largely determine the oxidative capacity of the atmosphere. The OH radical drives many processes in the atmosphere, especially during the day when photolysis of ozone drives OH concentrations (Atkinson, 2000). OH is a key species which reacts with nearly all the organic compounds in the troposphere, with only a few exceptions (Atkinson, 2000). Over land, isoprene (C₅H₈) and monoterpenes (C₁₀H₁₆) account for 50% and 30% of the OH reactivity (defined in section TODO) respectively (Fuentes et al., 2000).

Since radicals are involved in all oxidative chemistry in the atmosphere it is important for models to accurately represent them (eg. Travis2014). This is difficult as they are coupled with so many other species and measurements of OH are not readily available on a global scale. In the late 90's it was thought that OH radicals were formed exclusively from photolysis of O₃, HONO, HCHO, and other carbonyls (R₂C=O) Atkinson, 2000. It has been shown since that TODO. Isoprene (C₅H₈) was thought to be a sink of OH until it was shown by Paulot et al., 2009b that the radicals are recycled. This recycling process is discussed in more detail in section 1.3.3.

Ozone is an important precursor to OH, as excited oxygen atoms (O(¹D)) are created through its photolysis, which then go on to react with water to form OH, as shown in this reaction sequence (Atkinson, 2000; Atkinson and Arey, 2003):

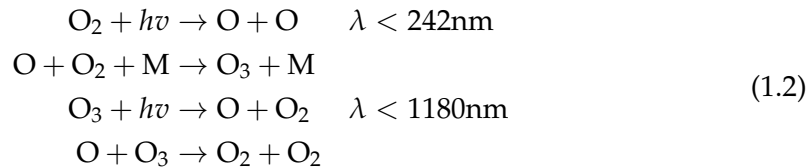


Where $h\nu$ represents radiation and M is an inert molecule. This shows that some of the O(¹D) recycles back to ozone, while some forms OH. Atkinson and Arey, 2003 discuss the relative rates of these reactions.

1.2 Ozone

Ozone (O₃) is mostly located in the stratosphere, where it prevents much of the shorter wavelength (UV) solar radiation from reaching the earth's surface. In the stratosphere ozone production is driven by the Chapman mechanism, as high energy radiation (with wavelengths $\lambda < 242$ nm) photolyses the molecular oxygen (O₂) in the atmosphere (Brasseur and Jacob, 2017, Chapter 3, section 2).

The Chapman mechanism involves several reactions which lead to rough equilibrium of O, O₂, O₃ and pressure, as follows:



The high energy photons ($\lambda < 242$ nm) are present from the top of the atmosphere but are mostly removed before reaching the troposphere as their energy is used to split the O₂ molecules. The lifetime of O against loss by O₂ is less than a second in the troposphere, and produced O₃ quickly returns to O and O₂, as low energy ($\lambda < 1180$ nm) photons and M are abundant. The reduced light penetration towards the surface, in addition to the logarithmic increase in atmospheric pressure (which affects M abundance) drives the vertical profile of ozone into what is called the *ozone layer*. This is a layer of relative ozone abundance within the stratosphere. The Chapman mechanism requires radiation so only takes place during the daytime, during the night this process slows to a halt, and the ozone concentrations remain stable unless NO_x pollution intrudes (Jacob, 1999, Chapter 10).

Since the Montreal Protocol on Substances that Deplete the Ozone Layer was established in August 1987, and ratified in August 1989, several satellites and many measurement stations were set up to monitor ozone in the stratosphere. However, in the southern hemisphere there are relatively few records of ozone (Huang et al., 2017). This affects our ability to accurately determine sources of ozone in the troposphere.

Generally there are two main drivers of tropospheric ozone concentrations; transport from the stratosphere and chemical production due to emissions of precursors. Tropospheric ozone is regulated by NO and NO₂ concentrations, which form an equilibrium (Cape, 2008; Young et al., 2017). However NO_x or VOC emissions affect this equilibrium and can lead to enhanced ozone formation, this can be seen in figure 1.2. At small to medium scales, pyrogenic (fire) and anthropogenic (man-made) emissions can be important. Smoke plumes from biomass burning can carry ozone precursors, creating higher ozone concentrations downwind of the plume's source. Emissions of precursors from large cities (such as NO_x emissions from traffic and power production) can impact ozone concentrations. These impacts are not always straightforwards due to the nonlinear relationship between ozone and its precursors.

A summary of processes affecting tropospheric ozone, copied from Young et al., 2017, is shown in Figure 1.2. This shows the major processes and emissions which affect tropospheric ozone concentrations. My work involves improving the highly uncertain natural emissions of NMVOCs from Australia.

NOx

NO_x ($\equiv \text{NO}_2 + \text{NO}$) is another important chemical family in the atmosphere which interacts with ozone and regulates the atmospheric oxidative capacity. NO_x compounds are short lived, with emissions (Power generation and combustion transport) being the main driver of concentrations (Delmas, Serca, and Jambert, 1997). NO_x and O₃ relative concentrations during the day are regulated by the following reactions

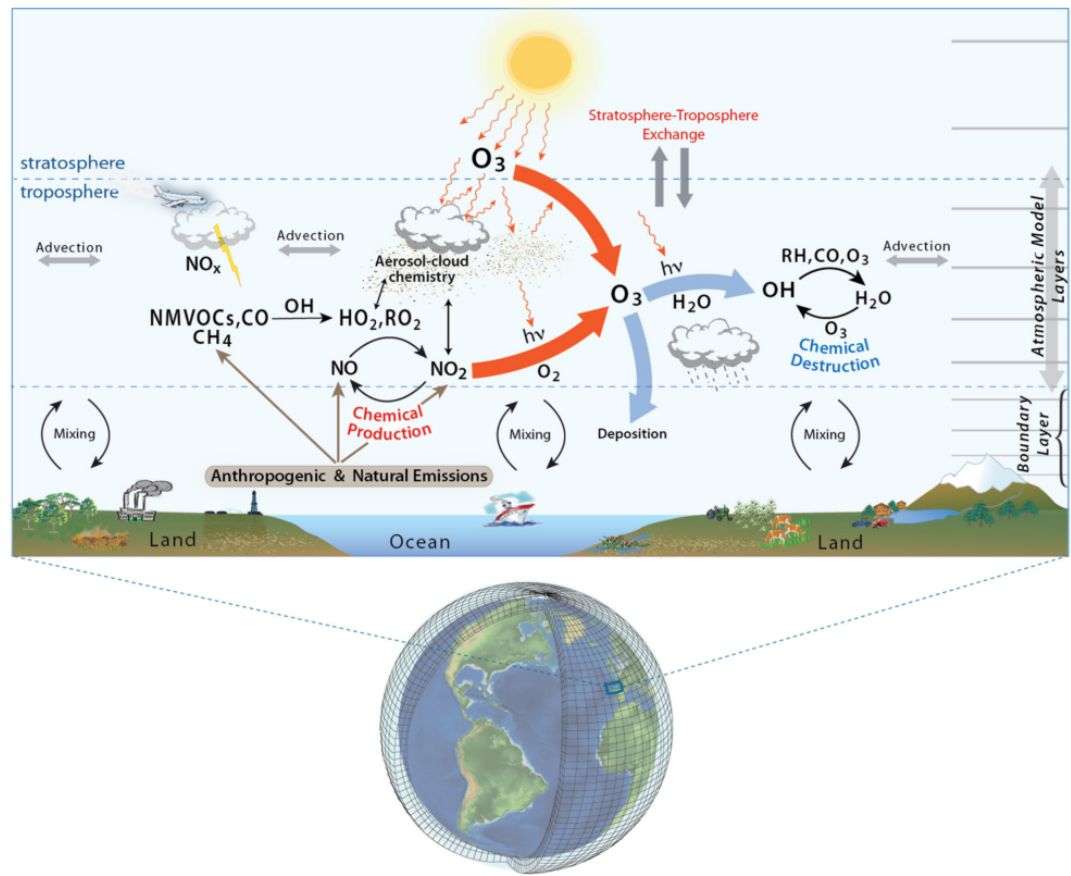
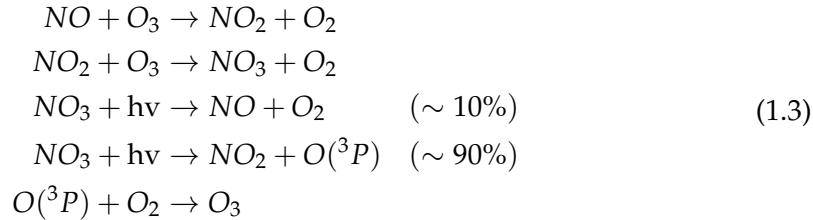


FIGURE 1.2: Tropospheric ozone processes, Figure 1 in Young et al., 2017. DOI: <https://doi.org/10.1525/elementa.265.f1>

(Sillman, 1999; Atkinson, 2000):



NO_x is removed primarily by conversion to nitric acid (HNO_3) followed by wet or dry deposition (Ayers and Simpson, 2006).

1.2.1 Stratosphere to troposphere transport

Historically (in the late 1990's), ozone transported down from the stratosphere was thought to contribute 10-40 ppb to tropospheric ozone levels, matching tropospheric production (Atkinson, 2000; Stohl et al., 2003). This number was revised down over the years as measurement and modelling campaigns improved our understanding of global scale transport, mixing, and chemistry (Monks et al., 2015). Recently Kuang et al., 2017 analysed tropospheric ozone measurements in south-east USA and observed STT influence which can be seen to affect surface ozone levels. In their work they use several different instruments and analyse the structure and temporal evolution of ozone and the local weather systems.

Ozone transported to the troposphere from the stratosphere can occur through diffusion (relatively slowly), or direct mixing. Intrusions of stratospheric air into the troposphere are often called Stratosphere to Troposphere Transport events (STT). STT often occur as tongues of stratospheric air descend and get disconnected from the stratosphere, potentially due to low pressure systems and jet streams Sprenger, Croci Maspoli, and Wernli, 2003. Recently global chemical transport models (CTMs) have been used to trace how much ozone is being transported to the troposphere in this manner. There are a few methods of doing this, such as Ojha et al., 2016, who use a model that keeps track of ozone formed in (and transported from) the stratosphere. Model based estimates require validation against actual measurements, such as those from ozonesondes or satellites. Hegglin and Shepherd, 2009 estimate that climate change will lead to increased STT due to an acceleration in the Brewer Dobson circulation. They estimate ~ 30 , and $\sim 121 \text{ Tg yr}^{-1}$ increases (relative to 1965) in the southern and northern hemispheres respectively

Liu et al., 2017 examine southern hemispheric ozone and the processes which control its inter-annual variability (IAV). IAV is the standard deviation of ozone anomalies from the monthly mean. They show that ozone transported from the stratosphere plays a major role in the upper troposphere, especially over the southern Indian ocean during austral winter. While stratospheric transport mostly impacts the upper troposphere, some areas are impacted right down to the surface. Liu et al., 2017 look at modelled tropospheric ozone sensitivity to changes in stratospheric ozone, ozone precursor emissions, and lightning over the southern hemisphere from 1992–2011. Their work suggests ozone at 430 hPa (roughly 6 km altitude) is mostly stratospheric in

September over 20°S to 60°S at all longitudes. They also see tropospheric ozone sensitivity to emissions from South America (0–20°S, 72.5–37.5°W), southern Africa (5–10°S, 12–38°E), and South to South-east Asia (70–125°E, 10°S–40°N). In the USA recent work by Lin et al., 2015 suggests that intrusions during spring are increasing surface ozone levels. Their work also recommends that understanding of the frequency and cause of STT needs to be improved to effectively implement air quality standards.

1.2.2 Chemical production

Ozone produced in the troposphere from precursors and radiation drive ozone levels, especially in the lower (near-surface) troposphere. The main processes involved are shown in figure 1.2, with ozone regulated by reactions 1.3. An analysis of the Atmospheric Chemistry and Climate Model Inter-comparison Project (ACCMIP) simulations by Young et al., 2013 found STT is responsible for $540 \pm 140 \text{ Tg yr}^{-1}$, equivalent to $\sim 11\%$ of the tropospheric ozone column, with the remainder produced photochemically (Monks et al., 2015). A recent summary by Young et al., 2017 estimates ozone production and loss in the troposphere to be $\sim 4900 \text{ Tg yr}^{-1}$, and $\sim 4500 \text{ Tg yr}^{-1}$ respectively, while STT sources are $\sim 500 \text{ Tg yr}^{-1}$. These numbers are at the global scale, and in order to understand the processes driving ozone concentrations at any specific site measurements must be analysed.

Tropospheric ozone concentrations rely on climate and ozone precursor emissions; including NO, NO₂, CO, VOCs, and HCHO (Atkinson, 2000; Young et al., 2013; Marvin et al., 2017). Ozone predictions are uncertain due to the vagaries of changing climate which affects both transport, deposition, destruction, and plant based precursor emissions. All of these processes are tightly coupled and difficult to accurately model, as they depend on uncertain assumptions such as CO₂ dependency (Young et al., 2013). Even with all the work done over the prior decades there remains large uncertainties about ozone precursors in the troposphere (Mazzuca et al., 2016).

Ozone is formed in the troposphere through oxidation of VOCs (described in Section 1.3) in the presence of NO_X. Net formation or loss of O₃ is determined by interactions between VOCs, NO_X, and HO_X, and is a complicated system of positive and negative feedbacks (Atkinson, 2000). Figure 1.3 shows the non-linear affect of NO_X and VOC concentrations on ozone production over Houston, as modelled in Mazzuca et al., 2016. Recently the relationship has been examined on the intradiel timescale showing that ozone production can be more or less sensitive to VOCs at different hours depending on location various other factors (Mazzuca et al., 2016). This shows how important it is to correctly determine the precursors concentrations in order to estimate ozone levels and production.

Tropospheric ozone is lost via chemical destruction and dry deposition, estimated to be $4700 \pm 700 \text{ Tg yr}^{-1}$ and $1000 \pm 200 \text{ Tg yr}^{-1}$, respectively (Stevenson et al., 2006; Young et al., 2017). The main loss channel is through equation 1.1, where photolysis and pressure create OH from the O₃.

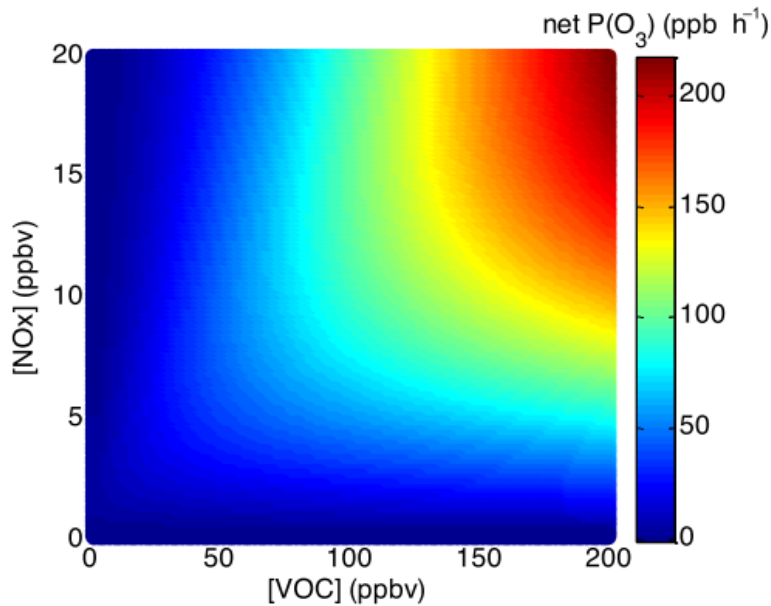


FIGURE 1.3: Ozone production rate dependent on NO_x and VOC concentrations (Mazzuca et al., 2016).

1.3 VOCs

The least well understood precursors to tropospheric ozone production belong to a class of organic compounds. Organic compounds are members of a large class of chemicals whose molecules contain carbon, with the exception of a few compounds such as carbides, carbonates (CO_3), and simple oxides of carbon and cyanides. Organic compounds can be categorised based on their vapour pressure, which is the tendency of a liquid or solid to vaporise. Compounds with high vapour pressures at standard temperature are classed as volatile, and have a facility to evaporate at low temperatures. Plants contain tens of thousands of organic compounds, it's likely that fewer than 40 have high enough volatility to be emitted (Guenther et al., 2000).

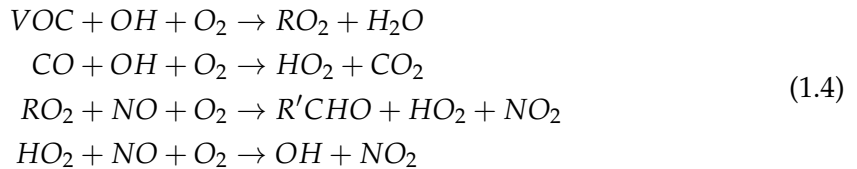
Atmospheric organic compounds are legion and differ by orders of magnitude with respect to their fundamental properties, such as volatility, reactivity, and cloud droplet formation propensity, etc. Volatile organic compounds (VOCs) have vapour pressure greater than 10^{-5} atm, and are mostly generated naturally by plants, which emit around 1000 Tg yr^{-1} (Guenther et al., 1995; Glasius and Goldstein, 2016). Due to their high volatility these compounds are generally seen in the gas phase. Organic compounds with a lower volatility are classed as semi-volatile (SVOCs: vapour pressure between 10^{-5} and 10^{-11} atm) are seen in both gas and particle phase depending on temperature and pressure. Organic compounds with even lower vapour pressure are generally found in the particle phase in aerosol particulate matter (Glasius and Goldstein, 2016). Understanding the drivers of trends in biogenic VOC emissions (BVOCs) is required in order to estimate future carbon fluxes, changes in the water cycle, ozone production, air quality, and other climate responses (Yue, Unger, and

Zheng, 2015). In the last 20 years anthropogenic emissions of VOCs have been increasing while biogenic VOC emissions have decreased, due to rapid economic growth and lower annual temperatures (Stavrakou et al., 2014; Kwon et al., 2017).

Methane (CH_4) is one of the more abundant and potent VOCs, however it is often classified separately and compared against non-methane VOCs (NMVOCs). NMVOCs are alkanes, alkenes, aromatic hydrocarbons and isoprene, with isoprene being the most prominent. Methane is relatively long lived (years) and is well mixed in the atmosphere while other VOC levels are spatially diverse due to their shorter lifetimes. In this thesis I work towards a better understanding of the NMVOC emissions coming from Australia.

VOCs are an important driver of atmospheric processes, especially near forests. VOCs are broken down into HCHO , O_3 , CO_2 and many other species, mainly through oxidation by OH. VOC emissions result in radical cycling, acid deposition, production of tropospheric ozone, and secondary organic aerosols (SOAs) (Atkinson, 2000; Kanakidou et al., 2005). VOC emissions affect surface pollution levels, potentially enhancing particulate matter (PM) and ozone levels. A regional-model study in Europe (Aksoyoglu et al., 2017) has also shown VOCs impact secondary inorganic aerosol concentrations. These have impacts on climate (through radiative forcing) and air quality (from ozone and SOA enhancements), affecting both human health and crop yields (Forster et al., 2007; Avnery et al., 2013; Lelieveld et al., 2015).

Ozone in rural areas is often higher than in populous cities, due to the more abundant VOCs concentrations. This occurs through the following reaction sequence (Sillman, 1999):



The reactions of VOCs or CO with OH convert NO to NO_2 , which leads to ozone formation as NO_2 production in reaction 1 of 1.3 is bypassed. R and R' are organic species in these reactions.

One problem associated with VOC emissions is the production of aerosols. Aerosols are suspended particulates and liquid compounds in the atmosphere, of which particulate matter (PM) is an important subset. PM in the atmosphere is a major problem, causing an estimated 2-3 million deaths annually (Hoek et al., 2013; Krewski et al., 2009; Silva et al., 2013; Lelieveld et al., 2015). Fine particulate matter ($\text{PM}_{2.5}$) penetrates deep into the lungs and is detrimental to human health. Some PM comes from small organic aerosols (OA) emitted in the particulate phase and referred to as primary OA (POA). A substantial amount of PM is due to gaseous organic compounds transforming in the troposphere leading to what's known as secondary OA (SOA) (Kroll and Seinfeld, 2008).

Formation of SOA is generally due to VOC oxidation and subsequent reactions, while removal from the atmosphere is largely due to wet or dry deposition, and cloud scavenging (Kanakidou et al., 2005). It can be difficult to attribute PM formation, in part due to the complex relationship between NO_x , OH, O_3 , and the uncertainty surrounding precursor emissions. Improved concentration estimates of these organic

compounds requires a better understanding of their emissions, which is one of the foci in this thesis.

1.3.1 Emissions

VOC emissions are often classified as either anthropogenic, biogenic, or pyrogenic. There are ten times as many emissions of NMVOCs from natural sources compared to anthropogenic sources (Guenther et al., 2006; Kanakidou et al., 2005; Millet et al., 2006). Methane and isoprene each comprise around a third of the global total emissions of VOCs (Guenther et al., 2006). Major emitters are tropical broadleafs (notably eucalypts), and shrubs (Guenther et al., 2006; Arneth et al., 2008; Niinemets et al., 2010; Monks et al., 2015). TODO: why do plants emit? increased canopy light penetration? Emissions are affected by various factors such as temperature, sunlight, soil moisture, etc.

It used to be thought that emissions of anthropogenic and biogenic VOCs (AVOCs, BVOCs respectively) were roughly similar (Müller, 1992, TODO: more cites). In the 1990's it became clear that biogenic emissions are in fact dominant. Global VOC levels are estimated at 85 %, 13 %, and 3 % from biogenic, anthropogenic, and pyrogenic sources respectively (Kanakidou et al., 2005; Kefauver, Filella, and Peñuelas, 2014). Although methane makes up a third of atmospheric VOCs, its emissions are low. The World Meteorological Organisation (WMO) estimated that we are emitting 360 Mt yr⁻¹ of methane, compared to biogenic emissions of around 200 Mt yr⁻¹ (Atkinson, 2000). In 1995 emissions of other VOCs were estimated at 1150 Tg C yr⁻¹ from biogenic sources, and 100 Tg C yr⁻¹ from anthropogenic sources (Guenther et al., 1995; Atkinson, 2000). The main non-methane BVOC emissions are isoprene (44%) and monoterpenes (11%) (Guenther et al., 2000; Kefauver, Filella, and Peñuelas, 2014). Land use changes can drastically affect isoprene sources, for instance in the tropics where large scale deforestation has converted forest into crop lands (Kanakidou et al., 2005).

VOCs are removed by wet and dry deposition, OH oxidation, reaction with NO₃, ozonolysis (at night time or in polluted areas) or photolysis (Atkinson and Arey, 2003; Brown et al., 2009). The process of deposition only accounts for a small fraction of the VOC loss, with the possible exception of the long lived methane compound (Atkinson and Arey, 2003).

1.3.2 Isoprene

Isoprene, or 2-methylbuta-1,3-diene, is a VOC with the chemical formula C₅H₈. It is of major importance to the atmosphere, as it is involved in various processes which alter the oxidative capacity of the atmosphere. Guenther et al., 1995, and subsequent updates (Guenther et al., 2000; Guenther et al., 2006; Guenther et al., 2012), have been used ubiquitously by the atmospheric community as a global estimate of isoprene emissions, at roughly 500-600 Tg yr⁻¹, emitted mostly during the day. Recently an estimate of global isoprene emissions has been made using a completely different model, of around 465 Tg C yr⁻¹, by Messina et al., 2016 using ORCHIDEE. The global emission factors model used to derive both these estimates is based on modelling emissions from different plant species (phenotypes), and relatively few Australian species are used when forming in these estimates.

Isoprene affects NO_X and HO_Y cycling, see for example formulae 1.1, 1.3. In the presence of NO_X, isoprene forms tropospheric ozone and SOAs (Wagner, 2002; Millet et al., 2006). It has a short lifetime during the day, roughly an hour due to OH oxidation (Atkinson and Arey, 2003)).

Measurements of isoprene are often uncertain or difficult to make accurately. Kanakidou et al., 2005 summarised how chamber experiments used to measure isoprene reactions may be unsuitable for comparison to the natural atmosphere. In Nguyen et al., 2014 many scientists and groups worked together on chamber measurements, to improve understanding of ambient atmospheric oxidation mechanisms of biogenic hydrocarbons (such as isoprene).

Isoprene emissions estimates are still fairly uncertain, as global measurements are difficult and regional emissions can be very different. The global uncertainty of isoprene emission was estimated to be a factor of 2 to 5 (250-750 Tg yr⁻¹) (Kanakidou et al., 2005). Improvements over the years have been incremental, and generally localised to regions of particular interest for air quality such as China and the USA TODO: find recent uncertainty estimate improvements examples. The lack of accuracy in BVOC emissions estimates prevents accurate determinations of the sources and distribution of pollutants including ozone and organic aerosols. Most of the tropospheric SOA comes from biogenic precursors, the evidence for this has grown over the last two decades (Guenther et al., 1995; Kanakidou et al., 2005; Guenther et al., 2012). Accuracy in VOC measurements is important: it has been shown that even the diurnal pattern of isoprene emissions has an effect on modelling ground level ozone (Hewitt et al., 2011; Fan and Zhang, 2004).

1.3.3 The isoprene cascade

Isoprene forms many products with various lifetimes, here I will present an overview of some important mechanisms and products which are useful to my work. Isoprene is emitted and enters the atmosphere in the gas phase, where it reacts quickly with OH and other radicals. One common compound which is produced by these reactions is HCHO, which is easier to measure and often used to estimate how much isoprene is being emitted. The reactions which occur are important to understand due to their impacts on air quality, ozone, and physical properties in the lower troposphere. The many children processes and products which begin with isoprene oxidation are often called the isoprene (photochemical) cascade Paulot2012; Crounse et al., 2012; Wolfe et al., 2016.

Photolysis and oxidation of many VOCs initially form alkyl radicals (\dot{R}). Alkenes (VOCs with double bonded carbon, such as isoprene) react with ozone leading to organic peroxy radicals (RO \dot{O}). These go on to form many products and lead to (amongst other things) aerosol, formaldehyde, and ozone formation, depending on sunlight and NO_X concentrations (Atkinson, 2000).

Oxidation

The primary first step for atmospheric isoprene is photooxidation, reacting with OH to form isoprene hydroxyperoxy radicals (RO \dot{O}) (Patchen2017; Wolfe et al., 2016; Marvin et al., 2017). There is still uncertainty about which pathways are most important

following RO \cdot production: HO $_2$ reactions predominantly produce hydroxyhydroperoxides (ISOPOOH), NO reactions largely produce methyl vinyl ketone (MVK) and methacrolein (MCR), and RO $_2$ reactions are also possible Liu et al., 2016b.

First isoprene has its double bond replaced by OH, as summarised by the equation from PATCHEN et al., 2007: R-CH=CH-R' + OH → R-CH(OH)CH-R' where R and R' represent hydrocarbons. This OH adduct then reacts with O $_2$ to produce a hydroxyperoxy radical (RO \cdot), which can be any of six different isomers (PATCHEN et al., 2007). These RO \cdot (also called organic-peroxy/alkyl-peroxyl/ISOPOO radicals, or RO $_2$) react with HO $_2$ or NO and produce stable products (often called oxidised VOCs or OVOCs) (Nguyen et al., 2014). Most of these reaction pathways produce HCHO (Wolfe et al., 2016).

RO \cdot reaction pathways depend on the NO X concentrations. Reactions with NO can lead to ozone production in environments rich in isoprene or other non-methane organic compounds (NMOCs) and NMVOCs (PATCHEN et al., 2007; Atkinson and Arey, 2003). These reactions are complex and coupled, for example NO $_2$ concentrations can be increased by NMOC and NO reactions (Atkinson and Arey, 2003).

In the presence of NO X , the RO \cdot may form organic nitrates after reacting with NO. Any organic nitrates which are formed affect levels of both HO X (H, OH, peroxy radicals) and NO X , acting as a sink (Mao et al., 2013 and references therein). Reaction with NO $_2$ forms isoprene nitrates, or hydroxynitrate (RONO $_2$). The first generation of organic nitrates produced by isoprene oxidation range from 7% to 12%, shown in laboratory experiments (Paulot et al., 2009a; Mao et al., 2013). A portion of isoprene nitrates are recycled back to NO X , so may serve as a reservoir of nitrogen and allow its transport to the boundary layer of remote regions (PATCHEN et al., 2007; Paulot et al., 2009a). The nitrates can also build up in the winter, when removal processes are not as dominant (Lelieveld et al., 2009).

Oxidation reactions are important and quickly stabilise the ratio of NO to NO $_2$. There is still large uncertainty around the fate of various RO \cdot , which limits understanding of the relative importance of some chemical processes (Crounse et al., 2013). Some portion of emitted isoprene leads to SOA, potentially through the formation of methacrylic acid epoxide (MAE) formed by decomposition of methacryloylperoxynitrate (MPAN, a second generation product of isoprene oxidation) as shown in smog chambers and field studies in Lin et al., 2013.

Low NO X scenario

Isoprene oxidation by OH is less well understood when lower concentrations of NO are present in the atmosphere. Initially isoprene was thought to be a sink for atmospheric oxidants (e.g. Guenther et al., 2000). It was thought that in low NO environments, like those far from anthropogenic pollution and fires, oxidation of isoprene would create ISOPOOH and lead to low concentrations of OH and HO $_2$ Paulot et al., 2009b. In Paulot et al., 2009b, the HO X levels are shown to be largely unaffected by isoprene concentrations. They show that ISOPOOH is formed in yields > 70%, and MACR and MVK is formed with yields < 30%. The formation of MACR and MVK produces some HO X , although not enough to close the gap. Paulot et al., 2009b goes on to suggest (and provide experimental evidence) that dihydroxyperoxides (IEPOX) are formed from oxidation of the ISOPOOH, which form precursors for SOAs as well

as closing the HO_x concentration gap. They then use GEOS-Chem, modified to include IEPOX formation, to estimate that one third of isoprene peroxy radicals react with HO₂, and two thirds react with NO. They estimated $95 \pm 45 \text{ Tg yr}^{-1}$ IEPOX being created in the atmosphere, which (at the time) was not modelled by CTMs. Their work showed another pathway for isoprene based SOA creation, through these IEPOX creation and HO_x recycling mechanisms. Peeters and Muller, 2010 suggested that the work of Paulot et al., 2009b only partially bridges the gap between clean air OH concentration measurements and models. They suggested four new mechanisms for OH recycling in these pristine conditions. These can be summarised as OH regenerating reactions which occur during photolysis of hydroperoxy-methyl-butens (HPALDs), and resulting photolabile peroxy-acid-aldehydes (PACALDs). These reactions are highly non-linear and subject to large uncertainty, however when compared against several campaigns they were shown to improve modeled HO_x concentrations. In Crounse et al., 2012, MACR products are examined and hydroxy recycling is observed in low NO conditions, backing up results from Peeters and Muller, 2010. Peeters and Muller, 2010 showed that HO₂ is produced at near unity yields following isoprene oxidation initiated by OH. TODO: read more Peeters2010

Nguyen et al., 2014 examine various measurement techniques to determine isoprene reactions in non-laboratory conditions. Their work discussed how large uncertainties persist in isoprene oxidation, which carries through to predictions by atmospheric models. Nguyen et al., 2014 show preliminary estimates of low-NO yields of MVK and MCR to be $6 \pm 3\%$ and $4 \pm 2\%$ respectively, consistent with TODO:Liu2013 but only when cold-trapping methods are employed. These yields each increase (due to interference by OVOCs) to greater than 40% when directly sampled by GC-FID.

Even with the recent boom in isoprene analysis, uncertainties remain in the isoprene oxidation mechanisms. Examples (taken from Nguyen et al., 2014) include isoprene nitrate yields, which range from 4-15% (Paulot et al., 2009a), 90% disagreements in MAC and MVK yields TODO:(Liu2013), various possible sources for SOA TODO:(Chan2010; “Reactive intermediates revealed in secondary organic aerosol formation from isoprene”; Lin et al., 2013), unknown HPALD fates, incomplete O₂ incorporation TODO:(Peeters2009; Crounse et al., 2013), and under-characterized RO₂ lifetime impacts TODO:(Wolfe2012). TODO: get those citations and read abstracts.

Ozononlysis

Ozononlysis is the splitting of carbon chains by ozone molecules, and is among the primary oxidation pathways for volatile alkenes (Nguyen et al., 2016). Criegee intermediates (carbonyl oxides with two charge centres) are formed when isoprene reacts with O₃. Nguyen et al., 2016 examine in detail a few of these, with proposed mechanisms for C₁ and C₄ Criegee intermediate reactions. The C₁ stabilised Criegee (CH₂OO, ~61%) is therein proposed to react with water yielding 73% hydroxymethyl hydroperoxide (HMHP), 6% HCHO + H₂O₂, and formic acid + H₂O, and the same products with yields of 40, 6, and 54% respectively when this Criegee reacts with (H₂O)₂.

Oxidation by NO₃

At night when OH concentrations have dropped, isoprene can remain in the atmosphere to be transported. Typically less than half of this night time isoprene is removed through ozonolysis (Atkinson and Arey, 2003), however, in polluted areas where high levels of NO_x exist, isoprene is consumed by a different radical. During the night isoprene is oxidised by nitrate radicals (NO₃), which joins to one of the double bonds and produces organic nitrates in high yield (65% to 85%) (Mao et al., 2013). (todo: read mao2013 para 3 cites) NO₃ are largely formed through ozone reactions, as in equation 1.3. A build up of NO₃ radicals can be seen at night, when photolysis is not removing them (Atkinson, 2000; Brown et al., 2009).

In areas with high NO_x levels, greater than 20% of the isoprene emitted late in the day ends up being oxidised by the NO₃ radical over night (Brown et al., 2009). At night isoprene has affects on both NO_x concentrations and ozone levels, and can form harmful organic nitrates and SOAs (Brown et al., 2009; Mao et al., 2013). These nitrates go on to produce further SOAs, largely due to NO₃ reacting with first generation isoprene oxidation products (Rollins et al., 2009). The night-time concentrations of OH and ozone also have a complex effect on NO_x removal in high latitude winters, when photolysis and NO reactions are reduced (Ayers and Simpson, 2006).

1.3.4 Radiative Forcing

One of the larger uncertainties in atmospheric modelling is how particles in the atmosphere affect radiative forcing. For 12 years it has been understood that most OA cool the atmosphere, with smaller particles having a larger effect as they matching the wavelengths of visible light (Kanakidou et al., 2005). Gas phase emissions with higher vapour pressures can be oxidised into lower vapour pressure products which will partition between gas and particle phase, often called semi or non-volatile. The aerosol products from these gas phase emissions (or the children thereof) are SOA (Kanakidou et al., 2005). SOA plays an indirect and complex role in cloud properties, with a net cooling effect (IPCC, 2013: *Climate Change 2013: The Physical Science Basis. Contribution of Working Group I to the Fifth Assessment Report of the Intergovernmental Panel on Climate Change*, Chapter 7,8)

Transport and indirect effects complicate matters further, with cloud creation and modification of cloud properties being quite difficult to accurately predict. In the third IPCC report (*Intergovernmental Panel on Climate Change (IPCC): Climate Change: The Scientific Basis* 2001), the uncertainty involved if OA forcing was a factor of 3 times the estimated effect. This has since been improved however OA and cloud formation still remains a large uncertainty in more recent IPCC reports (Forster et al., 2007). Figure 1.4 shows the radiative forcing (RF) of various atmospheric constituents, it's clear that OA uncertainty dominates. Figure 1.5 shows the same summary updated in chapter 8 of the fifth report, where the SOA uncertainty remains quite large.

In order to improve understanding of processes involved in radiative forcing, Kanakidou et al., 2005 highlight the need for improving VOC emissions and flux measurements. They also advocate utilising satellite data in models as a means of improving the emissions inventories. VOCs can lead to changes in cloud formation, as nucleation



FIGURE 1.4: The overall radiative forcings and uncertainties of several atmospheric constituents This is an image taken from Forster et al., 2007, found at https://www.ipcc.ch/publications_and_data/ar4/wg1/en/faq-2-1.html.

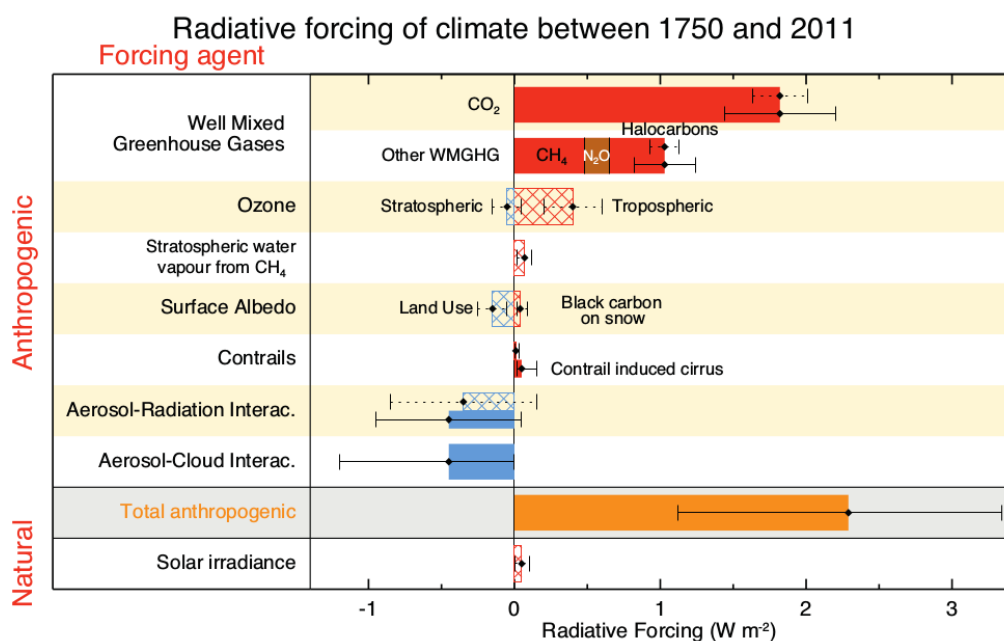


Figure 8.15 | Bar chart for RF (hatched) and ERF (solid) for the period 1750–2011, where the total ERF is derived from Figure 8.16. Uncertainties (5 to 95% confidence range) are given for RF (dotted lines) and ERF (solid lines).

FIGURE 1.5: The overall radiative forcings and uncertainties of several atmospheric constituents This is an image taken from *IPCC, 2013: Climate Change 2013: The Physical Science Basis. Contribution of Working Group I to the Fifth Assessment Report of the Intergovernmental Panel on Climate Change*, chapter 8.

can arise from the subsequent SOA. Kanakidou et al., 2005 concluded that it is very likely that organics contribute to particle growth and formation rates.

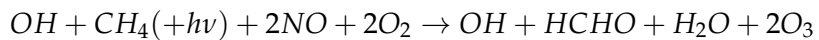
1.4 HCHO

One of the major products of isoprene chemistry is HCHO. HCHO is important both for its own atmospheric impacts, and as a proxy for determination of isoprene emissions. Given a modelled yield of HCHO from isoprene, it is possible to work backwards from measured HCHO concentrations to determine the isoprene emissions.

HCHO, aka methanal, methyl aldehyde, or methylene oxide, is of the aldehyde family. HCHO is an OVOC which is toxic, allergenic, and a potential carcinogen. It is dangerous at low levels, with WHO guidelines for prolonged exposure at 80 ppb. HCHO is used as an adhesive in plywood, carpeting, and in the creation of paints and wallpapers. Emissions in enclosed spaces can build up to dangerous levels, especially if new furnishings are installed (Davenport et al., 2015). At global scales HCHO in furniture is less important, as concentrations are driven by photochemical reactions with methane and other VOCs.

1.4.1 Sources and sinks

Background levels of HCHO in the atmosphere are driven by the oxidation of methane (CH_4) by the hydroxyl radical (OH^{-1}). Atkinson, 2000 summarised the background formation of HCHO with the following reaction:



which shows that photolysis and oxidation of methane forms HCHO and ozone in a process that regenerates the OH radicals. CH_4 concentrations are relatively well constrained in models, with the ACCMIP comparison showing only $\sim 3\%$ inter-quartile range (Young et al., 2013). There is a complex relationship between VOCs, HO_x , and NO_x : with higher levels of NO_x increase the speed that VOCs are converted into HCHO (Wolfe et al., 2016).

Within the continental boundary layer, the major source of HCHO enhancement is VOC emissions (which reacting with OH radicals in the presence of NO_x) (Wagner, 2002; Millet et al., 2006; Kefauver, Filella, and Peñuelas, 2014). Enhancements to regional and continental HCHO are largely driven by isoprene emissions (Guenther et al., 1995; Palmer, 2003; Shim et al., 2005; Kefauver, Filella, and Peñuelas, 2014). This is true except near fires or anthropogenic sources of HCHO and precursors (Guenther et al., 1995; Kefauver, Filella, and Peñuelas, 2014; Wolfe et al., 2016). Biomass burning (BB) can be a source of HCHO, and various other pollutants, precursors, and aerosols (Guenther et al., 1995; Andreae, 2001). Additionally HCHO is emitted into the atmosphere directly through fossil fuel combustion, natural gas flaring, ethanol refining, and agricultural activity (Wolfe et al., 2016).

Other terpenoids (monoterpenes, sesquiterpenes, etc.) can also produce HCHO, although generally to a lesser extent than isoprene, methane and biomass burning (Guenther et al., 2012). Many of the HCHO yields from terpenoids are estimated

through chamber studies which examine the products molecular mass and charge after mixing the compound of choice into a known volume of air (Nguyen et al., 2014, eg.). These conditions generally don't match those of the real world, where ambient air will have a cocktail of these compounds and other reactants. Nguyen et al., 2014 state that one of their goals is to recreate ambient atmosphere in their chamber studies with more accuracy, in order to improve interpretations and allow more accurate model parameters.

Millet et al., 2008 show that anthropogenic emissions of HCHO in America are mostly negligible, although improved sensitivity from oversampling allowed satellite detection of enhanced HCHO concentrations over Houston and Texas (Zhu et al., 2014). This is not the case in China, since massive population centres and industrial districts are emitting huge amounts of VOCs into the atmosphere (Fu et al., 2007). Fu et al., 2007 use GOME measurements over Asia and derive biogenic, anthropogenic, and pyrogenic VOC emissions, and Zhu et al., 2014 use oversampling of the OMI HCHO measurements to determine anthropogenic highly-reactive VOC emissions. Then with their updated emissions they show how surface ozone is affected, with a seasonal increase of 5-20 ppb simulated by GEOS-Chem.

In the past, HCHO levels were underestimated by models, often with large discrepancies, due to the poor understanding of methyl peroxy radical (CH_3OO) chemistry (Wagner, 2002). Nowadays HCHO concentrations are better understood, however precursor emissions are one of the main unknowns (Emmerson et al., 2016; Marvin et al., 2017, eg.). Marvin et al., 2017 found that discrepancies in modelled HCHO concentrations are primarily due to second and later generation isoprene oxidation chemistry.

HCHO has two major sinks, one being reactions with OH (oxidation), the other being photolysis: the process of being broken apart by photons (CRUTZEN, LAWRENCE, and PÖSCHL, 1999; Wagner, 2002; Levy, 1972; Kefauver, Filella, and Peñuelas, 2014). These reactions lead to a daytime lifetime of a few hours (Atkinson, 2000; Millet et al., 2006). Both these loss processes (photolysis, oxidation) form CO and hydroperoxyl radicals (HO_2), and have global significance to radiative forcing and oxidative capacity (Franco et al., 2015). The other notable sinks are wet and dry deposition, although these are not as significant (Atkinson, 2000) (TODO: add more cites here).

1.4.2 Measurement techniques

There are a few ways to measure HCHO, including Fourier Transform Infra-Red (FTIR) Spectrometry and Differential Optical Absorption Spectroscopy (DOAS). FTIR examines the Fourier transform of a measured spectrum in order to determine what trace gases are interfering within the IR range of light. DOAS methods are based on light interference and absorption through air masses.

The DOAS technique takes advantage of the optically thin nature of HCHO in order to linearise the radiance differential through air masses with and without HCHO, using the Beer-Lambert intensity law. This method is used both in the home, and from space, globally for HCHO detection (Guenther et al., 1995; Gonzalez Abad et al., 2015; Davenport et al., 2015). As a trace gas HCHO interferes with light over a few wavelength bands, which allows instruments to detect concentrations between a known light source and a detector. Figure 1.6 shows the interference spectrum of HCHO

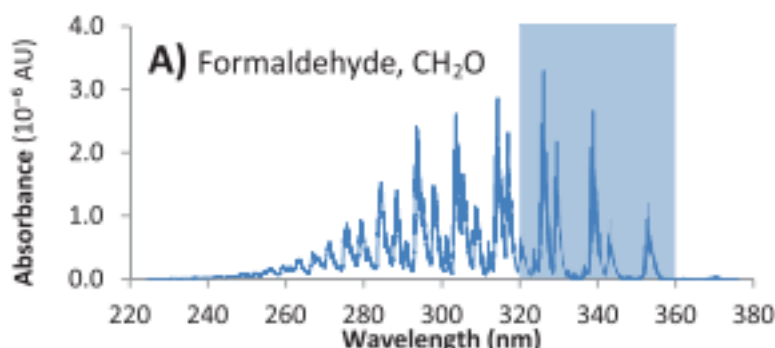


FIGURE 1.6: HCHO spectrum, with a typical band of wavelengths used for DOAS path measurements. This is a portion of an image from Davenport et al., 2015.

along with a typical band used to examine interference in the DOAS technique. One difficulty is that this interference is relatively small (HCHO is optically thin) and other compounds absorb light at similar wavelengths (Davenport et al., 2015).

FTIR and DOAS measurements have a range of uncertainties, including systematic and random measurement errors and uncertain apriori shape factors and water profiles (eg: Franco et al., 2015). Other types of measurement involve directly measuring the air, and determining chemical compounds through their physical properties. A proton transfer reaction mass spectrometer (PTR-MS) can be used to determine gas phase evolution of terpene oxidation products (Lee et al., 2006; Nguyen et al., 2014; Wolfe et al., 2016, eg.). This is done through analysis of mass to charge ratios (m/z) of ionised air masses which are then identified as chemical compounds. Nguyen et al., 2014 use and compare several instruments (including one which is PTR-MS based) in the analysis of isoprene and monoterpene products. A Gas Chromatography mass spectrometer (GC-MS) is also able to identify isoprene, monoterpenes, and their products Lerner2017; Nguyen et al., 2014, eg.

Other measurement techniques include chromatographic and fluorimetric methods, both of which differ widely from each other and the spectroscopic methods (Hak et al., 2005). Hak et al., 2005 examine a single air mass with 8 instruments using the four techniques (MAX-DOAS, FTIR, chromatographic, and fluorimetric), and show that reasonable agreements can be achieved. Generally the measurements were somewhat close, the five Hantzsch instruments agreeing to within 11% (after removing two potentially faulty measurements), although different calibration standards were used. Titration for the different calibration solutions could not be resolved, which may account for absolute offsets up to 30%. These differences and non-uniformities between measurements (even among identical instruments) are part of the reason HCHO does not have a consistent network for global measurements like those for GHGs or Ozone (Chevallier et al., 2012).

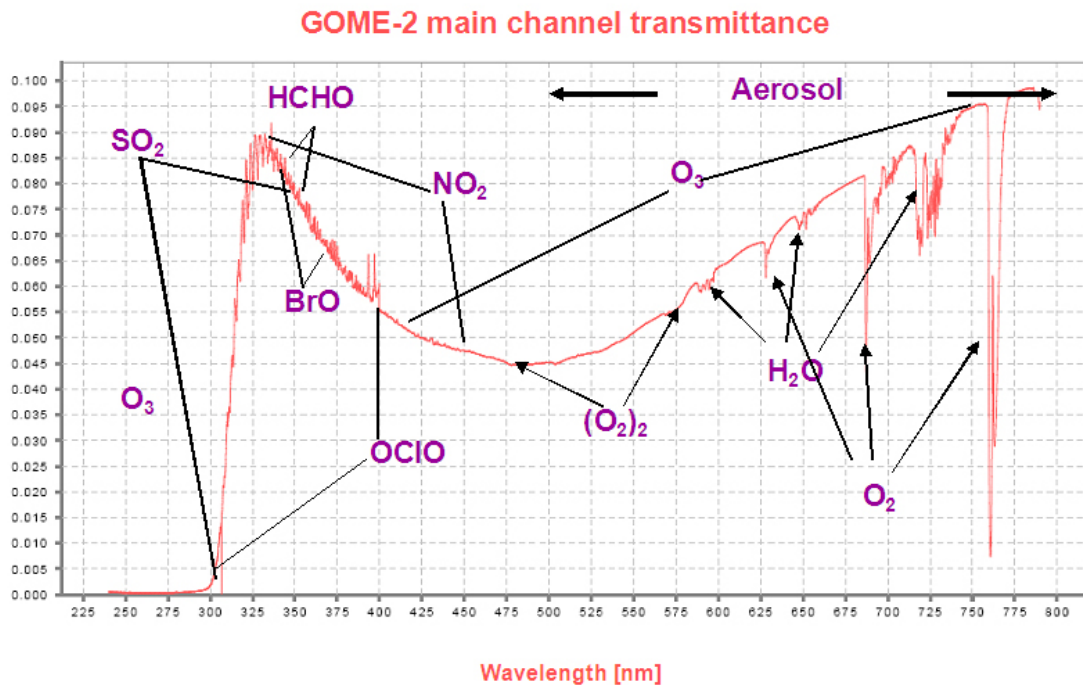


FIGURE 1.7: An example spectrum showing interferences used for species concentration measurements by GOME-2. Image by EUMETSAT and ESA (EUMETSAT, 2015).

Satellite measurements

Several satellites provide long term trace gas observations with near complete global coverage, including the ERS-2 launched in April 1995 which houses the GOME ultraviolet and visible (UV-Vis) spectrometer, the AURA launched in July 2004 which houses the OMI UV-Vis spectrometer, the MetOp-A and B launched in October 2006 and September 2012 respectively both housing a GOME-2 UV-Vis spectrometer. These satellites are on Low Earth Orbit (LEO) trajectories and overpass any area up to once per day. Satellites can use DOAS techniques with radiative transfer calculations on solar radiation absorption spectra to measure column HCHO. An example of a spectrum retrieved from the GOME-2 instrument is given in figure 1.7.

In conjunction with atmospheric chemistry and radiative models, satellite measurements can be used to quantify the abundance of several chemical species in the atmosphere. Isoprene is hard to measure directly due to its short lifetime and weak spectral absorption, instead HCHO is often used as a proxy (Millet et al., 2006; Fu et al., 2007; Dufour et al., 2008; Marais et al., 2012; Bauwens et al., 2013; Kefauver, Filella, and Peñuelas, 2014; Bauwens et al., 2016). This leads to a method of isoprene emissions estimation termed top-down (as opposed to bottom-up estimates). The existence of satellite data covering remote areas provides an opportunity to improve VOC emissions estimates leading to more robust models of global climate and chemistry. Satellite data allows us to verify large scale models of natural emissions, and their subsequent chemistry.

1.5 Atmospheric Chemistry Modelling

Models can fill the gaps (both spatial and temporal) in measurement records, and can help us improve our understanding of the world around us. They are used ideally to steer us away from unsustainable pollution by showing us the future outcomes resulting from our emissions, from small to large scales. They can be used to increase measurement accuracy (for instance in satellite measurements) and determine where we lack information, while also checking the performance of new instruments. Precisely representing various chemicals and reactions in the atmosphere allows efficient mitigation of pollution, since we can compare scenarios against one another. Models can always be expanded to include new compounds or processes, however validation is always necessary. Currently they require improved isoprene emissions and subsequent chemistry understanding for effective air quality determination (Marvin et al., 2017).

Atmospheric chemical models provide a simulation of chemical densities and transport over time, through the atmosphere. They require many inputs (such as wind velocities) in order to accurately represent scenarios or regions on earth. Models of emissions are often used as drivers for atmospheric chemistry models, which require initial and boundary conditions in order to run. Chemistry in the atmosphere is a complex system of coupled reactions and dynamics, which can be solved using numerical partial differential equation solvers.

Chemical Transport Models (CTMs) simulate production, loss, and transport of chemical species. This is generally calculated using one or both of the Eulerian (box) or Lagrangian (puff) frames of reference. CTMs normally solve the continuity equations simultaneously with chemical production and loss for chemicals under inspection. The continuity equations describe transport of a conserved quantity such as mass, which, solved together with production and loss of a chemical can provide detailed simulations of natural processes.

The general continuity equation links a quantity of a substance (q) to the field in which it flows and can be described by the formula:

$$\frac{\partial \rho}{\partial t} + \nabla \cdot j = \sigma$$

where ρ is density of q in the field, t is time, ∇ is divergence, j is the flux (q per unit area per unit time entering or leaving the field), and σ is the generation or loss of q per unit volume per unit time.

The type of model best suited to modelling the entire earth uses the Eulerian frame of reference, where the atmosphere is broken up into 3-D boxes with densities and transport calculated and stored for sequential steps in time at each location. The mass balance equation must be satisfied in any realistic long term box model and is as follows:

$$\begin{aligned} \frac{dm}{dt} &= \sum \text{sources} - \sum \text{sinks} \\ &= F_{in} + E + P - F_{out} - L - D \end{aligned}$$

where m is mass of a chemical, E and D are emission and deposition, P and L are

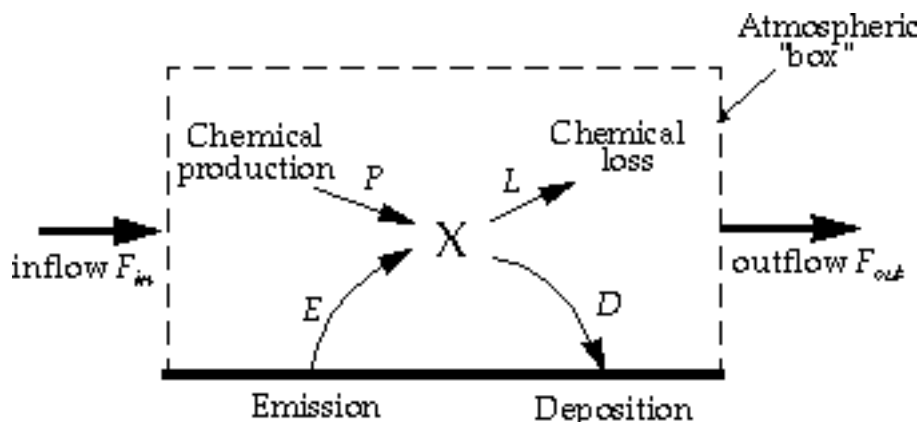


FIGURE 1.8: Standard box model parameters, image taken from Jacob, 1999.

production and loss, and F is chemical transport in and out, as shown in figure 1.8. Many chemical species interact with each other through production and loss. Any large chemical model will solve this mass balance equation over highly coupled arrays of partial differential equations, which becomes computation time expensive when looking at many species or resolved over many grid-boxes.

Contemporary models generally use mathematical differential solving tools of various complexity to solve chemical equations and reaction rates (often called chemical mechanisms) in order to predict an environments evolution over time. Different solvers may be slower or faster and more suited to particular situations based on the stability of the equations and systems involved, and chemical mechanisms may vary in how many reactions and chemicals are listed and grouped together. For example: Since $[O] \ll [O_3]$ the chemical family Ox ($Ox \equiv O + O_3$) can be used to simplify chemistry simulations and approximate O_3 concentrations (Brasseur and Jacob, 2017, Chapter 3). Zhang et al., 2012 examine the outputs from a regional model (WRF/Chem) using three different chemical mechanisms, and they show some model output sensitivity to the choice of mechanism.

1.5.1 Box models

Box models are much smaller scale than global CTMs, examining one uniform environment with many parametrisations such as transport and emissions. Box models can be used to check chemical mechanisms in specific scenarios, such as high or low NO_x environments. Marvin et al., 2017 use a box model matching conditions in southeast USA to evaluate isoprene mechanisms from several models. A box model involves modelling chemistry in a singular set of conditions without transport or any spatial gradients.

By allowing for interactions between boxes this concept can be extended to multiple-box models. These are simply multiple instances of single boxes with the addition of transport between them, which requires meteorological fields such as wind velocities and turbulence. The meteorology fields can be modelled, and/or input as parameters.

1.5.2 Emissions

There are two commonly used ways of estimating isoprene emissions, top-down or bottom-up. Bottom-up emission estimates generally model the flora and events which emit isoprene, like Eucalypts, factories, shrubs, etc. They use various properties of the emitters in order to estimate how much isoprene is being produced. Some of these properties include leaf areas, speciated responses to sunlight and temperature, moisture stress, etc (Guenther et al., 1995; Guenther et al., 2006). Understanding how much isoprene is emitted, when and by what, is complicated. One frequently used bottom up emissions model is the Model of Emissions of Gases and Aerosols from Nature (MEGAN, Guenther et al., 1995). Since little data exists with which to verify many of these bottom-up emission inventories, they can be uncertain on a large scale.

In many CTMs the isoprene emissions are calculated separately (for example by running MEGAN), and then used as boundary conditions (EG: Guenther et al., 2006). This can speed up calculations as the transport and concentrations can be simulated in various conditions without recalculating the emissions. Trace gases with short lifetimes and complex chemistry such as isoprene are often hard to measure which makes verifying model estimates difficult.

Bottom up models of VOC emissions are sensitive to parameters. For example Stavrakou et al., 2014 examined modelled Asian emissions and altered model parameters for temperature, plant type emission factors, incoming solar radiation (insolation) intensity, land use changes, and palm tree forest expansion. Changes were constrained by a network of radiation measurements and some experiments with south east Asian forest emissions - and led to reduction in isoprene emissions by a factor of two over the region.

Marais et al., 2014 examine factors affecting isoprene emissions, showing their sensitivity to environmental factors. Their work used MEGAN (Guenther et al., 1995) and GEOS-Chem to look at how these factors affect surface ozone and particulate matter in Africa. One of the important uncertainties seen in MEGAN within this work is the isoprene emissions due to plant type. Canopy level isoprene measurements are made using relaxed eddy accumulation (REA) at several sites in Africa. One plant type near a measurement site emits more than other species and it's actual distribution on a larger scale is completely unknown - leading to possible overestimations in MEGAN. Current emissions estimates require more validation against observations, and recently a comparison of two major VOC models (MEGAN and ORCHIDEE) was undertaken by Messina et al., 2016 reiterating this requirement. In their work they examine model sensitivities and show that the important parameters are leaf area index (LAI), emission factors (EF), plant functional type (PFT), and light density fraction (LDF). There is high uncertainty in LAI and EF, which require more or improved measurements at the global scale. LDF parameterisation needs improvement and these models require more PFTs. Global emissions inventories like MEGAN often have large areas based on extrapolations which can introduce uncertainties (Miller et al., 2014).

1.5.3 Uncertainties?

Here I will attempt to list and partially explain the major uncertainties models have in relation to VOCs, SOAs, and ozone. TODO: Is this a good idea or should I put any

pertinent uncertainties with the associated work/descriptions?

Emissions Inventories

Using different emissions inventories in an ACM can have large impacts on the simulation. Natural (biogenic or pyrogenic) and human driven (anthropogenic) emissions often drive a large fraction of atmospheric oxidation and radical chemistry, especially in the continental boundary layer. Zeng et al., 2015 examine the affects on CO and HCHO when running simulations with two different inventories. TODO: find where I took notes about Zeng2015 and put them here.

It is important to note that many estimates of isoprene emission are based on a few algorithms which can depend greatly on input parameters (Arneth et al., 2008; Niinemets et al., 2010). Arneth et al., 2008 argue that this monopoly of emissions estimates may be leading us to an incorrect understanding of isoprene chemistry. Yue, Unger, and Zheng, 2015 has shown that this is still a problem by looking at land carbon fluxes and modelling the sensitivity to VOC emissions estimates using two independent models of VOC emission. One model is photosynthesis based and estimates isoprene emissions using electron transfer energies and leaf physiology (Niinemets et al., 1999), while the other (MEGAN) uses the light and canopy temperature ((Guenther et al., 1995; Arneth et al., 2007) TODO: Read Arneth et al., 2007; Unger et al., 2013). Both are sensitive to light and temperature parameterisations.

Resolution

GEOS-Chem simulations are somewhat sensitive to the resolution at which you run. For example: Wild and Prather, 2006 show that reduced resolution increases OH concentrations and ozone production rates. Christian, Brune, and Mao, 2017 find small changes in OH (< 10%) in OH, HO₂ and ozone concentrations local to the north american arctic, when changing from 4 by 5 to 2 by 2.5 °resolution, however they continue at lower resolution to save computational time.

For many global scale analyses, errors from resolution are less important than those from chemistry, meteorology, and emissions (Christian, Brune, and Mao, 2017). Many models lack in-situ measurements with which to verify their chemical mechanisms, leading to large discrepancies, as seen in Marvin2017a TODO: briefly talk about Marvin2017a takeaways. Christian, Brune, and Mao, 2017 used GEOS-Chem v9-02, with 4° × 5° resolution, and while the low resolution adds errors in OH concentrations and O₃ production rates, the errors from chemistry, meteorology, and emissions are much larger.

Chemistry mechanisms

There is still much work to be done in models to correctly simulate the precursor emissions and processes which lead to HCHO. Often HCHO is used as a way of checking if these precursors are correctly modelled since HCHO measurements are more readily available (for instance from satellites). GEOS-Chem has recently been analysed for ozone and oxidant (OH and HO₂) sensitivity to the processes within the model along with inputs which drive it (Christian, Brune, and Mao, 2017). Christian, Brune, and

Mao, 2017 found that GEOS-Chem ozone was most sensitive to NO₂ photolysis, the NO₂ + OH reaction rate, and various emissions.

Marvin et al., 2017 suggest that isoprene mechanisms in several contemporary models (including GEOS-Chem) are inadequate. They show that for a specific measurement campaign, the HCHO concentrations are underestimated in a way that can not be easily fixed through rate constant changes. Recently Marvin et al., 2017 compared five global ACMs isoprene mechanisms by evaluating simulated HCHO mixing ratios compared to in situ measurements from the Southeast Nexus (SENEX) aircraft campaign (in southeastern USA). They compared five models (GEOS-Chem, CB05, CB6r2, MCMv3.2, and MCMv3.3.1) and found all of them underestimated the HCHO concentrations (by 15 – 30%).

Another important factor in determining the yield of HCHO and other products from BVOCs is the local concentration of NO_x. Travis et al., 2016 show how modelled surface ozone is overestimated due to high estimates of NO_x emissions, which affect oxidative capacity and VOC reactions.

Understanding of OH production/recycling in low NO conditions has been improved (see section 1.3.3), however many observations of OH were still quite underpredicted in models (Mao et al., 2012). Mao et al., 2012 showed how traditional OH measurements may be overestimated due to VOC oxidation. They looked at measurements in a remote forest in California and found that the instruments were generating OH internally. Nguyen et al., 2014 also see this VOC oxidation interference in measurements using a gas chromatographer (GC) with an equipped flame ionisation detector (FID). This lends more credence to the current understanding of VOC oxidation as it closed the gap between measurements and model predictions (Mao et al., 2012).

Clouds

One of the major uncertainties in chemical, climate, radiation, and weather models is cloud formation and dynamics. Clouds are remarkably complex at a much finer scale than can be accurately modelled by global chemistry models (with current processing power). Globally over half (50-60%) of the world is covered by clouds, with ~ 10% of them being rain-clouds (Kanakidou et al., 2005). Wet scavenging performed in clouds not only depends on large scale cloud processes, but also on the micro-physics of aerosols being scavenged, differing between aerosol sizes and hygroscopic properties.

Soil Moisture

Rowntree and Bolton, 1983 show how quickly soil moisture anomalies affect rainfall and other weather systems, while Chen and Dudhia, 2001 specifically show how important fine scale soil moisture information is when modelling land surface heat flux, and energy balances. Modelled emissions are sensitive to soil moisture, especially near the soil moisture threshold (or wilting point), below which trees stop emitting isoprene and other VOCs completely as they can no longer draw water (Bauwens et al., 2016). MEGAN accounts for soil moisture by applying it as an emission factor (EF) which scales the emission rate of various species.

Droughts affects can be difficult to measure, as it is a multi-scale problem which affects various aspects of the land-air interface including plant emissions and dry deposition (Wang et al., 2017). The Standardised Precipitation Evapotranspiration Index (SPEI) is a measure of drought using TODO *SPEI Drought Index*. This product covers 1901 - 2011, and uses the average over that period as the background, in order to compare drought stressed regions against those with sufficient or excess water *SPEI Drought Index*.

1.6 Australia and the southern hemisphere

Australia has a unique climate, along with soil moisture, clay content and other important properties which affect VOC emissions. These properties are poorly understood in Australia due to the continents size and the relative sparsity of population centres, which make many areas very difficult or expensive to reach. In Australia most long term air quality or composition measurements are performed in or near large cities. Australia is dominated by areas with little anthropogenic influence and no ground based measurements of the natural emissions taking place (VanDerA et al., 2008). Due to the lack of in-situ ground based measurements, estimates of VOC emissions are uncertain, with large scale extrapolation required Millet et al., 2006. Since many Australian cities are on the edge of regions with rich VOC emissions, it is very important to clarify the quantity, type, and cause of VOC emissions. Understanding of emissions from these areas is necessary to inform national policy on air pollution levels.

The trees in Australia are diverse, a great summary is provided by ABARES using the national forest inventory at <http://www.agriculture.gov.au/abares/forestsaustralia/australias-forests>. Figure 1.9 shows the different forest types and their locations within Australia, highlighting that much of our forested lands are near population centres along the east coast. 16% of Australia is covered by forest, most (75%) of which is Eucalyptus.

Fire emissions include a range of chemicals and each year the affects of fire or burning seasons blanket the northern and southern hemispheres independently. Biomass burning in southern Africa and South America has previously been shown to have a major influence on atmospheric composition in Australia (Oltmans et al., 2001; Gloudemanns et al., 2007; Edwards et al., 2006), particularly from July to December (Pak et al., 2003; Liu et al., 2016a). The ocean plays a role in VOC emissions as well, the Asian region is shown to have a strong correlation with the Oceanic Niño Index (ONI), with positive anomalies associated with El Niño (Stavrakou et al., 2014).

Guenther et al., 2006 estimated that the Australian outback is among the worlds strongest isoprene emitters with forests in SE Australia having emission factors greater than $16 \text{ mg m}^{-2} \text{ h}^{-1}$ (see figure 1.10). Measurement campaigns in SE Australia have since cast doubt on the emission factors used by MEGAN, as the Eucalyptus trees and soil moisture were poorly studied Emmerson et al., 2016. These emissions factor estimates are not well verified and measurements of isoprene (or other BVOC) emissions barely cover Australia either spatially or temporally. However, comprehensive coverage of one high yield product (HCHO) in the atmosphere over Australia exists in the form of satellite measurements.

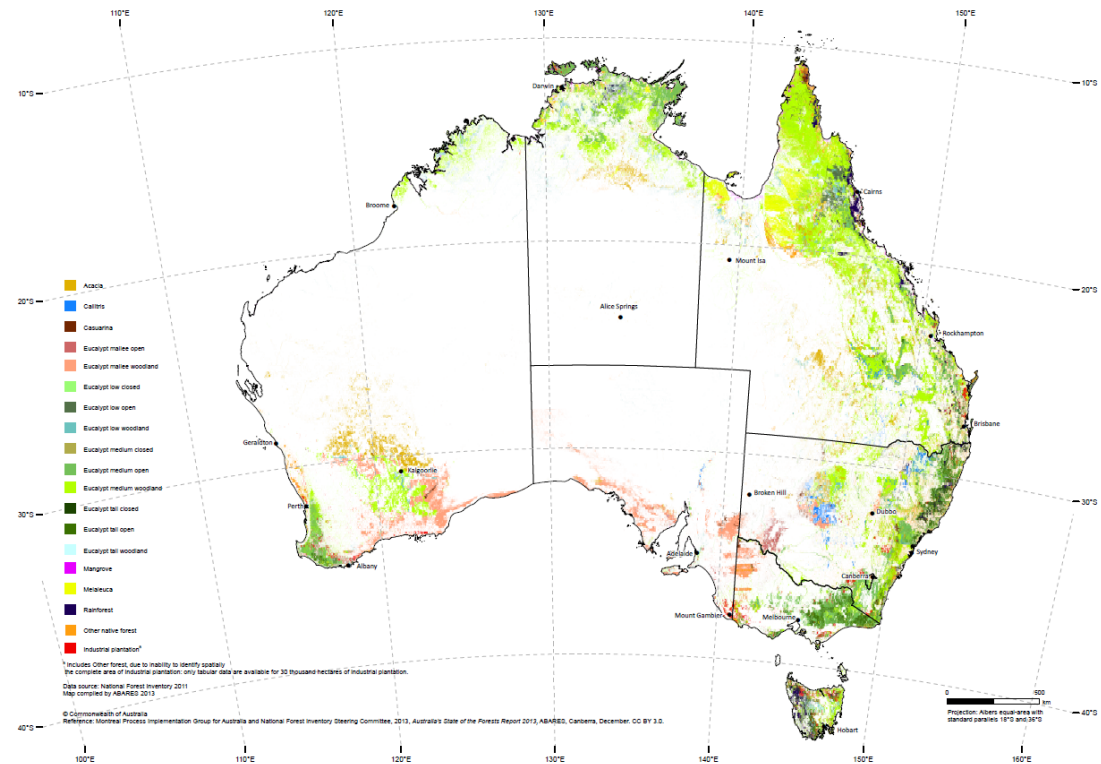


FIGURE 1.9: Forest types in Australia (<http://www.agriculture.gov.au/abares/forestsaustralia/australias-forests>)

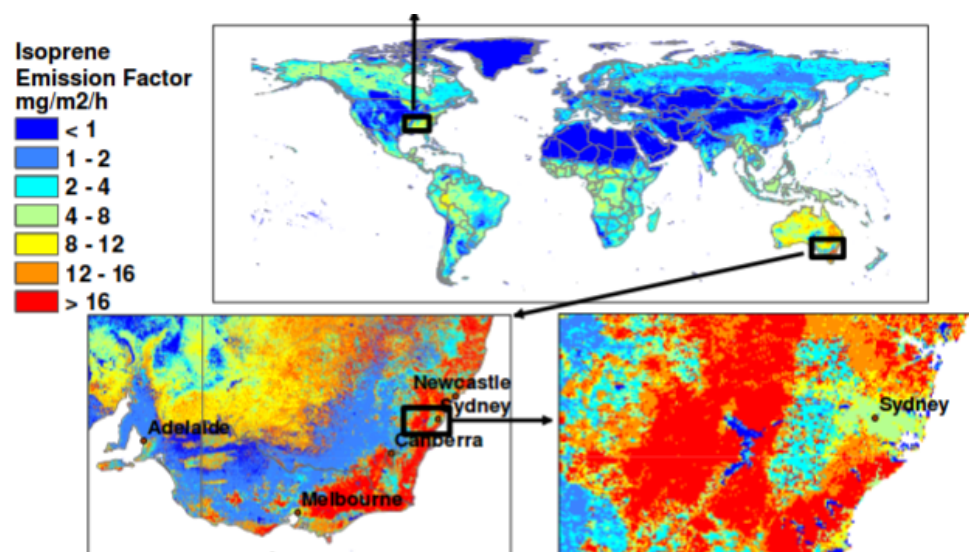


Fig. 2. Global distribution of landscape-average isoprene emission factors ($\text{mg isoprene m}^{-2} \text{ h}^{-1}$). Spatial variability at the base resolution ($\sim 1 \text{ km}$) is shown by regional images of the southeastern U.S. and southeastern Australia.

FIGURE 1.10: Part of a figure from Guenther et al., 2006 showing global isoprene emission factors.

1.6.1 Ozone

Ozone levels over Australia are relatively low, however it remains unclear how much we would expect this to change in the future as relatively little is known about precursors and influx for the continent. Australian air quality is monitored independently within each state, using several metrics. These metrics are measured by varying numbers of monitoring stations in each state. In New South Wales (NSW) the metrics used to determine air quality are: particulate matter (PM), O₃, CO, NO₂, SO₂, and visibility. An air quality index equal to the worst of these metrics is used for NSW as shown at <http://www.environment.nsw.gov.au/aqms/aqitable.htm>. Similar methods are used in other states to get an idea of air quality. Measurement stations are generally located in population centres, and don't regularly measure precursor emissions. This is an important omission as naturally emitted precursor gases often get transported into cities where they affect air quality through production of O₃ and other pollutants.

Generally STT over Australia affects the upper troposphere only, however ozone enhancements can reach quite low during heavy storms and cyclonic weather patterns (Alexander et al., 2013).

1.6.2 VOCs

Bottom up inventories of VOCs remain largely uncertain due to extensive extrapolation over plant functional types, changing land cover, and parameterised environmental stressors (Guenther et al., 2000; Kanakidou et al., 2005; Millet et al., 2006). VOC emission estimates are highly sensitive to many factors, several of which are not well characterised in Australia (Sindelarova et al., 2014; Bauwens et al., 2016). Changes in parameterisation of soil moisture in the MEGAN lead to massive changes in Australian isoprene emission estimates (Sindelarova et al., 2014). Over Australia MEGAN has problems involving unpublished plant functional types and their emissions, as well as poorly optimised soil moisture parameterisation (Emmerson et al., 2016).

Australia has the potential to be a major hotspot of isoprene emissions according to Guenther et al., 2006; Guenther et al., 2012, which shows heavy emissions factors in the region. Although recent work suggests that some Australian eucalypts may not be as egregious isoprene emitters as once thought Emmerson et al., 2016. Emissions in MEGAN are based on plant functional types, which can vary heavily even within species. TODO: more on Muller2008 Australia also lacks a clear estimate of emitted monoterpenes.

Emmerson et al., 2016 analyse EF sensitivity of a high resolution model of atmospheric chemistry over southeast Australia, comparing isoprene and monoterpene emissions against 4 separate campaigns. They show that the effect on total emissions is roughly linear and that no blanket EF changes are appropriate for all regions/seasons. They also mention that Australian eucalypt emissions are based on samples from young trees, which may emit more isoprene than older trees. Emmerson et al., 2016 suggest that monoterpenes may be emitted in similar quantities to isoprene, with more measurements required to determine if this is so. They compare emissions estimates from MEGAN against data from several field campaigns and see overestimated isoprene emissions, as well as underestimated monoterpene emissions.

Their work suggests that MEGAN estimates of isoprene emissions may be 2-6 times too high, and monoterpene emissions \sim 3 times too low over southeast Australia.

This problem is even more pronounced in Australia due to poor characterisation, or because emission factors are based on northern hemispheric data. Many plant emissions rates have not been published, such as those for any Australian acacias. Additionally soil moisture is not well quantified which has a large effect on emissions. Müller et al., 2008 show how isoprene is poorly captured by the MEGAN model and analyse the affect of changing the soil moisture parameter, which can reduce the overall bias for Australia. Sindelarova et al., 2014 show reductions in modelled Australian isoprene emissions of 50% when incorporating soil moisture in MEGAN estimates. Uncertainties in isoprene emissions could explain why models of HCHO over Australia are poor at reproducing satellite measurements (Stavrakou et al., 2009).

Improvements to emissions models require improved understanding of regions and their behaviour. Inaccuracies can arise due to lack of data, such as the large and sparsely measured Australian outback. MEGAN has been shown to overpredict isoprene and underpredict monoterpene emissions in southeast Australia, with peaks and troughs captured but not at the right magnitude (Emmerson et al., 2016). MEGAN output in Australia is adversely affected by poor emission factor estimation. An example can be seen in Müller et al. (2008) where MEGAN overestimates isoprene in northern Australia. Underestimates of monoterpenes may be due simply to underestimated emission rates for many Eucalypt species (Winters et al., 2009).

1.6.3 Measurements

TODO: Brief overview of all the measurement campaigns, pointing to Modelling and Data chapter for more details. There are relatively few measurements of isoprene in the southern hemisphere, including MUMBA(TODO CITE), SPSS(cite), and that girl from Macquarie University with an instrument in the daintree rainforest(TODO CITE, DESCRIBE). For details on the MUMBA campaign see Section ???. An airflight campaign (HIPPO) measuring isoprene was also performed in 2009-2011? TODO: ask Jenny re this one.

A particulate and air quality measurement campaign took place in Sydney using PTR-MS and GC-FID, for details see Section ??.

One method of measuring ozone in the troposphere and stratosphere is by releasing weather balloons (with attached ozone detectors) which take readings as they rise up to around 30 km, giving a vertical profile of concentrations. Since 1986, Lauder, New Zealand (45° S, 170° E) has released ozonesondes allowing a multi-decadal analysis of ozone concentrations over the city (Brinksma et al., 2002). Kerguelan Island (49.2° S, 70.1° E), also has a record of ozonesonde profiles, which are directly in the path of biomass burning smoke plumes transported off shore from Africa (Baray et al., 2012). SHADOZ is the southern hemispheric additional ozone project, which have released sondes from 15 sites at different times <http://tropo.gsfc.nasa.gov/shadoz/>.

A smaller network of ozonesonde release sites is operated by TODO: get details for sondes I use in ozone chapter.

1.7 Aims

TODO: outline of aims here (FIND THESE THEY ARE SOMEWHERE)

One of the aims in this thesis is to use the available satellite measurements to improve the estimates of isoprene emissions in Australia. Satellites which overpass daily record reflected solar (and emitted terrestrial) radiation, and give us measurements over all of Australia. Combining satellite data with model outcomes provides a platform for the understanding of natural processes which is especially useful over Australia. Due to the low availability of in-situ data over most of the Australian continent, a combination of the models with satellite can fill the gap of understanding of emissions from Australian landscapes. Improved emissions estimates will in turn improve the accuracy of CTMs, providing better predictions of atmospheric composition and its response to ongoing environmental change.

Calculation of isoprene to HCHO yields over Australia is required to create top-down estimates. This requires among other things an idea of which VOCs are present and their yields of HCHO. The technique of determining isoprene emissions from satellite detected HCHO is called satellite inversion. **Another aim to this end is to run and become familiar with GEOS-Chem in order to determine Australian emissions and yields, and the importance of the relevant parameters.** Soil moisture plays an important role in VOC emissions, as trees under stress may stop emitting various chemicals. This is especially true for Australia due to frequent droughts and wildfires. The argument for improved understanding of land surface properties, specifically soil moisture, is an old one(Mintz, 1982; Rowntree and Bolton, 1983; Chen and Dudhia, 2001).

To improve understanding of ozone over the southern hemisphere including Australia. Meteorology and precursor emissions are the largest drivers of tropospheric ozone concentrations, and an improved understanding of their effects in Australia would be facilitated by an analysis of STT as well as more confidence in the emitted precursors.

Chapter 2

Data and Modelling

2.1 Introduction

Models of ozone in the atmosphere are used broadly for international assessments of ozone related emissions (Young et al., 2017). Young et al., 2017 summarise current global ozone modelling standards and the metrics and processes used to evaluate these models. They show how models can be used to improve measurements, estimate concentrations in regions not sampled, and allow analysis of other processes which involve ozone (such as radiation).

2.2 List of runs and outputs used in my work TODO: good place for this?

TODO: Go through work process and clarify these items

2.2.1 GEOS-Chem

1. UCX
 - (a) Satellite output (1300-1400LT)
 - (b) Create shape factors for AMF recalculation in OMI
2. Tropchem (standard)
 - (a) satellite output, daily tracer averages
 - (b) Recreate the AMFs for OMI when running code from Dr. Paul Palmer, modified by Dr. Luke Surl.
 - (c) Combined with an identical run where isoprene emissions are halved in order to determine smearing.
 - (d) TODO: Compare total yearly isoprene emissions before and after new estimate.
3. Tropchem(isoprene emissions halved)
 - (a) Satellite output used to determine smearing.
4. Tropchem(biogenic emissions only, all other inventories turned off)

- (a) Satellite output, hourly biogenic emissions from MEGAN
- (b) Used to determine yield for new emissions estimates
- (c) TODO: compared to run with updated emissions

NB: for non-UCX runs, satellite output was modified to include tropopause height

2.2.2 CAABA/MECCA

2.2.3 Reading Data

CAABA/MECCA outputs

The box model can output in netcdf or text format, TODO: which way am I better off ? Text output from CAABA/MECCA was read using tailored python scripts modified from code written by dr. Luke Surl. Dr. Luke Surl also wrote the code which implements calculations of yield from runs using isoprene injections as described in Section ?? TODO: update to more specific reference.

GEOS-Chem Satellite output

HEMCO diagnostics

In order to get hourly MEGAN modelled isoprene emissions, HEMCO (the module of GEOS-Chem dealing with emissions inventories) diagnostic output was created. When working with globally gridded data, handling local time offsets becomes more important. The hourly output emissions of isoprene is saved using GMT, which needs to be offset based on longitude in order to retrieve local time. I do this by setting up a latitude by longitude array which matches the horizontal resolution of the data, filling each gridbox with its local time offset. This offset is determined as one hour per 15 degrees (since 360 degrees is 24 hours), and then used to retrieve global data at any specific local time. The retrieval of a daily local time global array is done by index matching the GMT+LT (modulo 24) with the desired hour on this grid over the 24 GMT hours.

2.3 GEOS-Chem

GEOS-Chem is an atmospheric chemical model (ACM), using a 3-D grid of boxes with transport driven by the GEOS meteorological model and chemistry calculated in each box independently. Many of these terms are described in Section ??.

GEOS-Chem uses many boxes covering the globe, each with chemistry and dynamic meteorological conditions. Different meteorological conditions such as wind and air pressure need to be handled within each box. GEOS-Chem has a meteorological model coupled to a chemical model, which simulates the world in a three dimensional grid of connected boxes.

GEOS-Chem is a well supported global, Eulerian CTM with a state of the science chemical mechanism, with transport driven by meteorological input from the Goddard Earth Observing System (GEOS) of the NASA Global Modeling and Assimilation Office (GMAO). GEOS-Chem simulates more than 100 chemical species from the

earth's surface up to the edge of space (0.01 hPa) and can be used in combination with remote and in-situ sensing data to give a verifiable estimate of atmospheric gases and aerosols. It was developed, and is maintained, by Harvard University staff as well as users and researchers worldwide. Several driving meteorological fields exist with different resolutions, the finest at 0.25 by 0.3125° horizontally at 5 minute time steps with 72 vertical levels.

Global CTMs are often run using one or several emission models (or the output from them) to determine boundary conditions for many gridboxes. TODO: is this the case? Doesn't GEOS-Chem have coupled chemistry and meteorology? Check the wiki. GEOS-Chem has boundary conditions based on several meteorological and emissions inventories, the following are the versions of theses used by GEOS-Chem v 10.01. Meteorological fields can be driven by NASA's GEOS-5 data ($0.5^\circ \times 0.666^\circ$) (Chen et al., 2009), which exists up to 2013, or GEOS-FP data ($0.25^\circ \times 0.3125^\circ$). Fire emissions come from the GFED4 product (Giglio, Randerson, and Van Der Werf, 2013). Anthropogenic VOC emissions come from the EDGAR inventory, while biogenic VOC emissions are coupled to the MEGAN model TODO:cites. The estimated biogenic VOC emissions are important for accurately simulating chemistry within models, as discussed in Sections ?? and 1.5.3.

2.3.1 GEOS-Chem isoprene modelling

Outline

The isoprene reactions simulated by GEOS-Chem were originally based on Horowitz et al., 1998. This involved simulating NO_x , O_3 , and NMHC chemistry in the troposphere at continental scale in three dimensions, with detailed NMHC chemistry with isoprene reactions and products. The mechanism was subsequently updated by Mao et al. (2013), who change the isoprene nitrates yields and add products based on current understanding as laid out in Paulot et al. (2009a) and Paulot et al. (2009b). Further mechanistic properties, like isomerisation rates, are based on results from four publications: citeCrounse2011,Crounse2012,Peeters2010,Peeters2011. (TODO: check abstracts Peeters papers). Crounse et al., 2011 examines the isomerisations associated with the oxidation of isoprene to six different isomers (ISO_2) formed in the presence of oxygen: isoprene $+ \text{OH} \rightarrow \text{O}_2 \text{ ISO}_2$. They determine rates and uncertainties involved in these reactions, and study the rate of formation of C_5 -hydroperoxyaldehydes (HPALDs) by isomerisation. Crounse et al., 2012 examine the fate of methacrolein (MACR), one of the products of isoprene oxidation. Prior to this work MACR oxidation chamber studies were performed in high NO or HO_2 concentrations, giving peroxy lifetimes of less than 0.1 s. In most environments this is not the case, and MACR products over various NO concentrations and peroxy radical lifetimes are determined in their work. Peeters and Muller, 2010 examine photolysis of hydroperoxy-methyl-butenals (HPALDs, produced by isoprene isomerisation), which regenerates OH levels in areas with high isoprene emissions. Additionally, photolysis of photolabile peroxy-acid-aldehydes creates OH and improved model agreement with continental observations. The OH and HPALD interactions are central to maintaining the OH levels in pristine and moderately polluted environments, which makes isoprene both a source and a sink of OH TODO: citation.

Formation of isoprene nitrates have an effect on ozone levels through NO_X sequestration, and the yields and destinies of these nitrates is analysed in Paulot et al. (2009a). They use anion chemical ionization mass spectrometry (CIMS) to determine products of isoprene photooxidation. In a chamber with clean air and high NO concentrations, isoprene photooxidation is initially driven by OH addition, followed by NO_X chemistry (150 min - 600 min), and finally HO_X dominated chemistry. The yields of various positional isomers of isoprene nitrates is estimated, and pathways of their oxidation products is shown and used in the GEOS-Chem isoprene mechanism (Paulot et al., 2009a; Mao et al., 2013).

In low NO_X conditions, isoprene oxidises to yield 70% hydroxyhydroperoxides (ISOPOOH), which then oxidises to create dihydroxyperoxides (IEPOX) with OH recycling maintaining the OH levels in the atmosphere (Paulot et al., 2009b). In older models isoprene produced ISOPOOH which then titrated OH, however, the loss of OH has not been seen in measurements (Paulot et al., 2009b; Mao et al., 2013). The isoprene mechanism in GEOS-Chem has been updated to include OH regeneration from oxidation of epoxydiols and slow isomerisation of ISOPO₂ (Mao et al., 2013).

ISOPN can be oxidised (by OH) to form nitrated organic products (Paulot et al., 2009a). In low NO_X ISOPOO reacts with HO₂ (producing hydroxy hydroperoxides, ISOPOOH), RO₂ (producing mainly MACR, MVK, and HCHO), or isomerises (1,5-H shift producing MACR, MVK, HCHO, or 1,6-H shift producing hydroperoxyenals HPALDs). ISOPOOH can be oxidised (by OH) to produce epoxydiols (IEPOX), precursors to SOA (Paulot et al., 2009b). HPALDs can photolyse to regenerate OH and small VOCs (Wolfe2012; Crounse et al., 2011; Jozef et al., 2014) TODO: Check out crounse2011. See section 1.3.3 for more information.

Under high NO_X conditions, isoprene undergoes OH addition at the 1 and 4 positions, becoming β (71%) or δ (29%) hydroxyl peroxy radicals (ISOPO₂). The β -hydroxyl reacts with NO_X and produces HCHO (66%), methylvinylketone (40%) (MVK), methacrolein (26%), and β -hydroxyl nitrates (6.7%) (ISOPNB). The δ -hydroxyl reacts with NO to form δ -hydroxyl nitrates (24%) (ISOPND), and ISOPNB (6.7%). ISOPNB and ISOPND yield first generation isoprene at 4.7% and 7% respectively.

Under low NO_X conditions, ISOPO₂ may react with HO₂ to form ISOPOOH. In this case there is also production of HCHO (4.7%), MVK(7.3%), and MACR (12%). As stated in earlier; most ISOPOOH will form IEPOX (epoxydiols) after reacting with OH and lead to OH regeneration. The other mechanism in low NO_X environments is unimolecular isomerisation of ISOPO₂. This leads to production of hydroperoxyaldehydes (HPALDS), which generally photolyse and have an OH yield of 100%. Mao et al. (2013) show that a lower (factor of 50) rate constant for ISOPO₂ isomerisation leads to better organic nitrate agreements with ICARTT.

This update leads to more accurate modelling of OH concentrations, especially in low NO_X conditions common in remote forests. Prior to Mao et al. (2012), measurements of OH in high VOC regions may have been up to double the real atmospheric OH levels, due to formation of OH inside the instrument. Mao et al. (2012) examine an upgraded method of measurement, and compare these against a regional atmospheric chemistry model (RACM2), with the OH recycling updates from Paulot et al. (2009b) as discussed in prior paragraphs.

The updates to isoprene chemistry by Mao et al. (2013), and those shown in Crounse

et al., 2011; Crounse et al., 2012 are the last before version 11, which was not used in this work.

The full current mechanism is described online at http://wiki.seas.harvard.edu/geos-chem/index.php/New_isoprene_scheme.

Emissions from MEGAN

MEGAN is a global model with resolution of around 1 km, and is used to generate the BVOC emissions used in various global chemistry models such as GEOS-Chem. MEGAN uses leaf area index, global meteorological data, and plant functional types (PFTs) to simulate terrestrial isoprene emissions. The model includes global measurements of leaf area index, plant functional type, and photosynthetic photon flux density, from remote sensing databases (Kefauver, Filella, and Peñuelas, 2014). The various PFTs are used to generate emission factors which represent quantities of a compound released to the atmosphere through an associated activity. For example, an emission factor for isoprene within a forest would include the requirement of sunshine and suitable temperature. The schematic for MEGAN, taken from Guenther (2016), is shown in figure 2.1

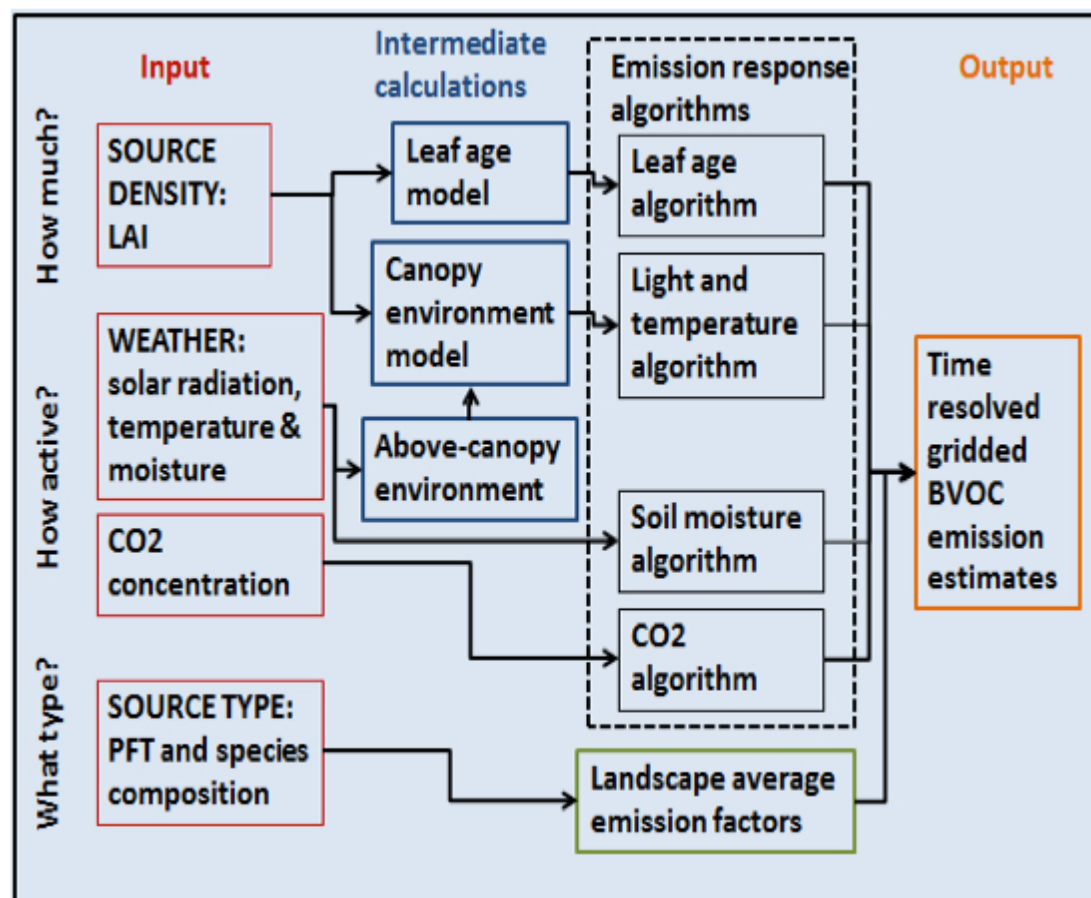


FIGURE 2.1: MEGAN schematic, copied from Guenther (2016)

MEGAN “is a modelling framework for estimating fluxes of biogenic compounds between terrestrial ecosystems and the atmosphere to account for the major known processes controlling biogenic emissions.” (Guenther et al., 2012). It allows parameterisation of various BVOC emissions, with descriptions given in Guenther et al., 2012. Instructions to run version 2.1 are available at http://lar.wsu.edu/megan/docs/MEGAN2.1_User_GuideWSU.pdf, and a version using the Community Land Model (CLM) is available at <http://www.cesm.ucar.edu>. It uses meteorological fields from the Weather Research and Forecasting (WRF) modelling system. Version 2.1 (updated from 2.0 (Guenther et al., 2006)) includes 147 species, in 19 BVOC classes, which can be lumped together to provide appropriate output for mechanisms in various chemical models.

MEGAN was developed as a replacement for two earlier canopy-environment emission models (BIES and GEIA), and initially included a simple canopy radiative transfer model, which parameterised sun-lit and shaded conditions through a canopy. Early models didn’t account for abiotic stresses, such as drought, prior rainfall and development processes, although these influenced species specific emissions by more than an order of magnitude (Niinemets et al., 1999). Isoprene emissions were based on temperature, leaf area, and light, but have since been updated to include leaf age activity (Guenther et al., 2000), and a leaf energy balance model (Guenther et al., 2006) in MEGANv2.0. This update included a parameter for soil moisture, to account for drought conditions, however this parameter is currently (as of version 2.1) not applied to isoprene (Sindelarova et al., 2014). Soil moisture effects on isoprene emission are very important, and can drastically affect estimates.

MEGAN has recently been analysed using 30 years of meteorological reanalysis information by Sindelarova et al., 2014. They estimate emissions of Biogenic VOCs (BVOCs) to be 760 Tg(C)yr⁻¹, 70% (532 Tg(C)yr⁻¹) of which is isoprene. This is similar to isoprene emission estimates from MEGAN itself, of 400-600 Tg(C)yr⁻¹ (Guenther et al., 2006). MEGAN emissions estimates are termed bottom-up, as opposed to top-down which are derived from satellite measurements of the products of various VOCs. Using GOME satellite HCHO and a Bayesian inversion technique to derive isoprene emissions, Shim et al., 2005 estimated global isoprene emissions to be $\sim 566 \text{ TgC yr}^{-1}$. This estimate is greater than initially thought and leads to decreased ($\sim 10\%$) simulated OH concentrations to $9.5 \times 10^5 \text{ molec cm}^{-3}$.

One of the important parameters in Australia is the soil moisture activity factor (γ_{SM}), which can have large regional affects on the isoprene emissions (Sindelarova et al., 2014; Bauwens et al., 2016). Generally if soil moisture is too low, isoprene emissions stop (Pegoraro et al., 2004; Niinemets et al., 2010), however in many Australian regions the plants may be more adapted to lower moisture levels. (TODO: Find cites for this - talk from K Emerson at Stanley indicated this) GEOS-Chem runs MEGANv2.1, which has three possible states for isoprene emissions based on the soil moisture (θ):

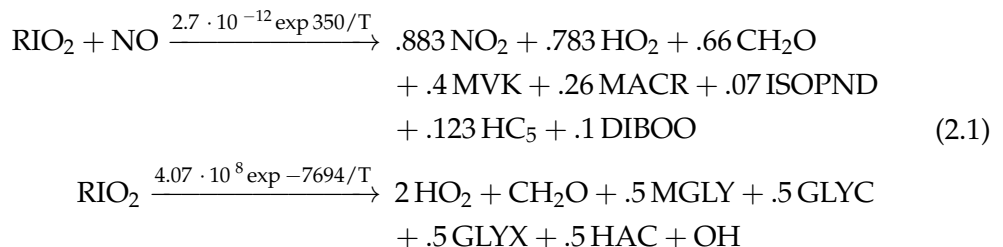
$\gamma_{SM} = 1$	$\theta > \theta_1$
$\gamma_{SM} = (\theta - \theta_w) / \Delta\theta_1$	$\theta_w < \theta < \theta_1$
$\gamma_{SM} = 0$	$\theta < \theta_w$

where θ_w is the wilting point, and θ_1 determines when plants are near the wilting point. The wilting point is set by a land based database from Chen and Dudhia (2001), while θ_1 is set globally based on Pegoraro et al. (2004).

In GEOS-Chem the isoprene emissions can be globally multiplied by a constant factor. By running the model two extra times, with the biogenic isoprene emissions turned off in one run and halved in another, while other parameters remain unchanged. These modified runs allow an estimate of model sensitivity to isoprene emissions and smearing impact as described in Section ??.

2.3.2 Chemical Mechanisms

Chemical reactions are turned into systems of differential equations (DEs) to be solved by the CPU for each gridbox in GEOS-Chem. Some of the important ones involving isoprene are copied here, including reaction rates in the form $k = A \exp -ER/T$.



2.3.3 Running GEOS-Chem (before isop?)

Installation and requirements

GEOS-Chem instructions for download, compilation, and running can be found in the user guide provided by Harvard: <http://acmg.seas.harvard.edu/geos/doc/man/>. In order to build and run GEOS-Chem a high-speed computing system is optimal, as globally gridded chemical calculations can take a long time to perform. I installed GEOS-Chem onto a suitably configured workspace on the National Computational Infrastructure (NCI, <http://nci.org.au/>). This workspace included access to compilers and libraries which are needed to build the Fortran based GEOS-Chem source code, and IDL, Python, and various editors and scripting languages to read, run, edit, and analyse both GEOS-Chem and its output.

After downloading GEOS-Chem, the code can be compiled with different options for resolution and chemical mechanisms.

Outputs

There are several outputs or diagnostics available from GEOS-Chem. GEOS-Chem models concentrations using a 15 minute time-step, however to save space one would generally only output the daily or monthly averages for many species. In my work when estimating model yields of isoprene to HCHO, I use daily averaged HCHO columns and compare them to colocated isoprene emissions from MEGAN.

Optionally one can save high temporally resolved data for a single (or list of) column(s). I've used this diagnostic to compare modelled ozone with ozonesonde profiles at three sonde release sites discussed in Chapter ??.

One of the more frequently used outputs in my work are the satellite overpass diagnostics, which look at averages within a window of time (for instance 1200-1300) using local time (LT) for each gridbox, each day. This diagnostic allows easier analysis of model data against a satellite as one can match the output with the satellite's overpass time.

Tropospheric chemistry run

UCX run

2.3.4 Run comparisons

There are many options available when running GEOS-Chem depending on the desired chemistry, resolution, meteorology, and boundary conditions. Here we compare the model output with and without enabling the Universal tropospheric-stratospheric Chemistry eXtension (UCX). Both runs use 2° latitude by 2.5° longitude, however the UCX mechanism is run with 72 vertical levels from the surface to the top of the atmosphere (TOA \sim 0.1 hPa), while the standard (tropchem) run uses 47 levels. The extra vertical levels are added in the stratosphere, providing finer vertical resolution from around 70 hPa to the top of the atmosphere. For both runs the input parameters such as MEGAN emissions and GEOS-5 meteorological fields are identical.

GEOS-Chem output of HCHO does not differ much between runs with or without the Unified Chemistry eXchange (UCX). Figure 2.2 shows an example of surface HCHO amounts with and without UCX turned on. The differences do not exceed 3% over Australia for the averaged month of January, 2005.

Figure 2.3 shows the differences in surface isoprene amounts over Australia. Here we start to see a higher relative difference in concentrations, although this is generally over the areas with less absolute concentrations. Very little isoprene is seen away from the continent (4-5 orders of magnitude less), due to the short lifetime of isoprene, and lack of emissions over the oceans. Generally isoprene is 0-30% higher over Australia when the UCX mechanism is turned on. This enhancement can be seen throughout the entire tropospheric column as shown by Figure TODO fix ref ??.

Figure TODO: shows the columns for isoprene and HCHO simulated by our two mechanisms over Australia in January of 2005. The differences are minimal compared to other uncertainties in both AMF calculation and emissions estimation.

TODO: The difference in isoprene between UCX and tropchem is likely caused by differences in the modelled radiation reaching the troposphere due to differences in simulated ozone in the stratosphere. With higher stratospheric ozone levels, less radiation would reach the troposphere, changing the photochemistry. Figure 2.4 shows the total column ozone between UCX and non-UCX runs, we can see that UCX has TODO: less or more ozone over Australia/USA in January.

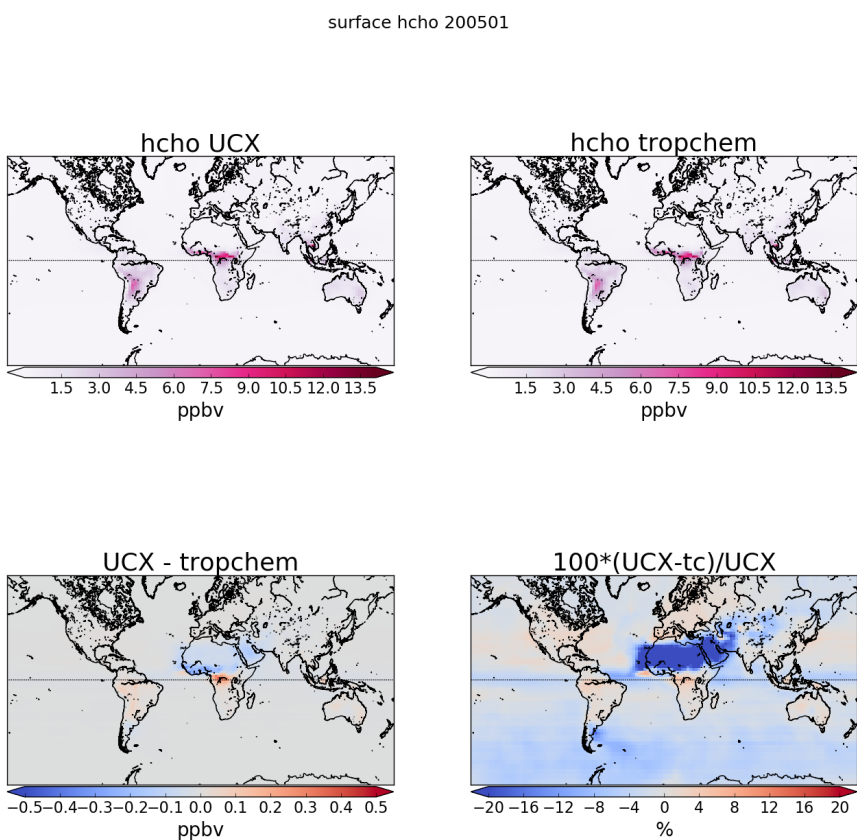


FIGURE 2.2: Surface HCHO simulated by GEOS-Chem with UCX (top left), and without UCX (top right), along with their absolute and relative differences (bottom left, right respectively). Amounts simulated by GEOS-Chem for the 1st of January, 2005.

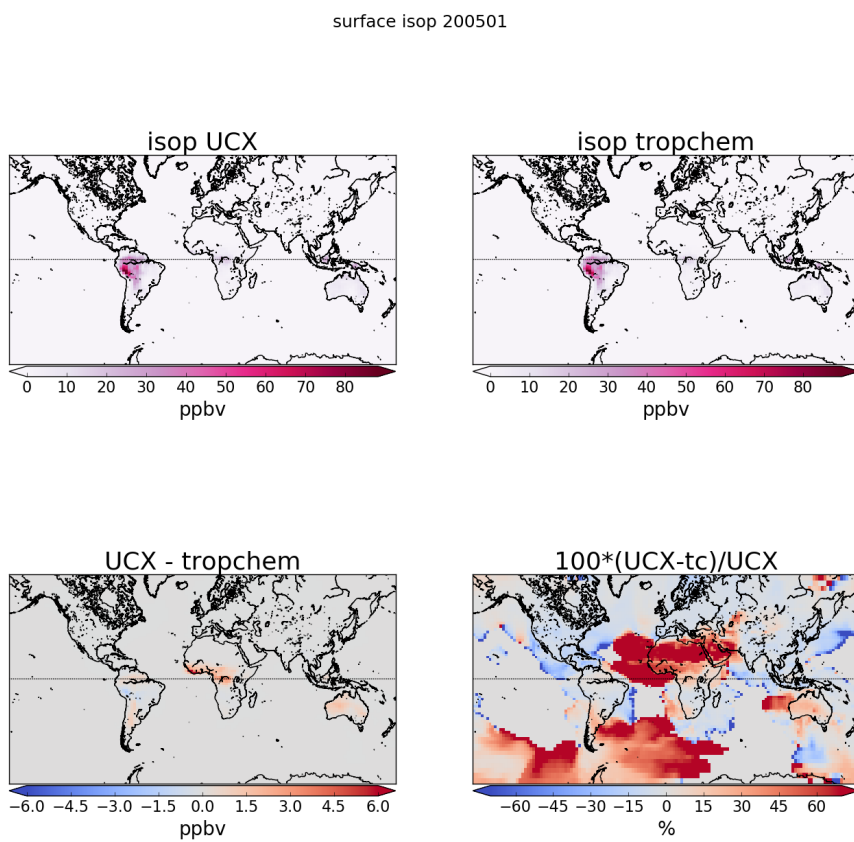


FIGURE 2.3: As figure 2.2, except looking at isoprene.

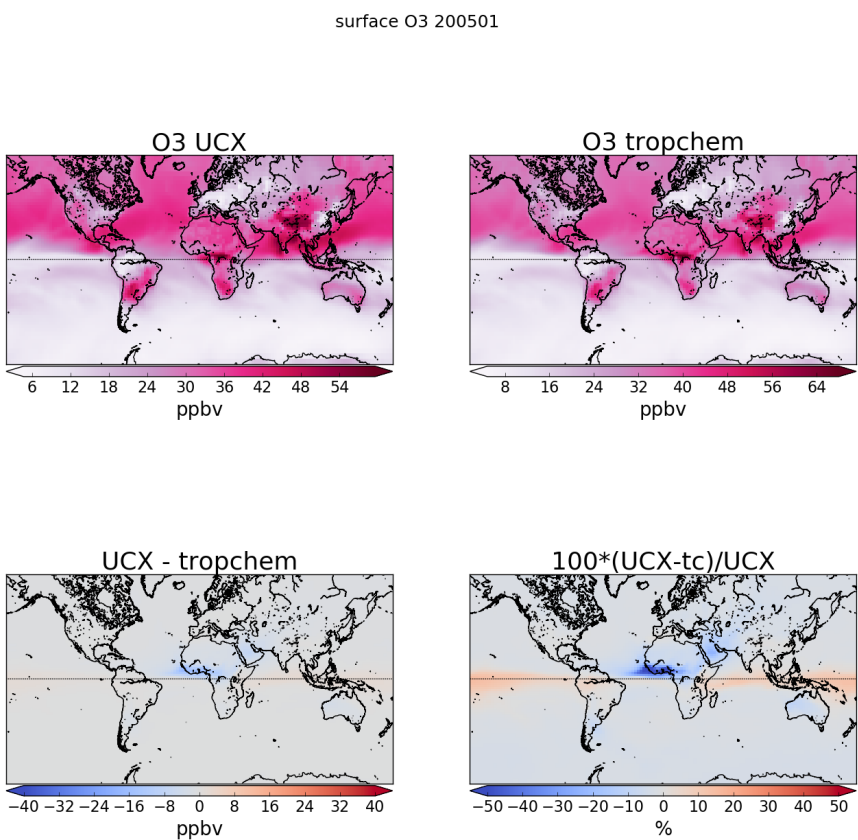


FIGURE 2.4: As figure 2.2, except looking at ozone.

2.4 Measurement Techniques

While I have not made any measurements myself, it is important to understand the techniques used in datasets I have utilised in order to understand possible anomalous datapoints or trends.

In-situ measurements contain errors, and depending on the device used and chemical being measured this error can be significant. Dunne et al., 2017 analyse the uncertainty of VOC measurements (including isoprene) using three different techniques during a campaign in Sydney in 2012. The major sources of uncertainty in measurement techniques included interference from non-target compounds and under-reporting. Overall isoprene uncertainty in their measurements was a factor of 1.5 to 2. This can feed into uncertainties in modelling and satellite retrievals, as verification and correlations are affected.

2.4.1 DOAS

The DOAS technique uses solar radiation absorption spectra to measure trace gases through paths of light. Beer's law states that $T = I/I_0 = e^{-\tau}$ with T being transmittance, τ being optical depth, and I, I_0 being radiant flux received at instrument and emitted at source respectively. From $\tau_i = \int \rho_i \beta_i ds$ we get:

$$I = I_0 \exp \left(\sum_i \int \rho_i \beta_i ds \right)$$

Where i represents a chemical species index, ρ is a species density(molecules per cm^3), β is the scattering and absorption cross section area (cm^2), and the integral over ds represents integration over the path from light source to instrument.

Generally satellites use a DOAS based technique, with chemical transport and radiative transfer models used to transform the non-vertical light path interference into vertical column amounts.

Multiple axis DOAS (MAX-DOAS) is a remote sensing technique which uses several DOAS measurements over different viewing paths. In these retrievals, the measurements of light absorption are performed over several elevations in order to add some vertical resolution to the measurement of trace gas concentrations. An example of this is shown in figure 2.5, which was taken from Lee et al., 2015. Recently MAX-DOAS has been used to examine HCHO profiles in the clean free troposphere (Franco et al., 2015; Schreier et al., 2016) as well as in polluted city air (Lee et al., 2015). Depending on orography and atmospheric composition (ie. the influence of interfering chemicals), MAX-DOAS can be used to split the tropospheric column into two partial columns; giving a small amount of vertical resolution to HCHO measurements (Franco et al., 2015; Lee et al., 2015, eg.). In Franco et al., 2015, an FTIR spectrometer at Jungfraujoch is compared against both MAX-DOAS and satellite data, with two CTMs; GEOS-Chem and IMAGES v2 used to compare total columns and vertical resolution of each instrument.

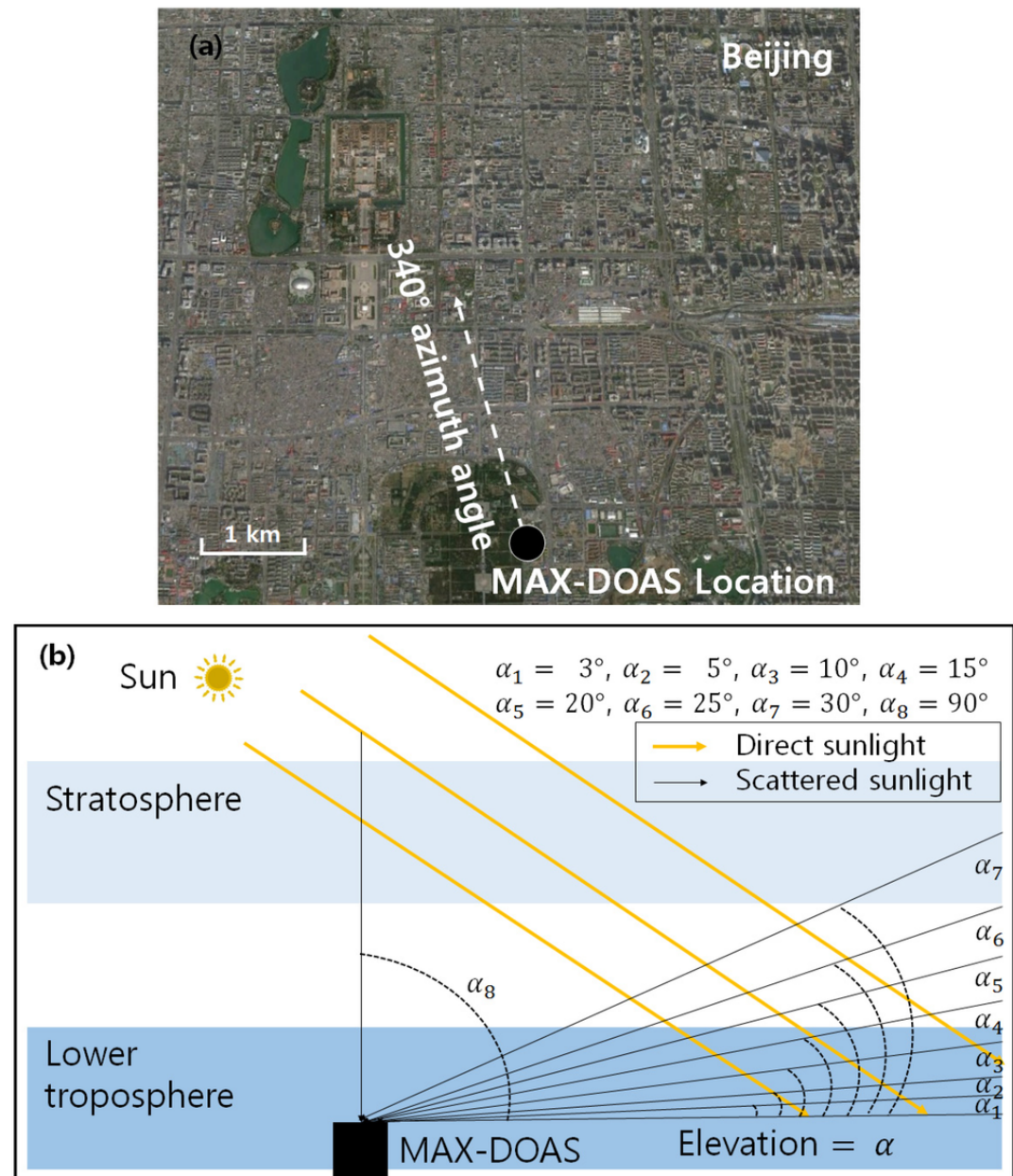


FIGURE 2.5: Image from Lee et al., 2015.

2.4.2 Satellites

Measurements done using DOAS often apply a forward radiative transfer model (RTM) such as LIDORT in order to determine a trace gas's radiative properties at various altitudes. The forward RTM used for satellite data products also involves functions representing extinction from Mie and Rayleigh scattering, and the efficiency of these on intensities from the trace gas under inspection, as well as accounting for various atmospheric parameters which may or may not be estimated (e.g. albedo).

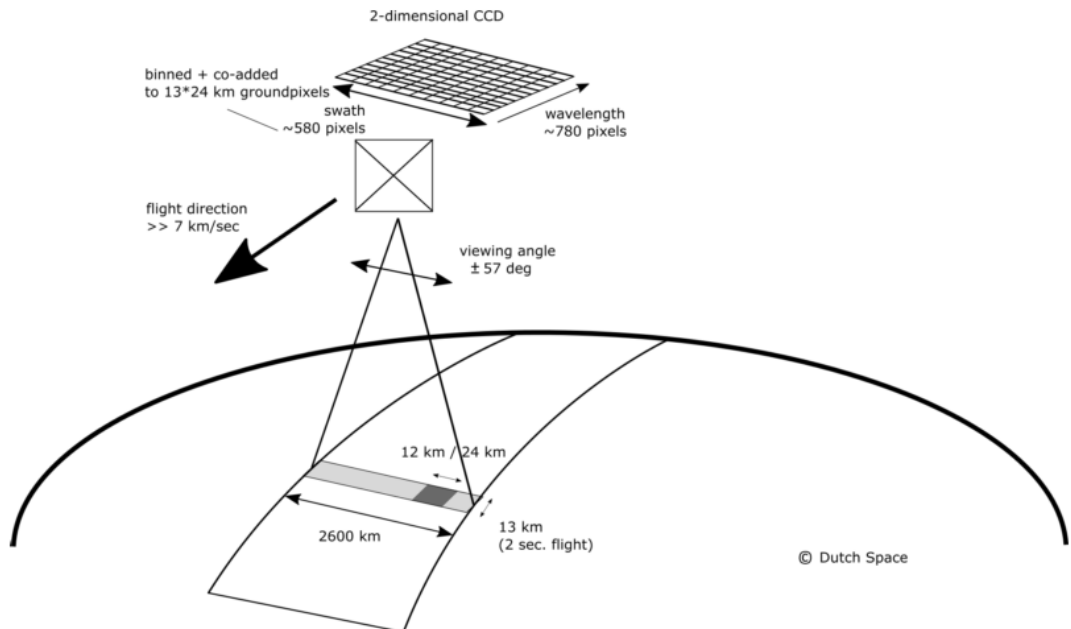
Satellites record near nadir (vertical) reflected spectra between around 250-700 nm split into spectral components at around 0.3 nm in order to calculate trace gases including O₃, NO₂, and HCHO (eg: Leue et al., 2001). Several public data servers are available which include products from satellites, including NASAs Earthdata portal (<https://earthdata.nasa.gov/>) and the Belgian Institute for Space Aeronomy (IASB-BIRA) Aeronomie site (<http://h2co.aeronomie.be/>).

Satellite measurements are generally performed using spectral fitting followed by conversion to vertical column densities. The use of multiple satellites can even be used to detect intradiel concentrations in trace gas columns, as shown in Stavrakou et al., 2015 using OMI and GOME-2 measurements, which have respective overpass times of 1330 and 0930 LT. Instruments including MODIS on board the AQUA and TERRA satellites are also able to determine aerosol optical depth (AOD), a measure of atmospheric scatter and absorbance. An AOD of under 0.05 indicates a clear sky, while values of 1 or greater indicate increasingly hazy conditions. This is important in order to determine where measurements from other instruments may be compromised by high interference. Satellite measured AOD requires validation by more accurate ground based instruments like those of AERONET which uses more than 200 sun photometers scattered globally.

Soon even more HCHO data will be available in the form of geostationary satellite measurements (Kwon et al., 2017). Kwon et al., 2017 examine simulated geostationary measurements against GEOS-Chem column simulations to determine the most important instrument sensitivities. Geostationary satellites can provide temporally rich measurements over an area, as they are not sweeping around the earth but fixed relative to one latitude and longitude.

OMI

The OMI instrument on board AURA has been active since July 2005, it records spectra from 264-504 nm using an array of 60 detectors with mid-resolution (0.4-0.6 nm). This band of wavelengths allows measurements of trace gases including O₃, NO₂, SO₂, HCHO, and various other quantities like surface UV radiation. Recently Schenkeveld et al., 2017 analysed the performance over time of the instrument and found irradiance degradation of 3-8%, changed radiances of 1-2%, and a stable wavelength calibration within 0.005-0.020 nm. They also provide a very nice summary of the OMI instrument copied here in Fig. 2.6, as it shows the instruments spectral, temporal, and spatial resolutions. These changes are measured excluding the row anomaly (RA) effect, which is relatively stable since 2011, although it is still growing and remains the most serious concern. An analysis of the row anomaly by Huang et al., 2017 state that OMI ozone



Channel	Wavelength range	Spectral resolution	Spectral sampling	Ground pixel size
UV1	264–311 nm	0.63 nm = 1.9 px	0.33 nm px ⁻¹	13 × 48 km
UV2	307–383 nm	0.42 nm = 3.0 px	0.14 nm px ⁻¹	13 × 24 km
VIS	349–504 nm	0.63 nm = 3.0 px	0.21 nm px ⁻¹	13 × 24 km

FIGURE 2.6: Figure 1 and Table 1 from Schenkeveld et al., 2017, with the following caption “An impression of OMI flying over the Earth. The spectrum of a ground pixel is projected on the wavelength dimension of the charge-coupled device (CCD; the columns). The cross-track ground pixels are projected on the swath dimension of the CCD (the rows). The forward speed of 7 kms^{-1} and an exposure time of 2 s lead to a ground pixel size of 13 km in the flight direction. The viewing angle of 114° leads to a swath width on the ground of 2600 km.” The table shows the optical properties for OMIs three channels.

columns remain suitable for scientific use, with recommendation for further evaluation. And analysis of OMI output by Schenkeveld et al., 2017 concludes that data is still of high quality and will deliver useful information for 5–10 more years, with radiances only changing by 1 – 2% outside of RA impacted areas. The RA began in June 2007, with some cross-track rows seemingly blocked. The most likely cause is some instrument insulation partially obscuring the radiance port (Schenkeveld et al., 2017).

AMF

To convert the trace gas profile from a reflected solar radiance column (slanted along the light path) into a purely vertical column requires calculations of an air mass factor (AMF). In satellite data, the AMF is typically a scalar value for each horizontal grid point which will equal the ratio of the total vertical column density to the total slant

column density. This value requires calculations to account for instrument sensitivities to various wavelengths over resolved altitudes, and is unique for each trace gas under consideration.

An AMF characterises measurement sensitivity to a trace gas at various altitudes Palmer et al., 2001, e.g. Lorente et al., 2017 show that AMF calculations can be the largest source of uncertainty in satellite measurements. Another way of describing AMFs are as measures of how radiance at the top of the atmosphere (TOA) changes with trace gas optical depths at specific altitudes (Lorente et al., 2017). Calculation of the AMF is important as it is multiplied against the estimated slant columns in order to give vertical column amounts.

Related to the AMF is the averaging kernal (AK), which is used to handle instrument measurements which are sensitive to concentrations at different altitudes in the atmosphere. DOAS methods can be heavily influenced by the initial estimates of a trace gas profile (the *a priori*) which is often produced by modelling, so when comparing models of these trace gases to satellite measurements extra care needs to be taken to avoid introducing bias from differing *a priori* assumptions. One way to remove these *a priori* influences is through the satellites AK (or by using AMFs), which takes into account the vertical profile of the modelled trace gas and instrument sensitivity to the trace gas (Eskes and Boersma, 2003; Palmer et al., 2001). Lamsal et al., 2014 recommends that when comparing satellite data to models, the AMF should first be recalculated using the model as an *a priori*. This is in order to remove any *a priori* bias between model and satellite columns.

Uncertainties

While satellite data is effective at covering huge areas (the entire earth) it only exists at a particular time of day, is subject to cloud cover, and generally does not have fine horizontal or vertical resolution. Concentrations retrieved by satellites have large uncertainties, which arise in the process of transforming spectra to total column measurements, as well as instrument degradation (satellite instruments are hard to tinker with once they are launched). Uncertainty in transforming satellite spectra comes from a range of things, including measurement difficulties introduced by clouds, and instrument sensitivity to particular aerosols (Millet et al., 2006). Many products require analysis of cloud and aerosol properties in order to estimate concentration or total column amounts (Palmer et al., 2001; Palmer, 2003; Marais et al., 2012; Vasilkov et al., 2017). The main source of error in satellite retrievals of HCHO are due to instrument detection sensitivities, and the vertical multiplication factor (discussed in more detail in Section ??) (Millet et al., 2006).

There are two types of measurement error, arguably the worst of these is systematic error (or bias) which normally indicates a problem in calculation or instrumentation. If the systematic error is known, it can be corrected for by either offsetting data in the opposite direction, or else fixing the cause. A proper fix can only be performed if the sources of error are known and there is a way of correcting or bypassing it. Random error is the other type (often reported as some function of a datasets variance, or uncertainty), and this can be reduced through averaging either spatially or temporally. By taking the average of several measurements, any random error can be reduced by

a factor of one over the square root of the number of measurements. This is done frequently for satellite measurements of trace gases (which are often near to the detection limit over much of the globe). For example: Vigouroux et al., 2009 reduce the measurement uncertainty (in SCIAMACHY HCHO columns) by at least a factor of 4 through averaging daily over roughly 500km around Saint-Denis, and only using days with at least 20 good measurements.

Satellite measurements of HCHO are relatively uncertain, however this can be improved by averaging over larger grid boxes or longer time scales. An example of this can be seen in Dufour et al., 2008, where monthly averaging is used to decrease the measurements uncertainty. They examine HCHO in Europe, which is low; near the detection limit of satellite measurements. Taking monthly averages allows enough certainty that useful inversions can be determined to estimate the source emissions of HCHO. The finer nadir resolution of OMI (13 by 24 km²) compared to other satellites reduces cloud influence (Millet et al., 2006; Millet et al., 2008). Although the uncertainty in each pixel is $\sim 2 \times 10^{16}$, which is 5 \times higher than GOME, there are $\sim 100 - 200 \times$ as many measurements due to the smaller footprint and better temporal resolution of OMI, which allows a greater reduction of uncertainty with averaging (Instrument, 2002; Millet et al., 2008).

In cloudy, hazy or polluted areas measurements are more difficult to analyse (e.g. Palmer, 2003; Marais et al., 2014). Recent work by Vasilkov et al., 2017 showed that updating how the surface reflectivity is incorporated into satellite measurements can change the retrievals by 50 % in polluted areas.

In satellite HCHO products, concentrations over the remote pacific ocean are sometimes used to analyse faulty instrument readings. This is due to the expected invariance of HCHO over this region. For instance GOME (an instrument which measures trace gases on board the ERS-2) corrects for an instrument artifact using modelled HCHO over the remote pacific (Shim et al., 2005). OMI HCHO products use a similar technique to account for sensor plate drift and changing bromine sensitivity (Gonzalez Abad et al., 2015)

For many places the tropospheric column HCHO measured by satellite is biased low, Zhu et al., 2016 examine six available datasets and show a bias of 20 - 51% over south east USA when compared against a campaign of aircraft observations (SEAC⁴RS). De Smedt et al., 2015 also found a low bias from 20 - 40% when comparing OMI and GOME2 observations against ground based vertical profiles, and Barkley et al., 2013 determine OMI to be 37% low compared with aircraft measurements over Guyana. These bias can be corrected by improving the assumed apriori HCHO profiles which are used to calculate the AMFs of the satellite columns. Millet et al., 2006 examine OMI HCHO columns over North America and determine overall uncertainty to be 40%, with most of this coming from cloud interference. Millet et al., 2008 shows that there also exists some latitude based bias, as well as a systematic offset between the OMI and GOME instruments. This does not appear to be due to the different overpass times of the two instruments.

Uncertainty in the OMI satellite instrument is calculated by the Smithsonian Astrophysical Observatory (SAO) group using the uncertainty in backscattered radiation retrievals (Gonzalez Abad et al., 2015; Abad et al., 2016). Another method of calculating the uncertainty is used by the Belgian Institute for Space Aeronomy (BIRA) group,

who determine uncertainty from the standard deviation of HCHO over the remote pacific ocean (De Smedt et al., 2012; De Smedt et al., 2015).

A full analysis of the AMF uncertainty in OMI measurements, as well as the structural uncertainty (between different systems of calculations applied to the same data) is performed by Lorente et al., 2017. They determine the structural uncertainty using ensemble techniques on seven AMF calculation approaches used by different retrieval groups. They show that in scenarios where the gas is enhanced in the lower troposphere, AMF calculation is the largest uncertainty in satellite measurements. In polluted environments the structural uncertainty is estimated at 42 %, or 31 % over unpolluted environments. The importance of apriori and ancillary data (such as surface albedo and cloud top height) is also shown, as it sharply affects the structural uncertainty.

GOME suffers from similar uncertainties to OMI, as the same general method of DOAS remote measurements are performed. The uncertainty from slant column fitting has been calculated for GOME to be 4×10^{15} molecules cm⁻² (Chance et al., 2000; Millet et al., 2006). The conversion factor for slant to vertical columns (AMF) calculation also suffers from errors; primarily from surface albedo, HCHO vertical profile apriori, aerosol, and cloud influence (Millet et al., 2006). AMF uncertainties for GOME are calculated to be 1 to 1.3×10^{15} molecules cm⁻² by Shim et al., 2005.

2.4.3 OMI Satellite measurements

OMI HCHO

Recalculated OMI formaldehyde columns are used as a basis for estimating isoprene emissions in Chapter ??

HCHO has been found to be biased low in several studies eg. Zhu et al., 2016; De Smedt et al., 2015; Barkley et al., 2013

OMI NO₂

2.5 Recalculation of OMI HCHO

The method used here largely follows that of Palmer et al. (2001). The AMFs for OMI are recalculated using shape factors based on GEOS-Chem HCHO profiles, averaged between 1200 and 1300 local time (LT). Using this one hour average should match the overpass time of OMI, and is similarly performed in Jin2017 When comparing satellite observations to a chemical model, recalculation of the satellite AMF using modelled vertical gas profiles removes any bias introduced by differences from the a-priori shape factor to the model. The AMF is needed to transform the slant column, as viewed by the satellite, into a vertical column:

$$AMF = \frac{\Omega_s}{\Omega_v} \quad (2.2)$$

where s and v subscripts refer to slant and vertical values, while Ω represents a column of absorber in molecules cm⁻².

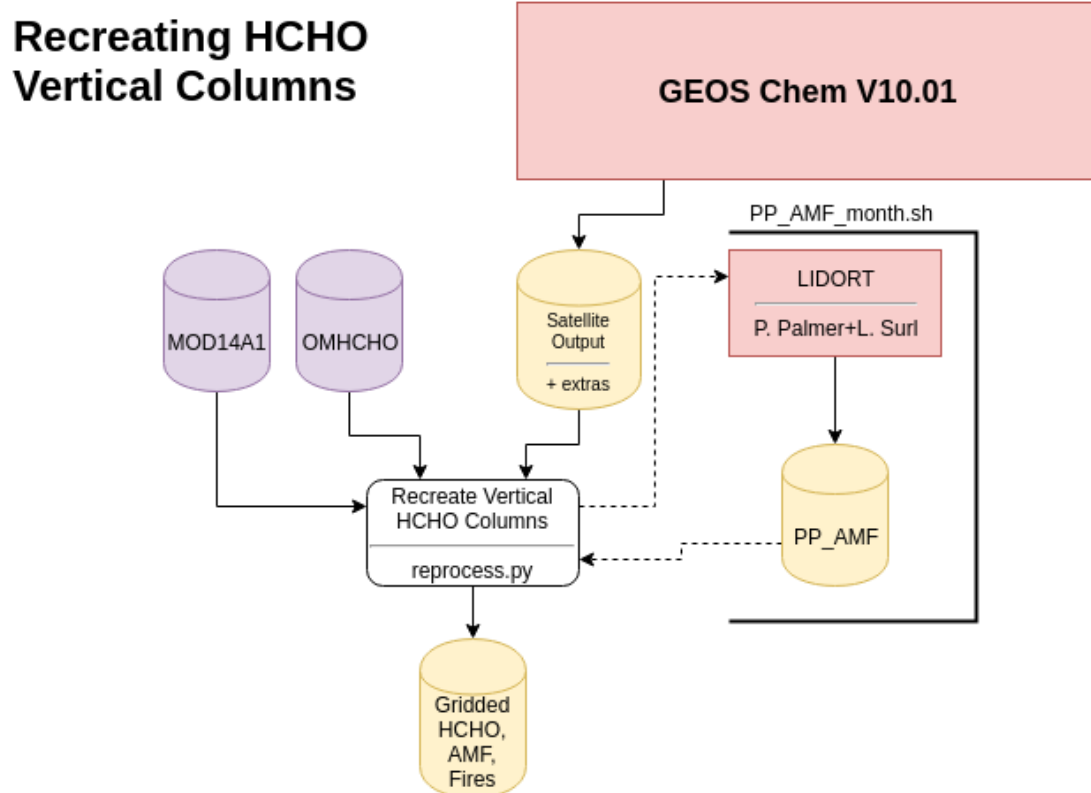


FIGURE 2.7: Depiction of processes and datasets used to recalculate OMI AMFs.

The vertical shape factor $S_z(z)$ is defined as a normalized vertical number density profile $S_z(z) = \frac{\eta(z)}{\Omega_v}$ where $\eta(z)$ is the number density in molecules m^{-3} . The AMF can be expressed as

$$AMF = AMF_G \int_0^{\infty} w(z)S_z(z)dz \quad (2.3)$$

Where $w(z)$ is the scattering weights describing the sensitivity of the backscattered spectrum to the abundance of an absorber at altitude z . It's worth noting that in the OMI satellite product, the provided $w(z)$ incorporates the AMF_G term and the equation 2.3 should be implemented without this term if using the satellite w . This is not noted in any of the papers which recalculate the AMF from the OMI product, due to them recalculating the w term themselves with a radiative transfer model such as LIDORT.

Figure 2.7 shows an overview of how this process is performed in my work. Output from GEOS-Chem is combined with both OMHCHO swath data and MOD14A1 gridded fire data in order to produce a gridded HCHO file which contains HCHO vertical columns and fire counts. The output keeps the original AMF as well as those recalculated using GEOS-Chem, and optionally those recalculated using GEOS-Chem and LIDORT.

Two HCHO products are created, both using GEOS-Chem output at global 2 by 2.5 °horizontal resolution. One uses the OMI product's ω_z and equation 2.3 in order

to calculate an AMF. While the other uses code provided by Dr. Paul Palmer, with alterations by Dr. Randal Martin, and Dr. Luke Surl to run LIDORT on the satellite slant columns and the GEOS-Chem output in order to calculate an AMF. These two calculations are compared over Australia in figure(s) TODO: Map comparison, regression, and time series once AMFpp is working properly. The effect of not recalculating the ω_z is can be seen in figure TODO which looks at the altered satellite vertical columns using each method. Figure TODO shows an analysis of the differences between running the recalculation with and without updating the ω_z .

The AMF calculated using Dr. Palmer's code uses a more strict series of filters, leading to fewer satellite based HCHO columns and reduced coverage over Australia. Stricter filtering must be balanced against both coverage and the sensitivity of the AMF determination to recalculating ω_z .

2.6 Campaigns

Here I will describe the various datasets I've used to analyse GEOS-Chem output. These datasets are also used to determine how suitable GEOS-Chem is in calculation of isoprene emissions estimations in chapter ?? and ozone transport extrapolations in chapter ??.

Figure 2.8 shows the locations of each of the campaigns I mention in this text. These took place over disparate times, and are in-situ datapoints which may not nicely compare with GEOS-Chem output which is averaged over a large horizontal space.

TODO: these summaries.

Daintree summary (P. Nelson)

2.6.1 Marine and Urban MBA ? (MUMBA)

2.6.2 Sydney Particle Studies (SPS1, SPS2)

Two VOC and other trace gas measurement campaigns took place at the Westmead Air Quality Station scientists from CSIRO, OEH, and ANSTO. Stage 1 (SPS1) was from 5 February to 7 March in 2011, while stage 2 (SPS2) ranged from 16 April to 14 May 2012.

Two instruments measured VOC concentrations: one was a Proton transfer reaction mass spectrometer (PTR-MS), the other a gas chromatograph (GC) with an equipped flame ionisation detector (FID). The PTR-MS uses chemical ionisation mass spectrometry and can quantify VOCs at high temporal resolution (< 1 s). It was calibrated several times per day against hcho, isoprene, α -pinene, and several more VOCs. Further details can be found in Dunne2012; Dunne et al., 2017 (TODO: Check papers). The output lists hourly averaged ppbv concentrations of trace gases based on the mass to charge ratio (m/z), which for isoprene is 69. It's possible that other chemicals (such as Furan, with the same m/z) interfered with this value, especially at low ambient isoprene concentrations and towards the end of autumn (SPS2) when wood fires usage starts to become frequent (TODO cite something). The GC-FID analysed samples collected in multi-absorbent tubes, with lower temporal resolution but no interferences. GC-FID data is averaged from 0500-1000 LT, and 1100-1900 LT. Further details for this method can be found in TODO: cite Min et al 2016.



FIGURE 2.8: Locations of Australian campaigns which are analysed within this thesis

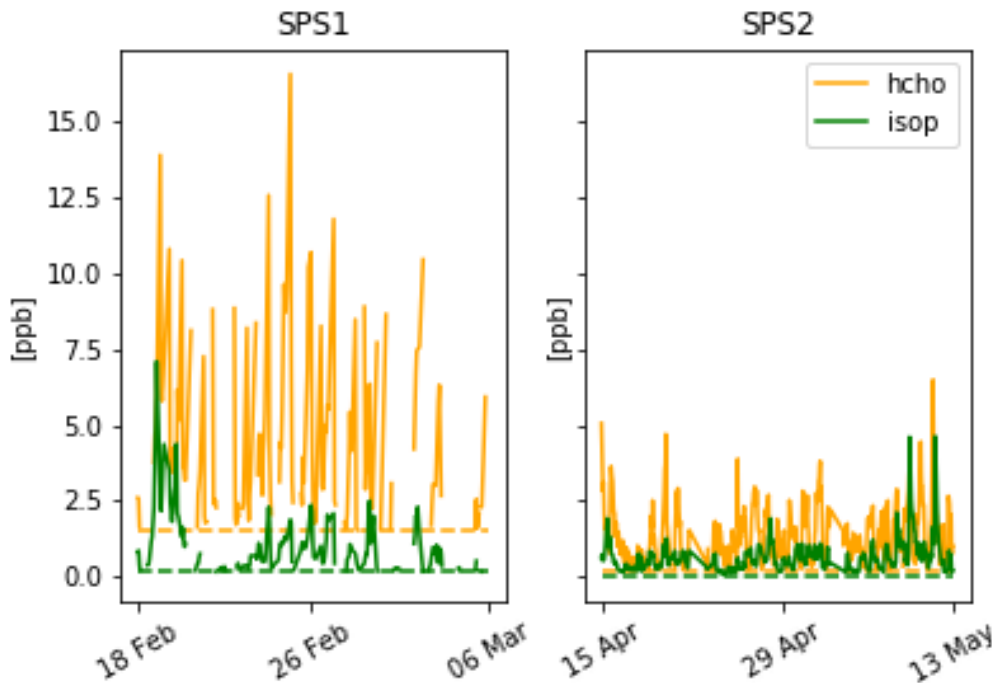


FIGURE 2.9: SPS 1 and 2 HCHO (yellow) and isoprene (green) time series, along with detection limits (dashed).

Figure 2.9 shows isoprene and formaldehyde over the course of these two campaigns, as well as the detection limits (dashed lines), as measured by PTR-MS. In order to compare with GEOS-Chem output a daily average and an overpass time (1200-1300 LT) average are both created from these data. In averaging, any measurements below the machine detection limit are set to half of the detection limit, as done in (TODO: doi:10.5194/acp-15-223-2015, 2015) which should minimise any introduced bias.

Figure 2.10 shows GEOS-Chem output in the gridsquare containing Sydney overlaid on SPS measurement data. Superficially the comparison is not too bad between these two datasets, however GEOS-Chem output is daily averaged over $2 \times 2.5^\circ$ (latitude by longitude). The SPS data is point-source and taken during the daytime when isoprene is higher, so it is very likely that GEOS-Chem HCHO and isoprene output is in fact too high.

2.7 Analysing output

2.7.1 Satellite HCHO recalculations

The HCHO columns provided in OMHCHO are described in TODO: ref other section. After recalculating the AMFs for each satellite pixel using GEOS-Chem v10.01, we are left with the new vertical columns which are essentially what the satellite would show given that the modelled column was known and correct. Comparing these new vertical columns to model output removes any bias caused by the apriori vertical column

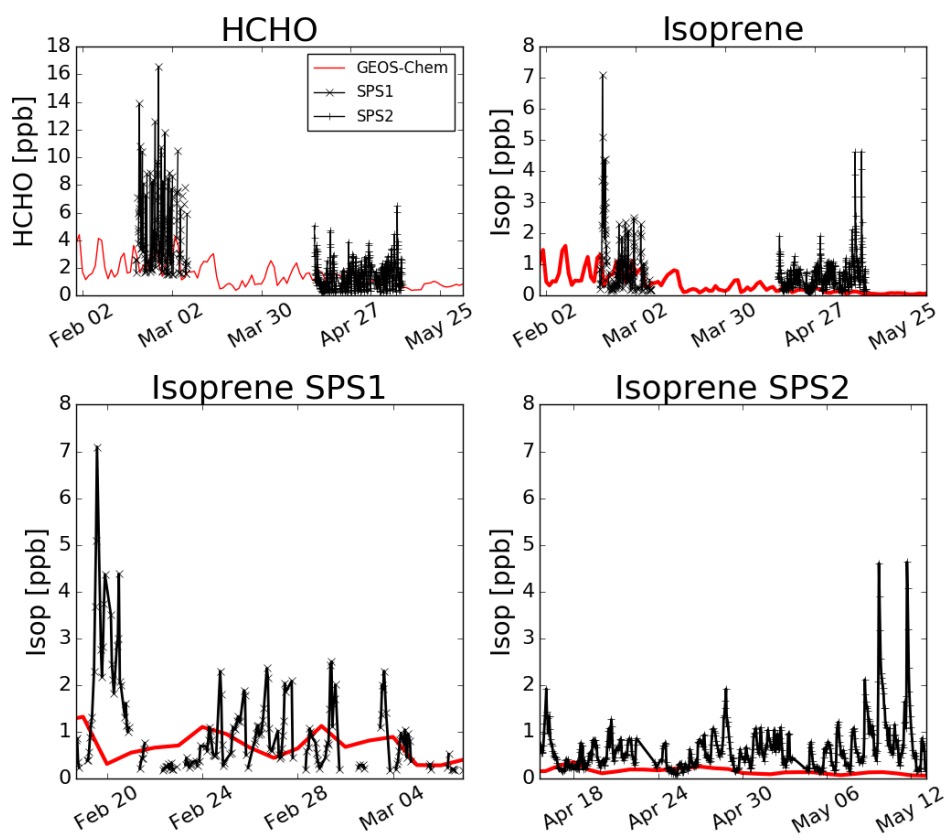


FIGURE 2.10: Comparison between GEOS-Chem HCHO concentrations in the gridsquare containing Sydney for the duration of the SPS 1 and 2 campaigns

in the satellite product, since now biases in the modelled column affect both data sets equally.

Figure (TODO: figure) shows vertical columns of HCHO for: column 1) the original satellite swaths, column 2) recalculated without changing the provided scattering weights, and column 3) fully recalculated vertical columns. Each grid square (at 0.25 by 0.3125 lat lon resolution) has been created by binning the recalculated satellite pixels within the month. The average pixels per land square is overlaid and changes due to how a fire filter is applied. Each row has a stricter fire filter applied from top to bottom, with no fire filter on the first row up to filtering pixels from squares with fires up to 8 days prior.

2.7.2 Circadian emissions cycle

HEMCO diagnostics provide the simulated MEGAN isoprene emissions at high temporal resolution. TODO: Figure X shows the daily emissions cycles for a few regions over each season. The regions are labelled in the top panel, and seasonally averaged emissions from grid-boxes in each region are shown below. TODO: Figure XX shows the emissions from SPS1 and 2 compared against GEOS-Chem estimates in the same grid square.

2.7.3 HCHO: Simulated vs Measured

HCHO precursors are heavily tied to temperature (TODO:cite), and model output shows how higher temperature leads to an increase in HCHO levels. Figures 2.11 - 2.13 show the relationship between temperature and HCHO, for January 2005, within subsets of Australia. A reduced major axis regression is used to determine the linear slopes between surface temperature (X axis) and HCHO (Y axis). This gives us a linear regression for each region however it's clear from the straight line and from literature that the relationship is not linear but rather exponential (TODO: cite and example studies). Using the natural log of HCHO we can take the linear regression and then exponentiate each side in the equation $\ln Y = mX + b$ to get $Y = \exp(mX + b)$. This gives us the exponential fit as shown, with the corellation coefficient between $\ln HCHO$ and temperature, which is not directly comparable to the linear coefficient. The distributions of exponential corellation coefficients and exponential 'm' terms is shown in the embedded plot, with one datapoint available for each grid square where the regression is performed.

2.7.4 Accounting for Fires

TODO: look at yearly corellation, compare to exponential curve and look for fire outliers As seen in TODO: citation, HCHO concentrations scale exponentially with temperature. This allows another method for detecting the influence of non-biogenic HCHO emission/creation by looking for outliers above the curve at low temperature. Zhu et al., 2013 has a similar analysis over south-eastern USA showing an exponential correlation of $HCHO = \exp(0.15 * T - 9.07)$.

In GEOS-Chem we can simply turn off pyrogenic emissions, however in satellite datasets we need to mask pixels affected by biomass burning. This can be done using

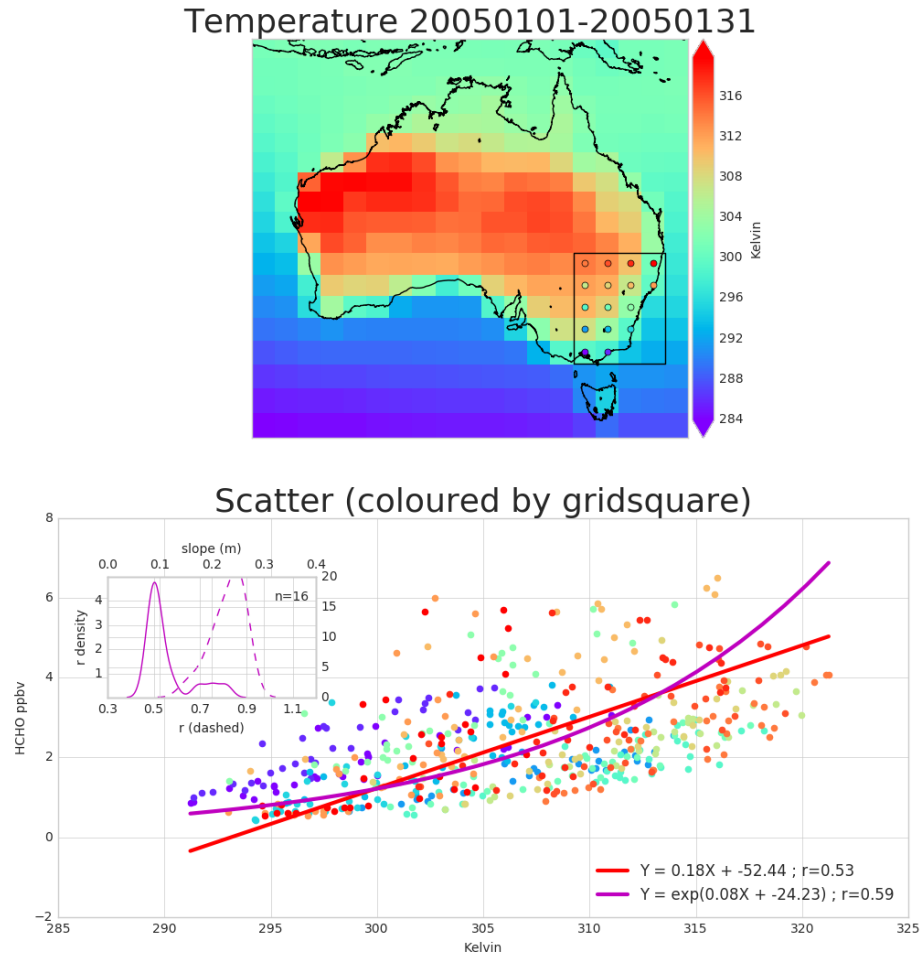


FIGURE 2.11: Top panel: surface temperature averaged over January 2005. Bottom panel: surface temperature correlated against temperature over January 2005, with different colours for each gridbox, and the combined correlation. A reduced major axis regression is used within each gridbox (shown in top panel) using daily overpass time surface temperature and HCHO amounts (ppbv). The distribution of slopes and regression corellation coefficients (one datapoint per gridbox) for the exponential regression is shown in the embedded plot.

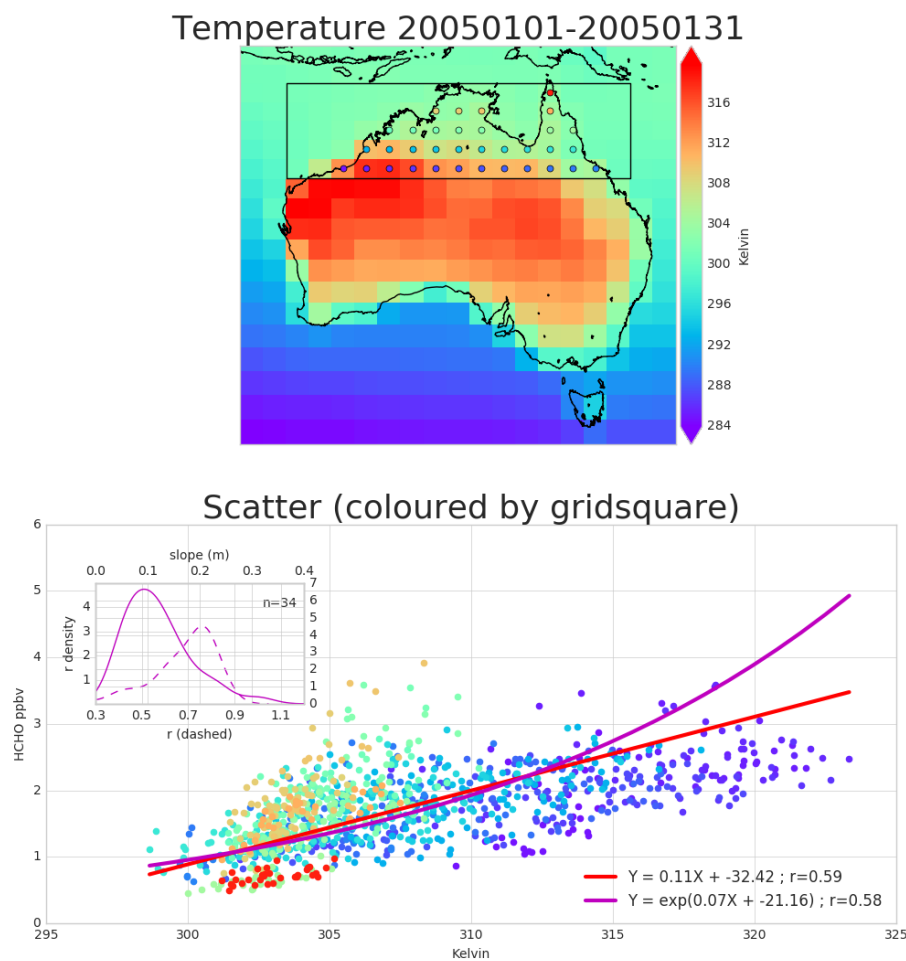


FIGURE 2.12: As figure 2.11 but for northern Australia.

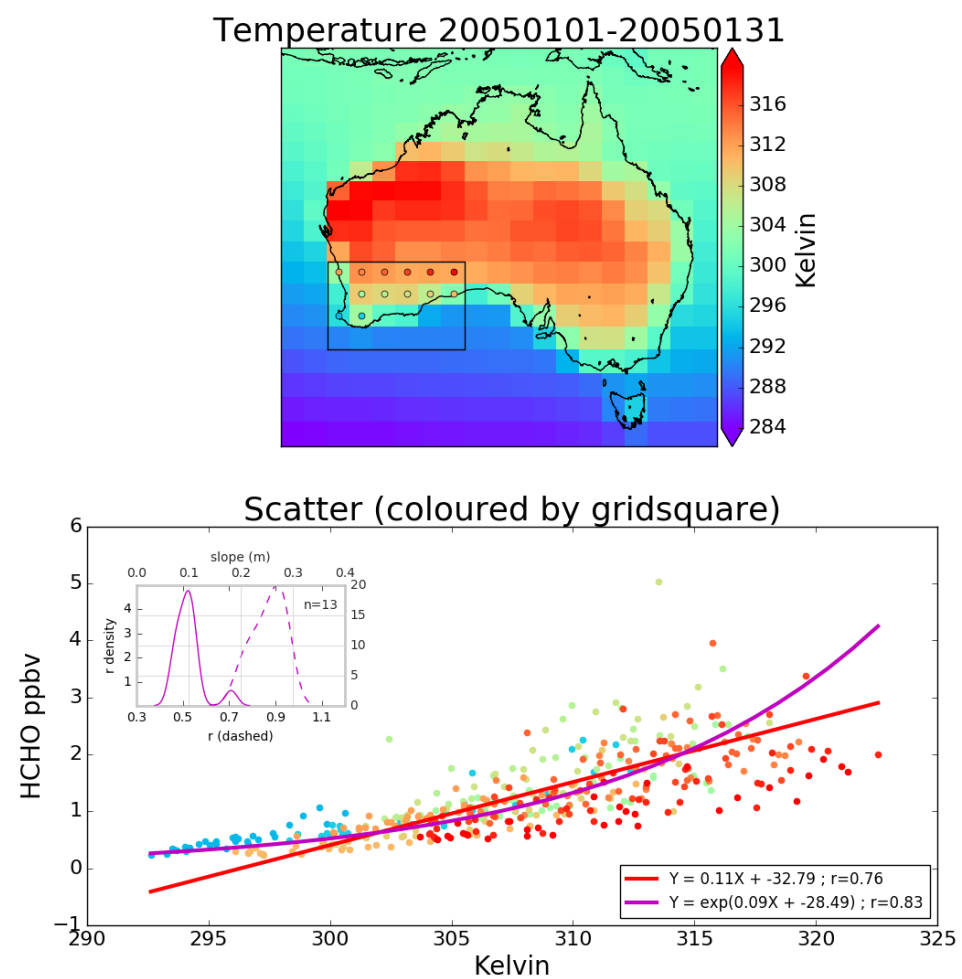


FIGURE 2.13: As figure 2.11 but for south-western Australia.

the MODIS fire counts, detected from space using the combined product from Terra and Aqua (Terra at 10:30, 22:30 LT; Aqua at 13:30, 01:30 LT). Marais et al., 2012 remove pixels colocated with non zero fire counts in any of the prior eight days, within grid squares with $1 \times 1^\circ$ resolution. Barkley et al., 2013 use fires from the preceding and concurrent day, within local or adjacent grid squares, with grid resolution of $0.25 \times 0.3125^\circ$.

Filtering active fires does not account for transported smoke plumes, which can carry HCHO precursors. Smoke plumes can be filtered using the aerosol absorption optical depth (AAOD) seen by OMI (product OMAERUVd), although care needs to be taken when deciding the threshold for smoke detection (Marais et al., 2012).

When analysing satellite OMHCHO vertical columns (Ω), the following steps are performed in order to mask influence from biomass burning:

1. MOD14A1 daily gridded Aqua/Terra combined fire counts are read at $1 \times 1 \text{ km}^2$ resolution, and binned into $0.25 \times 0.3125^\circ$ bins, matching the resolution of binned Ω .
2. A rolling mask is formed which removes Ω if one or more fires are detected in a grid square, or in the adjacent grid square, up to 8 days previously. This includes the 'current' day, making 9 days of fires in total being filtered out on each day.
3. AAOD at 500 nm is mapped from OMAERUVd $1 \times 1^\circ$ resolution onto the $0.25 \times 0.3125^\circ$ resolution.
4. An AAOD threshold is determined using some technique (TODO).
5. Grid squares with AAOD over this threshold (TODO) are additionally masked.

2.7.5 Accounting for NO_x

NO_x concentrations affect HCHO yield, isoprene lifetimes, and other things due to affects on the atmospheres oxidative capacity. This means that if the model is poorly simulating NO_x, the yield (and transport, see ??) may be poorly estimated. In order to determine if rescaling the NO emissions over Australia is necessary in GEOS-Chem, I looked at modelled NO₂ amounts compared to satellite data for most of 2005.

Simulated GEOS-Chem tropospheric NO₂ columns averaged from 1300-1400 LT are compared against OMNO2d data (Sec. 2.4.3). Figure 2.14 shows the direct comparison between these datasets averaged over January to February, 2005. It's clear that the OMNO2d product can pick out Sydney and Melbourne as NO₂ hotspots, which are underestimated by GEOS-Chem (potentially due to averaging over the $2 \times 2.5^\circ$ horizontal resolution). Over much of the country GEOS-Chem overestimates NO₂ by 10-60%, except in NA and northern Queensland where up to 50% underestimation occurs.

This comparison is expanded, including a comparison against modelled emissions, and repeated for autumn (MAM), winter (JJA), and spring (SON) in figures 2.15 to 2.22. These show an analysis of GEOS-Chem NO emissions and their correlations with the bias between GEOS-Chem NO₂ mid-day columns and the OMNO2d product, averaged over each season in 2005. The scatter plots have one datapoint for each land square over Australia.

GC NO vs OMNO2d 20050101-20050228

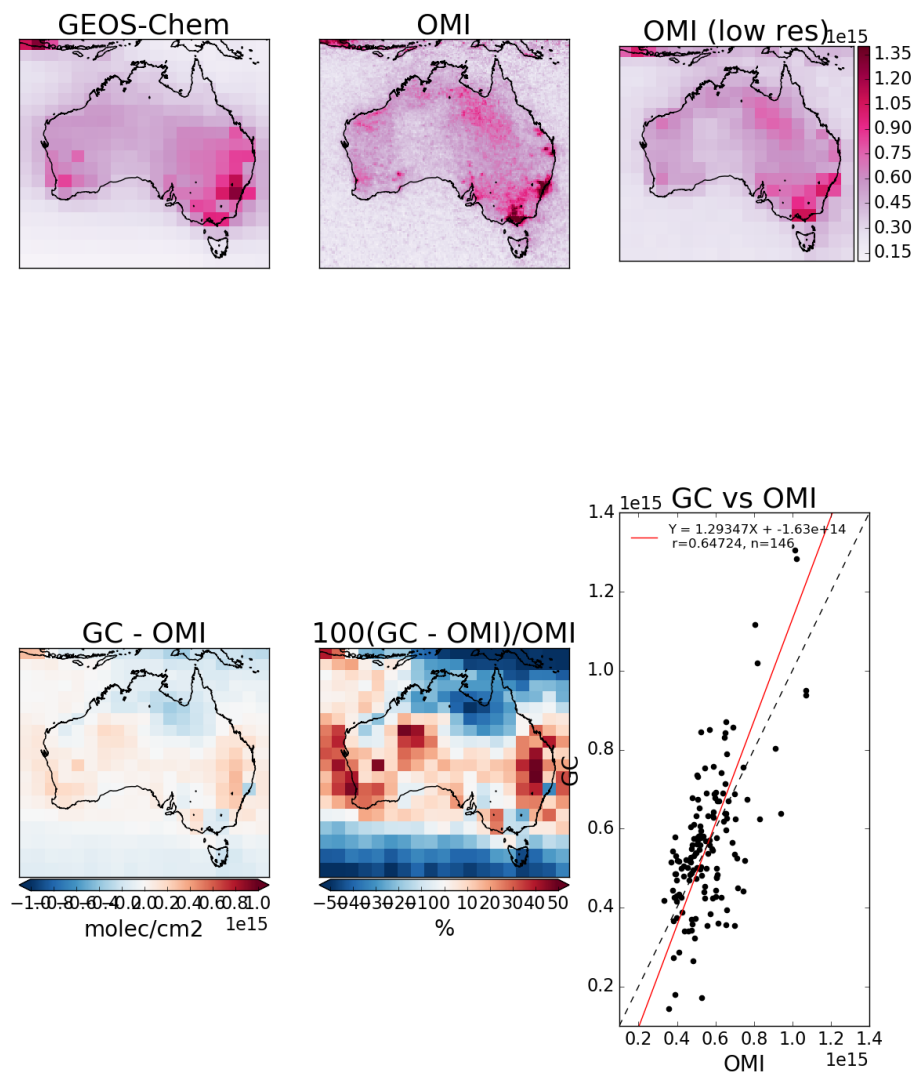


FIGURE 2.14: GEOS-Chem mid-day tropospheric column NO₂ vs OMNO₂d columns (averaged to match GEOS-Chem's lower resolution). Absolute and relative differences, along with correlation shown on bottom row.

The corellation between model and satellite NO₂ columns is OK throughout the year over Australia, with some overestimation in the north during non-summer months. There is also slight underestimation over Sydney and Melbourne throughout the year. Figures 2.15 to 2.22 show that the visible biases are not over Australia are not driven by modelled emissions of NO. While the corellation between column NO₂ and emitted NO is clear, emissions do not appear to bias the model in either direction away from the satellite data.

2.7.6 HCHO Comparisons

TODO: GOME2 HCHO stuff? During days with more than one HCHO column measurement we can more confidently fit the cycle. For example EOS AURA's OMI measurements from 2004 can be combined with MetOp-A's GOME2 after October 2006, with daily overpasses by OMI and GOME2 at 1345 and 0930 respectively.

2.8 Data Access

TODO: ADD MORE HERE

OMNO2d Daily satellite NO₂ product downloaded from <https://search.earthdata.nasa.gov/search>, DOI:10.5067/Aura/OMI/DATA3007. See more information in section

SPEI Monthly standardised precipitation evapotranspiration index (metric to determine drought stress) downloaded from <http://hdl.handle.net/10261/153475> with DOI:10.20350/digitalCSIC/8508. See more information in section

OMHCHO Satellite swaths of HCHO slant columns downloaded from TODO, with DOI TODO

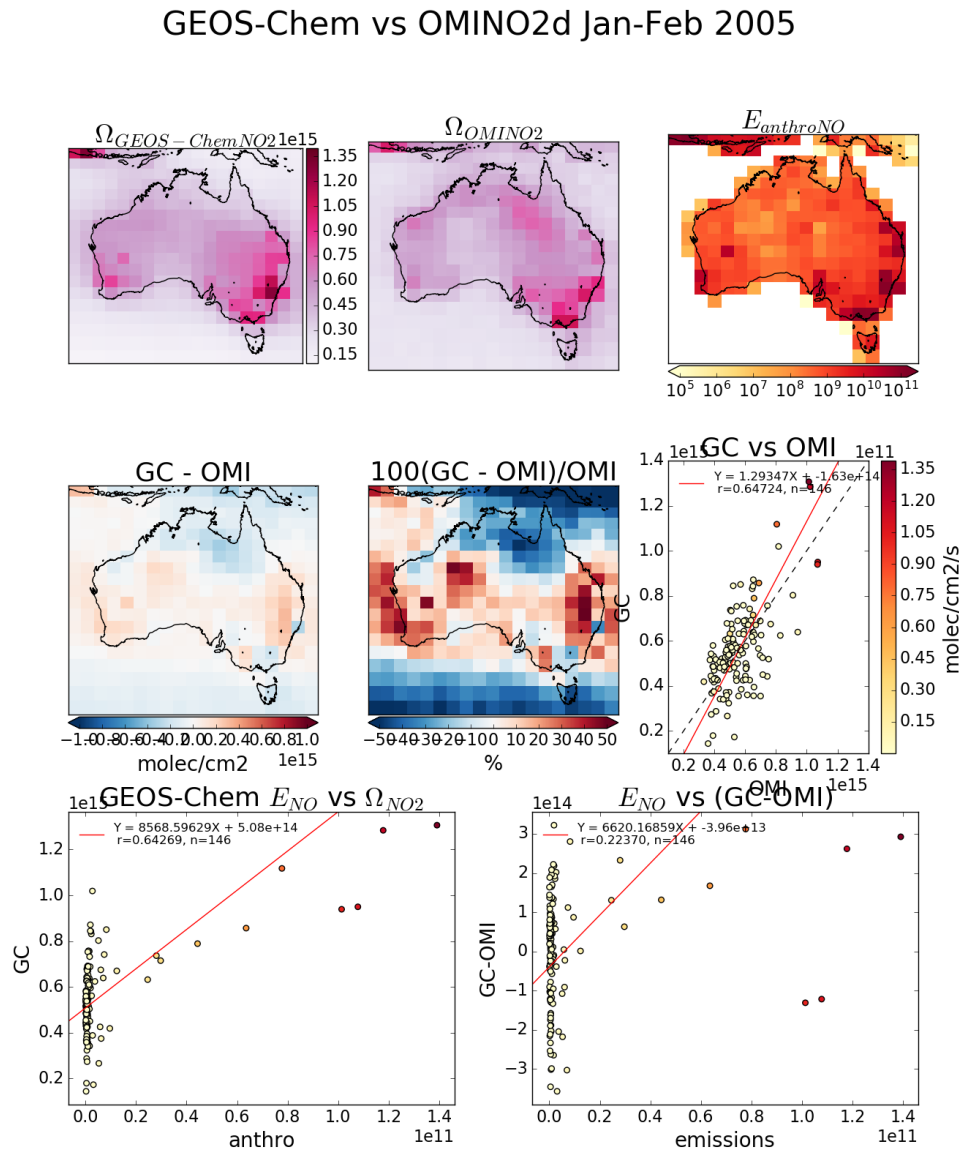


FIGURE 2.15: Top row (left to right): GEOS-Chem NO₂ mid-day tropospheric columns, OMNO2d NO₂ columns, modelled anthropogenic NO emissions. Second row: absolute and relative difference between GEOS-Chem and OMI NO₂ data, and the corellation. Third row: corellation between GEOS-Chem tropospheric column NO₂ and emitted NO, then between the model-satellite bias and the emissions. All corellation plots are coloured by emission rates.

GEOS-Chem vs OMINO2d Sprint (SON) 2005

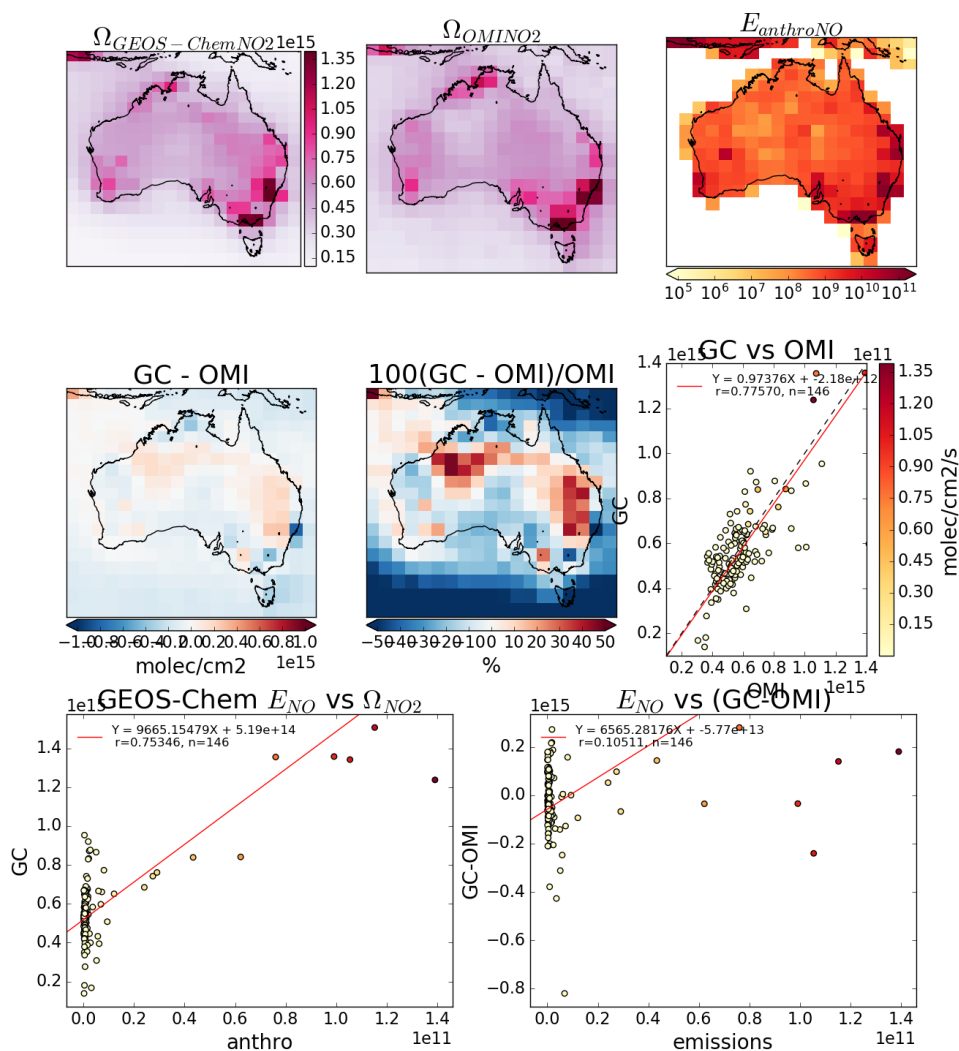


FIGURE 2.16: As figure 2.15, for Autumn 2005.

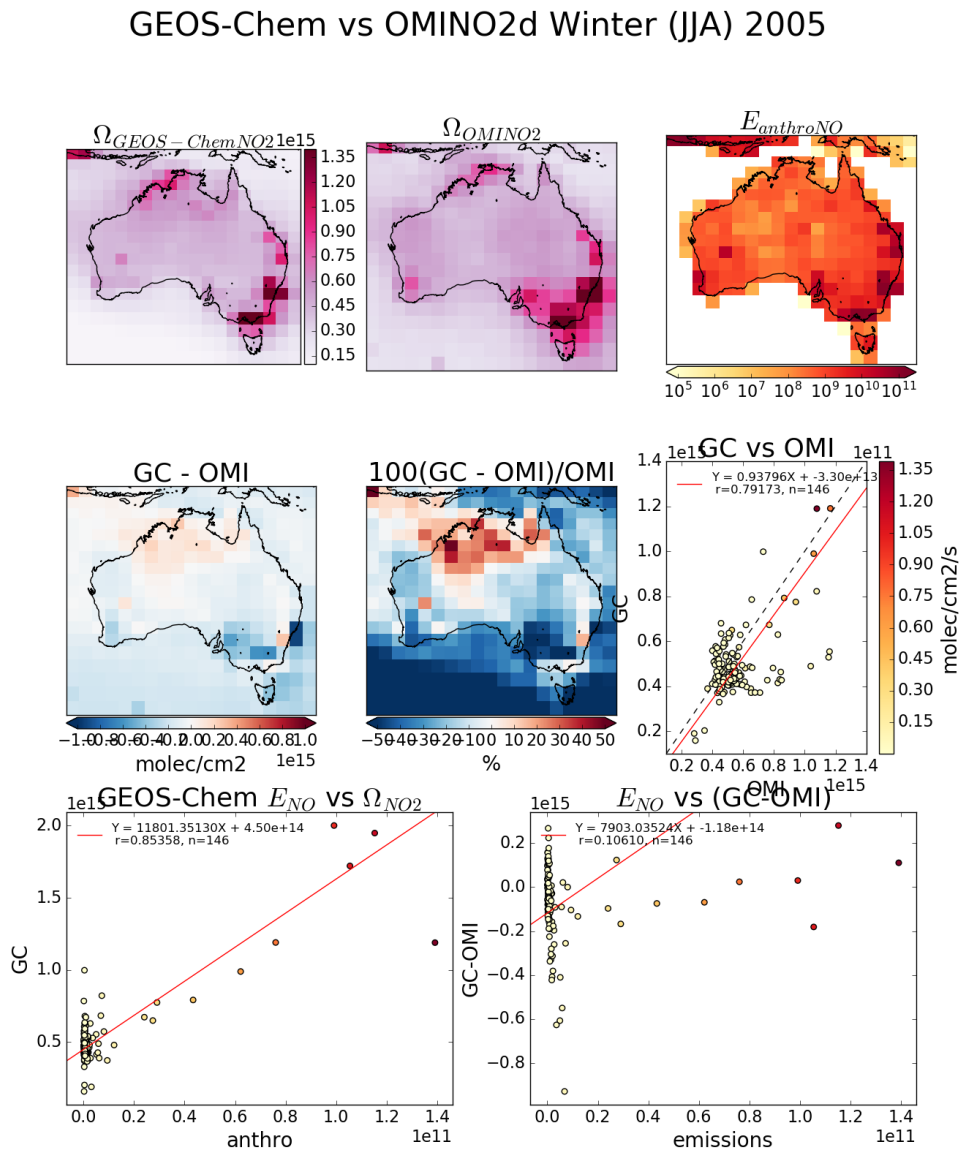


FIGURE 2.17: As figure 2.15, for Winter 2005.

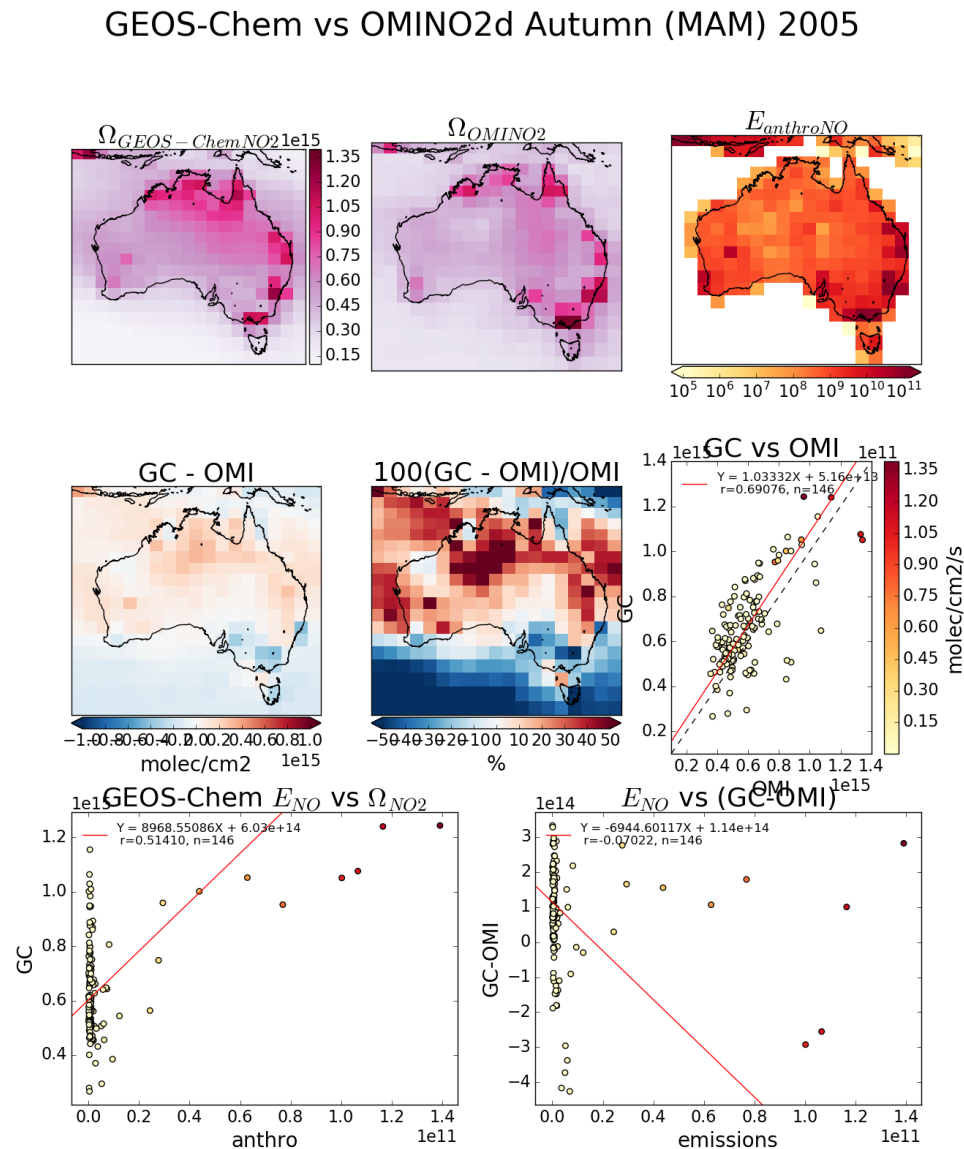


FIGURE 2.18: As figure 2.15, for Spring 2005.

GEOS-Chem vs OMINO2d 20050101-20050228

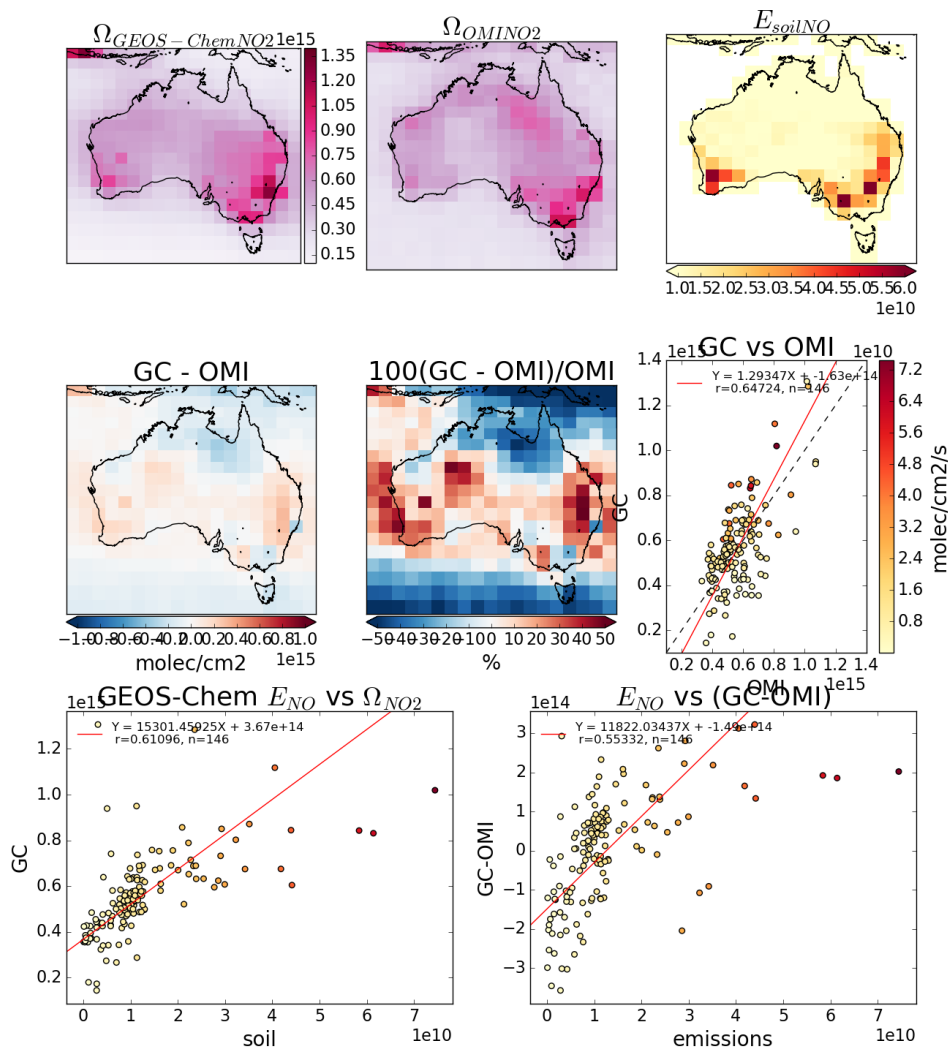


FIGURE 2.19: As figure 2.15, except anthropogenic NO emissions are replaced by soil NO emissions.

GEOS-Chem vs OMINO2d 20050301-20050531

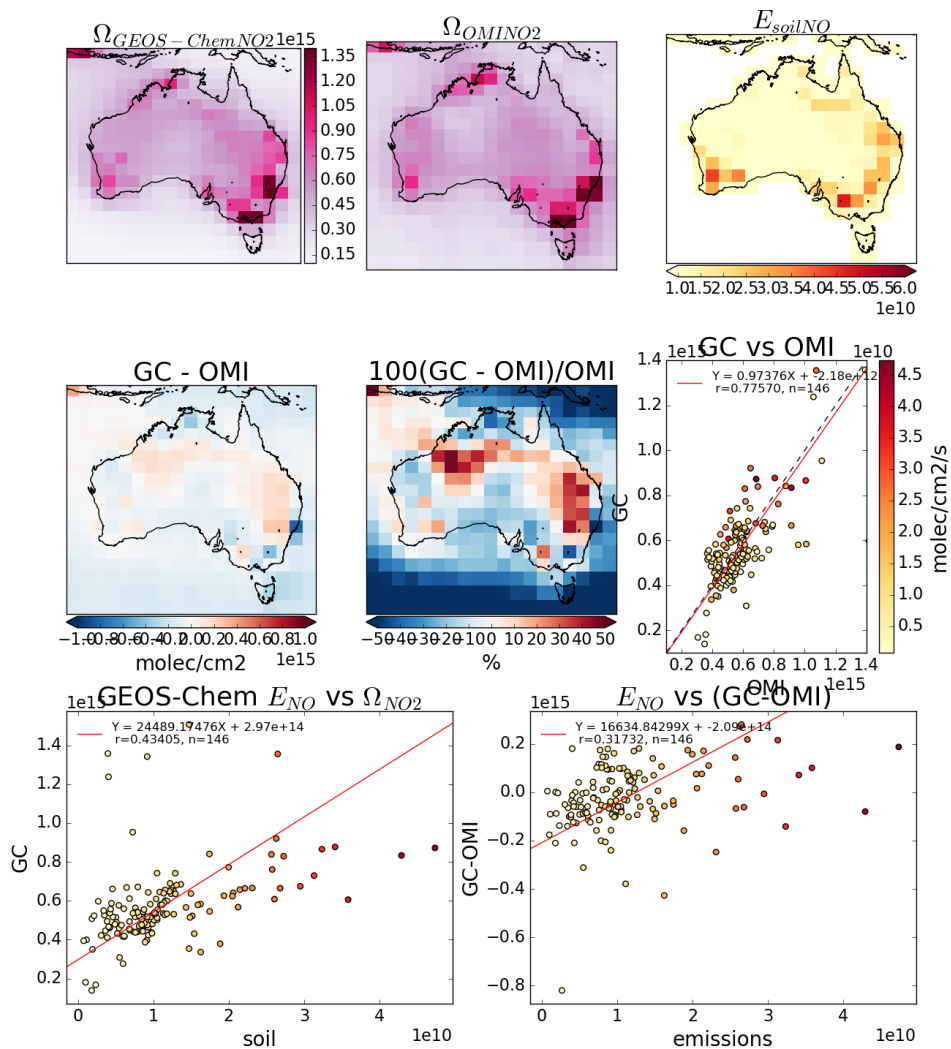


FIGURE 2.20: As figure 2.15, for Autumn 2005, with soil NO emissions replacing anthropogenic NO emissions.

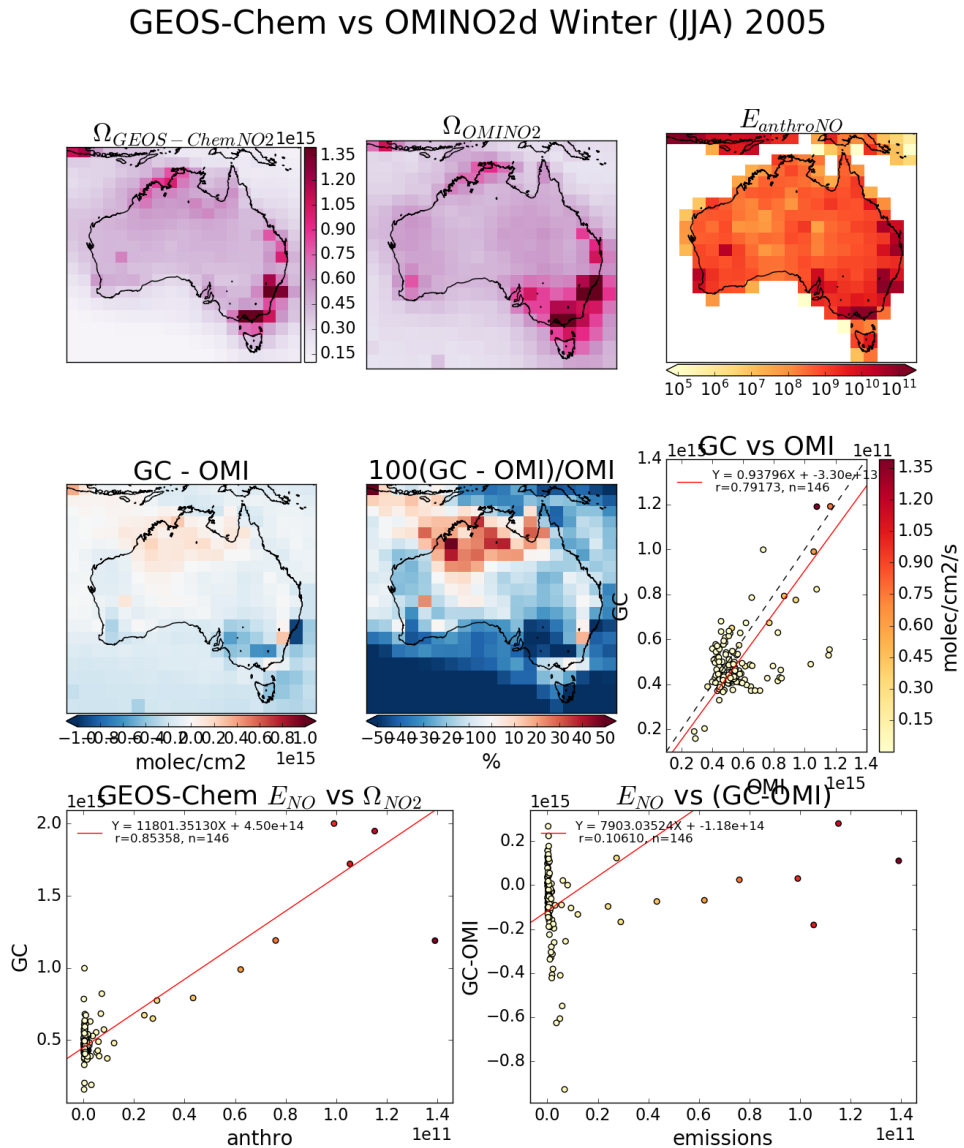


FIGURE 2.21: As figure 2.15, for Winter 2005, with soil NO emissions replacing anthropogenic NO emissions.

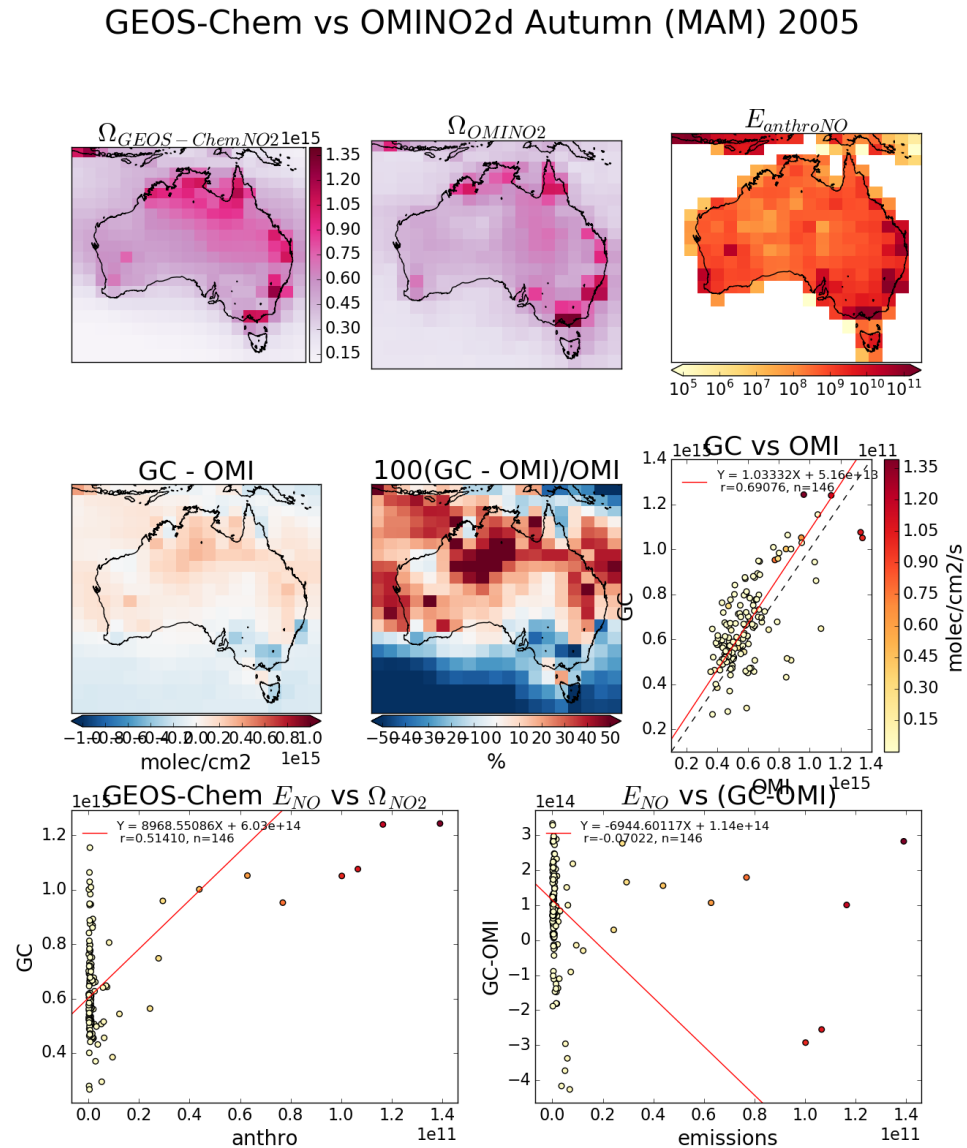


FIGURE 2.22: As figure 2.15, for Spring 2005, with soil NO emissions replacing anthropogenic NO emissions.

Bibliography

- Brasseur, Guy P and Daniel J Jacob (2017). *Modeling of Atmospheric Chemistry*. Cambridge University Press. DOI: [10.1017/9781316544754](https://doi.org/10.1017/9781316544754).
- Hsieh, Nan-Hung and Chung-Min Liao (2013). "Fluctuations in air pollution give risk warning signals of asthma hospitalization". In: *Atmospheric Environment* 75, pp. 206–216. DOI: [10.1016/j.atmosenv.2013.04.043](https://doi.org/10.1016/j.atmosenv.2013.04.043). URL: <http://dx.doi.org/10.1016/j.atmosenv.2013.04.043>.
- Avnery, Shiri et al. (2013). "Global crop yield reductions due to surface ozone exposure: 2. Year 2030 potential crop production losses and economic damage under two scenarios of O₃ pollution". In: *Atmospheric Environment* 71.13, pp. 408–409. ISSN: 13522310. DOI: [10.1016/j.atmosenv.2012.12.045](https://doi.org/10.1016/j.atmosenv.2012.12.045). URL: <http://dx.doi.org/10.1016/j.atmosenv.2011.01.002>.
- Yue, Xu et al. (2017). "Ozone and haze pollution weakens net primary productivity in China". In: *Atmospheric Chemistry and Physics* 17.9, pp. 6073–6089. ISSN: 1680-7324. DOI: [10.5194/acp-17-6073-2017](https://doi.org/10.5194/acp-17-6073-2017). URL: <https://www.atmos-chem-phys.net/17/6073/2017/>.
- Myhre, G and D Shindell (2013). Chapter 8: *Anthropogenic and Natural Radiative Forcing*, in *Climate Change 2013: The Physical Science Basis, Working Group 1 Contribution to the Fifth Assessment Report of the Intergovernmental Panel on Climate Change*, 2013. Fifth Assessment Report of the Intergovernmental Panel on Climate Change, 2013.
- Monks, P. S. et al. (2015). "Tropospheric ozone and its precursors from the urban to the global scale from air quality to short-lived climate forcer". In: *Atmospheric Chemistry and Physics* 15.15, pp. 8889–8973. ISSN: 1680-7324. DOI: [10.5194/acp-15-8889-2015](https://doi.org/10.5194/acp-15-8889-2015). URL: <https://www.atmos-chem-phys.net/15/8889/2015/>.
- Lelieveld, J. et al. (2013). "Model calculated global, regional and megacity premature mortality due to air pollution". In: *Atmospheric Chemistry and Physics* 13.14, pp. 7023–7037. ISSN: 16807324. DOI: [10.5194/acp-13-7023-2013](https://doi.org/10.5194/acp-13-7023-2013).
- Ayers, James D and William R Simpson (2006). "Measurements of N₂O₅ near Fairbanks, Alaska". In: *Journal of Geophysical Research: Atmospheres* 111.D14, n/a–n/a. ISSN: 2156-2202. DOI: [10.1029/2006JD007070](https://doi.org/10.1029/2006JD007070). URL: <http://dx.doi.org/10.1029/2006JD007070>.
- Lelieveld, J. et al. (2009). "Severe ozone air pollution in the Persian Gulf region". In: *Atmospheric Chemistry and Physics* 9, pp. 1393–1406. ISSN: 1680-7324. DOI: [10.5194/acp-9-1393-2009](https://doi.org/10.5194/acp-9-1393-2009).
- Ashmore, M R, Lisa. Emberson, and Murray Frank (2003). *Air pollution impacts on crops and forests : a global assessment*. Ed. by Lisa Emberson, Mike Ashmore, and Frank Murray. Imperial College Press London ; River Edge, NJ, xiii, 372 p. : ISBN: 186094292.

- Stevenson, D. S. et al. (2013). "Tropospheric ozone changes, radiative forcing and attribution to emissions in the Atmospheric Chemistry and Climate Model Intercomparison Project (ACCMIP)". In: *Atmospheric Chemistry and Physics* 13.6, pp. 3063–3085. ISSN: 16807316. DOI: [10.5194/acp-13-3063-2013](https://doi.org/10.5194/acp-13-3063-2013).
- Selin, N E et al. (2009). "Global health and economic impacts of future ozone pollution". In: *Environmental Research Letters* 4.4, p. 044014. ISSN: 1748-9326. DOI: [10.1088/1748-9326/4/4/044014](https://doi.org/10.1088/1748-9326/4/4/044014).
- Atkinson, Roger (2000). "Atmospheric chemistry of VOCs and NO(x)". In: *Atmospheric Environment* 34.12-14, pp. 2063–2101. ISSN: 13522310. DOI: [10.1016/S1352-2310\(99\)00460-4](https://doi.org/10.1016/S1352-2310(99)00460-4).
- Fuentes, J. D. et al. (2000). "Biogenic Hydrocarbons in the Atmospheric Boundary Layer: A Review". In: *Bulletin of the American Meteorological Society* 81.7, pp. 1537–1575. ISSN: 00030007. DOI: [10.1175/1520-0477\(2000\)081<1537:BHITAB>2.3.CO;2](https://doi.org/10.1175/1520-0477(2000)081<1537:BHITAB>2.3.CO;2). arXiv: [arXiv : 1011.1669v3](https://arxiv.org/abs/1011.1669v3). URL: [http://journals.ametsoc.org/doi/abs/10.1175/1520-0477\(2000\)081%3C1537%3ABHITAB%3E2.3.CO%3B2](http://journals.ametsoc.org/doi/abs/10.1175/1520-0477(2000)081%3C1537%3ABHITAB%3E2.3.CO%3B2).
- Paulot, Fabien et al. (2009b). "Unexpected Epoxide Formation in the". In: *Science* 325.2009, pp. 730–733. ISSN: 0036-8075. DOI: [10.1126/science.1172910](https://doi.org/10.1126/science.1172910).
- Atkinson, Roger and Janet Arey (2003). "Gas-phase tropospheric chemistry of biogenic volatile organic compounds: A review". In: *Atmospheric Environment* 37.SUPPL. 2. ISSN: 13522310. DOI: [10.1016/S1352-2310\(03\)00391-1](https://doi.org/10.1016/S1352-2310(03)00391-1).
- Jacob, Daniel J (1999). *Introduction to Atmospheric Chemistry*. Ed. by Daniel J Jacob. Princeton University Press. URL: <http://acmg.seas.harvard.edu/people/faculty/djj/book/index.html>.
- Huang, Guanyu et al. (2017). "Validation of 10-year SAO OMI Ozone Profile (PROFOZ) Product Using Aura MLS Measurements". In: *Atmospheric Measurement Techniques Discussions*, pp. 1–25. ISSN: 1867-8610. DOI: [10.5194/amt-2017-92](https://doi.org/10.5194/amt-2017-92). URL: <https://www.atmos-meas-tech-discuss.net/amt-2017-92/>.
- Cape, J. N. (2008). "Surface ozone concentrations and ecosystem health: Past trends and a guide to future projections". In: *Science of the Total Environment* 400.1-3, pp. 257–269. ISSN: 00489697. DOI: [10.1016/j.scitotenv.2008.06.025](https://doi.org/10.1016/j.scitotenv.2008.06.025). URL: [http://dx.doi.org/10.1016/j.scitotenv.2008.06.025](https://doi.org/10.1016/j.scitotenv.2008.06.025).
- Young, P J et al. (2017). "Tropospheric Ozone Assessment Report (TOAR): Assessment of global-scale model performance for global and regional ozone distributions, variability, and trends". In: *Elementa: Science of the Anthropocene*, pp. 0–84. ISSN: 2325-1026. DOI: [10.1525/elementa.265](https://doi.org/10.1525/elementa.265). URL: http://eprints.lancs.ac.uk/88836/1/TOAR_Model_Performance_07062017.pdfhttp://www.igacproject.org/sites/default/files/2017-05/TOAR-Model_Performance_draft_for_open_comment.pdf.
- Delmas, R, D Serca, and C Jambert (1997). "Global inventory of NOx sources". In: *Nutrient cycling in agroecosystems* 48.x, pp. 51–60. ISSN: 1385-1314. DOI: [10.1023/A:1009793806086](https://doi.org/10.1023/A:1009793806086). URL: [http://link.springer.com/article/10.1023/A:1009793806086](https://doi.org/10.1023/A:1009793806086).
- Sillman, Sanford (1999). "The relation between ozone , NO and hydrocarbons in urban and polluted rural environments". In: *Atmospheric Environment* 33. DOI: [https://doi.org/10.1016/S1352-2310\(98\)00345-8](https://doi.org/10.1016/S1352-2310(98)00345-8). URL: <http://www-personal>.

- umich . edu /\$ \sim \\$ sillman / web - publications / Sillmanreview99 . pdf https : //www.sciencedirect.com/science/article/pii/S1352231098003458.
- Stohl, Andreas et al. (2003). "A new perspective of stratosphere-troposphere exchange". In: *Bulletin of the American Meteorological Society* 84.11, pp. 1565–1573+1473. ISSN: 00030007. DOI: 10.1175/BAMS-84-11-1565.
- Kuang, Shi et al. (2017). "Summertime tropospheric ozone enhancement associated with a cold front passage due to stratosphere-to-troposphere transport and biomass burning: Simultaneous ground-based lidar and airborne measurements". In: *Journal of Geophysical Research: Atmospheres* 122.2, pp. 1293–1311. ISSN: 21698996. DOI: 10.1002/2016JD026078. URL: <http://doi.wiley.com/10.1002/2016JD026078>.
- Sprenger, Michael, Mischa Croci Maspoli, and Heini Wernli (2003). "Tropopause folds and cross-tropopause exchange: A global investigation based upon ECMWF analyses for the time period March 2000 to February 2001". In: *Journal of Geophysical Research* 108.D12. ISSN: 2156-2202. DOI: 10.1029/2002JD002587. URL: <http://dx.doi.org/10.1029/2002JD002587>.
- Ojha, Narendra et al. (2016). "Secondary ozone peaks in the troposphere over the Himalayas". In: *Atmospheric Chemistry and Physics Discussions* 17.November, pp. 1–25. ISSN: 1680-7375. DOI: 10.5194/acp-2016-908. URL: <http://www.atmos-chem-phys-discuss.net/acp-2016-908/>.
- Hegglin, Michaela I and Theodore G Shepherd (2009). "Large climate-induced changes in ultraviolet index and stratosphere-to-troposphere ozone flux". In: *Nature Geoscience* 2.10, pp. 687–691. DOI: 10.1038/ngeo604. URL: <http://dx.doi.org/10.1038/ngeo604>.
- Liu, Junhua et al. (2017). "Causes of interannual variability over the southern hemispheric tropospheric ozone maximum". In: *Atmos. Chem. Phys* 17.5, pp. 3279–3299. ISSN: 1680-7324. DOI: 10.5194/acp-17-3279-2017. URL: www.atmos-chem-phys.net/17/3279/2017/.
- Lin, Meiyun et al. (2015). "Climate variability modulates western US ozone air quality in spring via deep stratospheric intrusions." In: *Nature communications* 6.May, p. 7105. ISSN: 2041-1723. DOI: 10.1038/ncomms8105. URL: <http://www.nature.com/ncomms/2015/150512/ncomms8105/full/ncomms8105.html>.
- Young, P. J. et al. (2013). "Preindustrial to present-day changes in tropospheric hydroxyl radical and methane lifetime from the Atmospheric Chemistry and Climate Model Intercomparison Project (ACCMIP)". In: *Atmospheric Chemistry and Physics* 13.10, pp. 5277–5298. ISSN: 16807316. DOI: 10.5194/acp-13-5277-2013.
- Marvin, Margaret R. et al. (2017). "Impact of evolving isoprene mechanisms on simulated formaldehyde: An inter-comparison supported by in situ observations from SENEX". In: *Atmospheric Environment* 164, pp. 325–336. ISSN: 13522310. DOI: 10.1016/j.atmosenv.2017.05.049. URL: https://ac.els-cdn.com/S1352231017303618/1-s2.0-S1352231017303618-main.pdf?_tid=3de7eaaa-06ff-11e8-99a9-0000aacb360&acdnat=1517455576_09d7334af609ed43470155c1c42fad5fhttp://www.sciencedirect.com/science/article/pii/S1352231017303618.
- Mazzuca, Gina M. et al. (2016). "Ozone production and its sensitivity to NO_x and VOCs: Results from the DISCOVER-AQ field experiment, Houston 2013". In: *Atmospheric Chemistry and Physics* 16.22, pp. 14463–14474. ISSN: 16807324. DOI: 10.5194/acp-16-14463-2016.

- Stevenson, D S et al. (2006). "Multimodel ensemble simulations of present-day and near-future tropospheric ozone". In: *Journal of Geophysical Research* 111.D8. DOI: [10.1029/2005jd006338](https://doi.org/10.1029/2005jd006338). URL: <http://dx.doi.org/10.1029/2005JD006338>.
- Guenther, Alex et al. (2000). "Natural emissions of non-methane volatile organic compounds, carbon monoxide, and oxides of nitrogen from North America". In: *Atmospheric Environment* 34.12-14, pp. 2205–2230. ISSN: 13522310. DOI: [10.1016/S1352-2310\(99\)00465-3](https://doi.org/10.1016/S1352-2310(99)00465-3).
- Guenther, Alex et al. (1995). "A global model of natural volatile organic compound emissions". In: *Journal of Geophysical Research* 100.D5, pp. 8873–8892. ISSN: 0148-0227. DOI: [10.1029/94JD02950](https://doi.org/10.1029/94JD02950). URL: <http://onlinelibrary.wiley.com/doi/10.1029/94JD02950/full>.
- Glasius, Marianne and Allen H. Goldstein (2016). "Recent Discoveries and Future Challenges in Atmospheric Organic Chemistry". In: *Environmental Science and Technology* 50.6, pp. 2754–2764. ISSN: 15205851. DOI: [10.1021/acs.est.5b05105](https://doi.org/10.1021/acs.est.5b05105).
- Yue, X., N. Unger, and Y. Zheng (2015). "Distinguishing the drivers of trends in land carbon fluxes and plant volatile emissions over the past 3 decades". In: *Atmospheric Chemistry and Physics* 15.20, pp. 11931–11948. ISSN: 16807324. DOI: [10.5194/acp-15-11931-2015](https://doi.org/10.5194/acp-15-11931-2015).
- Stavrakou, T. et al. (2014). "Isoprene emissions over Asia 1979–2012: Impact of climate and land-use changes". In: *Atmospheric Chemistry and Physics* 14.9. ISSN: 16807324. DOI: [10.5194/acp-14-4587-2014](https://doi.org/10.5194/acp-14-4587-2014).
- Kwon, Hyeong-Ahn et al. (2017). "Sensitivity of formaldehyde (HCHO) column measurements from a geostationary satellite to temporal variation of the air mass factor in East Asia". In: *Atmospheric Chemistry and Physics* 17.7, pp. 4673–4686. ISSN: 1680-7324. DOI: [10.5194/acp-17-4673-2017](https://doi.org/10.5194/acp-17-4673-2017). URL: <http://www.atmos-chem-phys.net/17/4673/2017/>.
- Kanakidou, M et al. (2005). "Physics Organic aerosol and global climate modelling : a review". In: *Atmospheric Chemistry and Physics* 5, pp. 1053–1123.
- Aksoyoglu, Sebnem et al. (2017). "Secondary inorganic aerosols in Europe: sources and the significant influence of biogenic VOC emissions, especially on ammonium nitrate". In: *Atmospheric Chemistry and Physics* 17.12, pp. 7757–7773. ISSN: 1680-7324. DOI: [10.5194/acp-17-7757-2017](https://doi.org/10.5194/acp-17-7757-2017). URL: <https://www.atmos-chem-phys.net/17/7757/2017/>.
- Forster, P. et al. (2007). *Changes in Atmospheric Constituents and in Radiative Forcing*. In: *Climate Change 2007: The Physical Science Basis. Contribution of Working Group I to the Fourth Assessment Report of the Intergovernmental Panel on Climate Change* [Solomon, S., D. Qin, M. Man. URL: https://www.ipcc.ch/publications_and_data/ar4/wg1/en/ch2.html (visited on 01/14/2016).
- Lelieveld, J et al. (2015). "The contribution of outdoor air pollution sources to premature mortality on a global scale". In: *Nature* 525.7569, pp. 367–371. DOI: [10.1038/nature15371](https://doi.org/10.1038/nature15371). URL: <http://dx.doi.org/10.1038/nature15371>.
- Hoek, Gerard et al. (2013). "Long-term air pollution exposure and cardio-respiratory mortality: a review". In: *Environmental Health* 12.1, p. 43. DOI: [10.1186/1476-069x-12-43](https://doi.org/10.1186/1476-069x-12-43). URL: <http://dx.doi.org/10.1186/1476-069x-12-43>.

- Krewski, D et al. (2009). "Extended follow-up and spatial analysis of the American Cancer Society study linking particulate air pollution and mortality". In: *Res Rep Health Eff Inst* 140, pp. 5–36. ISSN: 1041-5505 (Print) 1041-5505 (Linking). URL: <http://www.ncbi.nlm.nih.gov/pubmed/19627030>.
- Silva, Raquel A et al. (2013). "Global premature mortality due to anthropogenic outdoor air pollution and the contribution of past climate change". In: *Environ. Res. Lett.* 8.3, p. 34005. DOI: [10.1088/1748-9326/8/3/034005](https://doi.org/10.1088/1748-9326/8/3/034005). URL: <http://dx.doi.org/10.1088/1748-9326/8/3/034005>.
- Kroll, Jesse H. and John H. Seinfeld (2008). "Chemistry of secondary organic aerosol: Formation and evolution of low-volatility organics in the atmosphere". In: *Atmospheric Environment* 42.16, pp. 3593–3624. ISSN: 13522310. DOI: [10.1016/j.atmosenv.2008.01.003](https://doi.org/10.1016/j.atmosenv.2008.01.003). URL: <http://www.sciencedirect.com.ezproxy.uow.edu.au/science/article/pii/S1352231008000253>.
- Guenther, A et al. (2006). "Estimates of global terrestrial isoprene emissions using MEGAN (Model of Emissions of Gases and Aerosols from Nature)". In: *Atmospheric Chemistry and Physics* 6.11, pp. 3181–3210. DOI: [10.5194/acp-6-3181-2006](https://doi.org/10.5194/acp-6-3181-2006). URL: <http://dx.doi.org/10.5194/acp-6-3181-2006>.
- Millet, Dylan B et al. (2006). "Formaldehyde distribution over North America: Implications for satellite retrievals of formaldehyde columns and isoprene emission". In: *J. Geophys. Res.* 111.D24. DOI: [10.1029/2005jd006853](https://doi.org/10.1029/2005jd006853). URL: [TODO](#).
- Arneth, A et al. (2008). "Why are estimates of global terrestrial isoprene emissions so similar (and why is this not so for monoterpenes)?" In: *Atmos. Chem. Phys* 8.x, pp. 4605–4620. ISSN: 1680-7375. DOI: [10.5194/acpd-8-7017-2008](https://doi.org/10.5194/acpd-8-7017-2008).
- Niinemets, U. et al. (2010). "The emission factor of volatile isoprenoids: Stress, acclimation, and developmental responses". In: *Biogeosciences* 7.7, pp. 2203–2223. ISSN: 17264170. DOI: [10.5194/bg-7-2203-2010](https://doi.org/10.5194/bg-7-2203-2010).
- Müller, Jean-François (1992). "Geographical distribution and seasonal variation of surface emissions and deposition velocities of atmospheric trace gases". In: *Journal of Geophysical Research: Atmospheres* 97.D4, pp. 3787–3804. ISSN: 2156-2202. DOI: [10.1029/91JD02757](https://doi.org/10.1029/91JD02757). URL: <http://dx.doi.org/10.1029/91JD02757>.
- Kefauver, Shawn C., Iolanda Filella, and Josep Peñuelas (2014). "Remote sensing of atmospheric biogenic volatile organic compounds (BVOCs) via satellite-based formaldehyde vertical column assessments". en. In: *International Journal of Remote Sensing*. URL: <http://www.tandfonline.com/doi/abs/10.1080/01431161.2014.968690#.VkjEubNM61M>.
- Brown, S. S. et al. (2009). "Nocturnal isoprene oxidation over the Northeast United States in summer and its impact on reactive nitrogen partitioning and secondary organic aerosol". In: *Atmospheric Chemistry and Physics* 9.9, pp. 3027–3042. ISSN: 16807316. DOI: [10.5194/acp-9-3027-2009](https://doi.org/10.5194/acp-9-3027-2009).
- Guenther, A. B. et al. (2012). "The model of emissions of gases and aerosols from nature version 2.1 (MEGAN2.1): An extended and updated framework for modeling biogenic emissions". In: *Geoscientific Model Development* 5.6, pp. 1471–1492. ISSN: 1991959X. DOI: [10.5194/gmd-5-1471-2012](https://doi.org/10.5194/gmd-5-1471-2012).
- Messina, Palmira et al. (2016). "Global biogenic volatile organic compound emissions in the ORCHIDEE and MEGAN models and sensitivity to key parameters". In: *Atmospheric Chemistry and Physics* 16.22, pp. 14169–14202. ISSN: 16807324. DOI: [10.5194/acp-16-14169-2016](https://doi.org/10.5194/acp-16-14169-2016).

- 5194/acp-16-14169-2016. URL: <http://www.atmos-chem-phys.net/16/14169/2016/acp-16-14169-2016.pdf>.
- Wagner, V (2002). "Are CH₂O measurements in the marine boundary layer suitable for testing the current understanding of CH₄ photooxidation?: A model study". In: *Journal of Geophysical Research* 107.D3, p. 4029. ISSN: 0148-0227. DOI: [10.1029/2001JD000722](https://doi.wiley.com/10.1029/2001JD000722). URL: <http://doi.wiley.com/10.1029/2001JD000722>.
- Nguyen, T. B. et al. (2014). "Overview of the Focused Isoprene eXperiment at the California Institute of Technology (FIXCIT): Mechanistic chamber studies on the oxidation of biogenic compounds". In: *Atmospheric Chemistry and Physics* 14.24. ISSN: 16807324. DOI: [10.5194/acp-14-13531-2014](https://doi.org/10.5194/acp-14-13531-2014).
- Crounse, John D et al. (2012). "Atmospheric Fate of Methacrolein. 1. Peroxy Radical Isomerization Following Addition of OH and O₂". In: *Physical Chemistry m.*
- Wolfe, G. M. et al. (2016). "Formaldehyde production from isoprene oxidation across NO_x regimes". In: *Atmospheric Chemistry and Physics* 16.x, pp. 2597–2610. ISSN: 16807324. DOI: [10.5194/acp-16-2597-2016](https://doi.org/10.5194/acp-16-2597-2016). URL: www.atmos-chem-phys.net/16/2597/2016/.
- Liu, Yingjun et al. (2016b). "Isoprene photochemistry over the Amazon rainforest". In: *Proceedings of the National Academy of Sciences* 113.22, pp. 6125–6130. ISSN: 0027-8424. DOI: [10.1073/pnas.1524136113](https://doi.org/10.1073/pnas.1524136113). URL: <http://www.pnas.org/content/113/22/6125.abstract>.
- PATCHEN, AMIE K. et al. (2007). "Direct Kinetics Study of the Product-Forming Channels of the Reaction of Isoprene-Derived Hydroxyperoxy Radicals with NO". In: *International journal of Chemical Kinetics* 31.5, pp. 493–499. ISSN: 13000527. DOI: [10.1002/kin.20248/full](https://doi.org/10.1002/kin.20248). URL: <http://onlinelibrary.wiley.com/wol1/doi/10.1002/kin.20248/full>.
- Mao, Jingqiu et al. (2013). "Ozone and organic nitrates over the eastern United States: Sensitivity to isoprene chemistry". In: *Journal of Geophysical Research Atmospheres* 118.19, pp. 11256–11268. ISSN: 21698996. DOI: [10.1002/jgrd.50817](https://doi.org/10.1002/jgrd.50817).
- Paulot, F. et al. (2009a). "Isoprene photooxidation: new insights into the production of acids and organic nitrates". In: *Atmospheric Chemistry and Physics* 9.4, pp. 1479–1501. ISSN: 1680-7324. DOI: [10.5194/acp-9-1479-2009](https://doi.org/10.5194/acp-9-1479-2009).
- Crounse, John D. et al. (2013). "Autoxidation of organic compounds in the atmosphere". In: *Journal of Physical Chemistry Letters* 4.20, pp. 3513–3520. ISSN: 19487185. DOI: [10.1021/jz4019207](https://doi.org/10.1021/jz4019207). URL: <http://pubs.acs.org/doi/abs/10.1021/jz4019207>.
- Lin, Ying-Hsuan et al. (2013). "Epoxide as a precursor to secondary organic aerosol formation from isoprene photooxidation in the presence of nitrogen oxides". In: DOI: [10.1073/pnas.1221150110](https://doi.org/10.1073/pnas.1221150110). URL: <http://www.pnas.org/content/110/17/6718.full.pdf>.
- Peeters, Jozef and Jean-Francis Muller (2010). "HO_x radical regeneration in isoprene oxidation via peroxy radical isomerisations. II: experimental evidence and global impact". In: *Physical Chemistry Chemical Physics* 12.42, p. 14227. ISSN: 1463-9076. DOI: [10.1039/c0cp00811g](https://doi.org/10.1039/c0cp00811g). URL: <http://pubs.rsc.org/en/content/articlepdf/2010/cp/c0cp00811g>.

- Mao, J. et al. (2012). "Insights into hydroxyl measurements and atmospheric oxidation in a California forest". In: *Atmospheric Chemistry and Physics* 12.17, pp. 8009–8020. ISSN: 16807316. DOI: [10.5194/acp-12-8009-2012](https://doi.org/10.5194/acp-12-8009-2012).
- Surratt, Jason D et al. "Reactive intermediates revealed in secondary organic aerosol formation from isoprene". In: DOI: [10.1073/pnas.0911114107](https://doi.org/10.1073/pnas.0911114107). URL: <http://www.pnas.org/content/107/15/6640.full.pdf>.
- Nguyen, Tran B. et al. (2016). "Atmospheric fates of Criegee intermediates in the ozonolysis of isoprene". In: *Phys. Chem. Chem. Phys.* 18.15, pp. 10241–10254. ISSN: 1463-9076. DOI: [10.1039/C6CP00053C](https://doi.org/10.1039/C6CP00053C). URL: <http://xlink.rsc.org/?DOI=C6CP00053C>.
- Rollins, A W et al. (2009). "Isoprene oxidation by nitrate radical: alkyl nitrate and secondary organic aerosol yields". In: *Atmos. Chem. Phys. Atmospheric Chemistry and Physics* 9, pp. 6685–6703. URL: www.atmos-chem-phys.net/9/6685/2009/.
- Intergovernmental Panel on Climate Change (IPCC): *Climate Change: The Scientific Basis* (2001). Tech. rep. Cambridge University Press. URL: <http://www.ipcc.ch/ipccreports/tar/>.
- Stocker, T.F. et al. *IPCC, 2013: Climate Change 2013: The Physical Science Basis. Contribution of Working Group I to the Fifth Assessment Report of the Intergovernmental Panel on Climate Change*. Tech. rep. Cambridge University Press, Cambridge, United Kingdom and New York, NY, USA. DOI: [10.1017/CBO9781107415324](https://doi.org/10.1017/CBO9781107415324).
- Davenport, J. J. et al. (2015). "A measurement strategy for non-dispersive ultra-violet detection of formaldehyde in indoor air : spectral analysis and interferent gases". In: *Measurement Science and Technology* 015802. December 2015, p. 15802. ISSN: 0957-0233. DOI: [10.1088/0957-0233/27/1/015802](https://doi.org/10.1088/0957-0233/27/1/015802). URL: <http://dx.doi.org/10.1088/0957-0233/27/1/015802>.
- Palmer, Paul I (2003). "Mapping isoprene emissions over North America using formaldehyde column observations from space". In: *J. Geophys. Res.* 108.D6. DOI: [10.1029/2002jd002153](https://doi.org/10.1029/2002jd002153). URL: <http://dx.doi.org/10.1029/2002jd002153>.
- Shim, Changsub et al. (2005). "Constraining global isoprene emissions with Global Ozone Monitoring Experiment (GOME) formaldehyde column measurements". In: *Journal of Geophysical Research Atmospheres* 110.24, pp. 1–14. ISSN: 01480227. DOI: [10.1029/2004JD005629](https://doi.org/10.1029/2004JD005629).
- Andreae, M O (2001). "Emission of trace gases and aerosols from biomass burning". In: *Biogeochemistry* 15.4, pp. 955–966. URL: <http://onlinelibrary.wiley.com/doi/10.1029/2000GB001382/epdf>.
- Millet, Dylan B. et al. (2008). "Spatial distribution of isoprene emissions from North America derived from formaldehyde column measurements by the OMI satellite sensor". In: *Journal of Geophysical Research Atmospheres* 113.2, pp. 1–18. ISSN: 01480227. DOI: [10.1029/2007JD008950](https://doi.org/10.1029/2007JD008950).
- Zhu, Lei et al. (2014). "Anthropogenic emissions of highly reactive volatile organic compounds in eastern Texas inferred from oversampling of satellite (OMI) measurements of HCHO columns". In: *Environmental Research Letters* 9.11, p. 114004. ISSN: 1748-9326. DOI: [10.1088/1748-9326/9/11/114004](https://doi.org/10.1088/1748-9326/9/11/114004). URL: <http://stacks.iop.org/1748-9326/9/i=11/a=114004?key=crossref.3d2869ee02fd4f0792f831ac8cbec117>.
- Fu, Tzung-may et al. (2007). "Space-based formaldehyde measurements as constraints on volatile organic compound emissions in east and south Asia and implications for ozone". In: 112, pp. 1–15. DOI: [10.1029/2006JD007853](https://doi.org/10.1029/2006JD007853).

- Emmerson, Kathryn M. et al. (2016). "Current estimates of biogenic emissions from eucalypts uncertain for southeast Australia". In: *Atmospheric Chemistry and Physics* 16.11, pp. 6997–7011. ISSN: 1680-7324. DOI: [10.5194/acp-16-6997-2016](https://doi.org/10.5194/acp-16-6997-2016). URL: <http://www.atmos-chem-phys.net/16/6997/2016/>.
- CRUTZEN, PAUL J, MARK G LAWRENCE, and ULRICH PÖSCHL (1999). "On the background photochemistry of tropospheric ozone". In: *Tellus A* 51.1, pp. 123–146. ISSN: 1600-0870. DOI: [10.1034/j.1600-0870.1999.t01-1-00010.x](https://doi.org/10.1034/j.1600-0870.1999.t01-1-00010.x). URL: <http://dx.doi.org/10.1034/j.1600-0870.1999.t01-1-00010.x>.
- Levy, Hiram (1972). "Photochemistry of the lower troposphere". In: *Planetary and Space Science* 20.6, pp. 919–935. ISSN: 00320633. DOI: [10.1016/0032-0633\(72\)90177-8](https://doi.org/10.1016/0032-0633(72)90177-8).
- Franco, B. et al. (2015). "Retrievals of formaldehyde from ground-based FTIR and MAX-DOAS observations at the Jungfraujoch station and comparisons with GEOS-Chem and IMAGES model simulations". In: *Atmospheric Measurement Techniques* 8.4, pp. 1733–1756. ISSN: 18678548. DOI: [10.5194/amt-8-1733-2015](https://doi.org/10.5194/amt-8-1733-2015).
- Gonzalez Abad, G. et al. (2015). "Updated Smithsonian Astrophysical Observatory Ozone Monitoring Instrument (SAO OMI) formaldehyde retrieval". In: *Atmospheric Measurement Techniques* 8.1, pp. 19–32. ISSN: 18678548. DOI: [10.5194/amt-8-19-2015](https://doi.org/10.5194/amt-8-19-2015).
- Lee, Anita et al. (2006). "Gas-phase products and secondary aerosol yields from the ozonolysis of ten different terpenes". In: 111.Ci, pp. 1–18. DOI: [10.1029/2005JD006437](https://doi.org/10.1029/2005JD006437).
- Hak, C. et al. (2005). "Intercomparison of four different in-situ techniques for ambient formaldehyde measurements in urban air". In: *Atmospheric Chemistry and Physics Discussions* 5.3, pp. 2897–2945. ISSN: 1680-7316. DOI: [10.5194/acpd-5-2897-2005](https://doi.org/10.5194/acpd-5-2897-2005).
- Chevallier, F. et al. (2012). "The formaldehyde budget as seen by a global-scale multi-constraint and multi-species inversion system". In: *Atmospheric Chemistry and Physics* 12.15, pp. 6699–6721. ISSN: 16807316. DOI: [10.5194/acp-12-6699-2012](https://doi.org/10.5194/acp-12-6699-2012). URL: <http://www.atmos-chem-phys.net/12/6699/2012/acp-12-6699-2012.pdf>.
- EUMETSAT (2015). GOME2. URL: <http://www.eumetsat.int/website/home/Satellites/CurrentSatellites/Metop/MetopDesign/GOME2/index.html>.
- Dufour, G. et al. (2008). "SCIAMACHY formaldehyde observations: constraint for isoprene emissions over Europe?" In: *Atmospheric Chemistry and Physics* 8.6, pp. 19273–19312. ISSN: 1680-7324. DOI: [10.5194/acpd-8-19273-2008](https://doi.org/10.5194/acpd-8-19273-2008).
- Marais, E A et al. (2012). "Isoprene emissions in Africa inferred from OMI observations of formaldehyde columns". In: *Atmospheric Chemistry and Physics* 12.3, pp. 7475–7520. DOI: [10.5194/acp-12-6219-2012](https://doi.org/10.5194/acp-12-6219-2012). URL: <http://dx.doi.org/10.5194/acp-12-6219-2012>.
- Bauwens, M et al. (2013). "Satellite-based isoprene emission estimates (2007–2012) from the GlobEmission project". In: *Proceedings of the ACCENT-Plus Symposium, Atmospheric Composition Change-Policy Support and Science, Urbino*, pp. 17–20.
- Bauwens, Maite et al. (2016). "Nine years of global hydrocarbon emissions based on source inversion of OMI formaldehyde observations". In: *Atmospheric Chemistry and Physics Discussions* March, pp. 1–45. ISSN: 1680-7375. DOI: [10.5194/acp-2016-221](https://doi.org/10.5194/acp-2016-221). URL: <http://www.atmos-chem-phys-discuss.net/acp-2016-221/>.

- Zhang, Yang et al. (2012). "Impact of gas-phase mechanisms on Weather Research Forecasting Model with Chemistry (WRF/Chem) predictions: Mechanism implementation and comparative evaluation". In: *Journal of Geophysical Research: Atmospheres* 117.D1, n/a-n/a. DOI: [10.1029/2011JD015775](https://doi.wiley.com/10.1029/2011JD015775). URL: <http://doi.wiley.com/10.1029/2011JD015775>.
- Marais, E A et al. (2014). "Improved model of isoprene emissions in Africa using Ozone Monitoring Instrument (OMI) satellite observations of formaldehyde: implications for oxidants and particulate matter". In: *Atmospheric Chemistry and Physics* 14.15, pp. 7693–7703. DOI: [10.5194/acp-14-7693-2014](https://doi.org/10.5194/acp-14-7693-2014). URL: <http://dx.doi.org/10.5194/acp-14-7693-2014>.
- Miller, C. et al. (2014). "Glyoxal retrieval from the Ozone Monitoring Instrument". In: *Atmospheric Measurement Techniques* 7.11, pp. 3891–3907. ISSN: 1867-8548. DOI: [10.5194/amt-7-3891-2014](https://doi.org/10.5194/amt-7-3891-2014). URL: <http://www.atmos-meas-tech.net/7/3891/2014/>.
- Zeng, G. et al. (2015). "Multi-model simulation of CO and HCHO in the Southern Hemisphere: comparison with observations and impact of biogenic emissions". In: *Atmospheric Chemistry and Physics* 15.13, pp. 7217–7245. ISSN: 1680-7324. DOI: [10.5194/acp-15-7217-2015](https://doi.org/10.5194/acp-15-7217-2015). URL: <http://www.atmos-chem-phys.net/15/7217/2015/>.
- Niinemets, U. et al. (1999). "A model of isoprene emission based on energetic requirements for isoprene synthesis and leaf photosynthetic properties for Liquidambar and Quercus". In: *Plant, Cell and Environment* 22.11, pp. 1319–1335. ISSN: 01407791. DOI: [10.1046/j.1365-3040.1999.00505.x](https://doi.org/10.1046/j.1365-3040.1999.00505.x).
- Arneth, Almut et al. (2007). "CO₂ inhibition of global terrestrial isoprene emissions: Potential implications for atmospheric chemistry". In: *Geophysical Research Letters* 34.18, p. L18813. DOI: [10.1029/2007GL030615](https://doi.wiley.com/10.1029/2007GL030615). URL: <http://doi.wiley.com/10.1029/2007GL030615>.
- Hewitt, C N et al. (2011). "Ground-level ozone influenced by circadian control of isoprene emissions". In: *Nature Geoscience* 4.10, pp. 671–674. DOI: [10.1038/ngeo1271](https://doi.org/10.1038/ngeo1271). URL: <http://dx.doi.org/10.1038/ngeo1271>.
- Fan, Jiwen and Renyi Zhang (2004). "Atmospheric oxidation mechanism of isoprene". In: *Environmental Chemistry* 1.3, pp. 140–149. ISSN: 14482517. DOI: [10.1071/EN04045](https://doi.org/10.1071/EN04045). URL: <http://dx.doi.org/10.1071/en04045>.
- Müller, J.-F. et al. (2008). "Global isoprene emissions estimated using MEGAN ECMWF analyses and a detailed canopy environment model". In: *Atmospheric Chemistry and Physics Discussions* 7.6, pp. 15373–15407. DOI: [10.5194/acpd-7-15373-2007](https://doi.org/10.5194/acpd-7-15373-2007). URL: <http://dx.doi.org/10.5194/acpd-7-15373-2007>.
- Winters, Anthony J et al. (2009). "Emissions of isoprene, monoterpene and short-chained carbonyl compounds from Eucalyptus spp. in southern Australia". In: *Atmospheric Environment* 43.19, pp. 3035–3043. ISSN: 13522310. DOI: [10.1016/j.atmosenv.2009.03.026](https://doi.org/10.1016/j.atmosenv.2009.03.026).
- Wild, Oliver and Michael J. Prather (2006). "Global tropospheric ozone modeling: Quantifying errors due to grid resolution". In: *Journal of Geophysical Research Atmospheres* 111.11, pp. 1–14. ISSN: 01480227. DOI: [10.1029/2005JD006605](https://doi.org/10.1029/2005JD006605).
- Christian, Kenneth E, William H Brune, and Jingqiu Mao (2017). "Global sensitivity analysis of the GEOS-Chem chemical transport model: ozone and hydrogen oxides

- during ARCTAS (2008)". In: *Atmos. Chem. Phys* 17, pp. 3769–3784. DOI: [10.5194/acp-17-3769-2017](https://doi.org/10.5194/acp-17-3769-2017). URL: www.atmos-chem-phys.net/17/3769/2017/.
- Travis, Katherine R et al. (2016). "Why do models overestimate surface ozone in the Southeast United States?" In: *Atmos. Chem. Phys* 16, pp. 13561–13577. DOI: [10.5194/acp-16-13561-2016](https://doi.org/10.5194/acp-16-13561-2016). URL: www.atmos-chem-phys.net/16/13561/2016/.
- Rowntree, P. R. and J. A. Bolton (1983). "Simulation of the atmospheric response to soil moisture anomalies over Europe". In: *Quarterly Journal of the Royal Meteorological Society* 109.461, pp. 501–526. ISSN: 00359009. DOI: [10.1002/qj.49710946105](https://doi.org/10.1002/qj.49710946105). URL: <http://doi.wiley.com/10.1002/qj.49710946105>.
- Chen, Fei and Jimy Dudhia (2001). "Coupling an Advanced Land Surface–Hydrology Model with the Penn State–NCAR MM5 Modeling System. Part I: Model Implementation and Sensitivity". In: *Monthly Weather Review* 129. URL: <https://journals.ametsoc.org/doi/pdf/10.1175/1520-0493%282001%29129%3C0569%3ACAALSH%3E2.0.CO%3B2>.
- Wang, Yuxuan et al. (2017). "Adverse effects of increasing drought on air quality via natural processes". In: *Atmos. Chem. Phys* 175194, pp. 12827–12843. DOI: [10.5194/acp-17-12827-2017](https://doi.org/10.5194/acp-17-12827-2017). URL: <https://www.atmos-chem-phys.net/17/12827/2017/acp-17-12827-2017.pdf>.
- SPEI Drought Index. URL: <http://spei.csic.es/home.html> (visited on 12/19/2017).
- VanDerA, R J et al. (2008). "Trends seasonal variability and dominant NO x source derived from a ten year record of NO 2 measured from space". In: *J. Geophys. Res.* 113.D4. DOI: [10.1029/2007jd009021](https://doi.org/10.1029/2007jd009021). URL: <http://dx.doi.org/10.1029/2007jd009021>.
- Oltmans, J et al. (2001). "Ozone in the Pacific tropical troposphere from ozonesonde observations". In: *Journal of Geophysical Research* 106.D23, pp. 32503–32525.
- Gloudemans, Annemieke et al. (2007). "Evidence for long-range transport of carbon monoxide in the Southern Hemisphere from SCIAMACHY observations". In: *European Space Agency, (Special Publication)* 33.SP-636, pp. 1–5. ISSN: 03796566. DOI: [10.1029/2006GL026804](https://doi.org/10.1029/2006GL026804).
- Edwards, D. P. et al. (2006). "Satellite-observed pollution from Southern Hemisphere biomass burning". In: *Journal of Geophysical Research* 111.14, pp. 1–17. ISSN: 01480227. DOI: [10.1029/2005JD006655](https://doi.org/10.1029/2005JD006655).
- Pak, B.C.a et al. (2003). "Measurements of biomass burning influences in the troposphere over southeast Australia during the SAFARI 2000 dry season campaign". In: *Journal of Geophysical Research* 108.13, pp. 1–10. ISSN: 0148-0227. DOI: [10.1029/2002JD002343](https://doi.org/10.1029/2002JD002343). URL: <http://www.scopus.com/inward/record.url?eid=2-s2.0-0742322536&partnerID=40&md5=cafaf3b948fb456696583ed3ab9a5>.
- Liu, Junhua et al. (2016a). "Causes of interannual variability of tropospheric ozone over the Southern Ocean". In: *Atmospheric Chemistry and Physics Discussions* October, pp. 1–46. ISSN: 1680-7316. DOI: [10.5194/ACP-2016-692](https://doi.org/10.5194/ACP-2016-692).
- Alexander, S. P. et al. (2013). "High resolution VHF radar measurements of tropopause structure and variability at Davis, Antarctica (69 S, 78 E)". In: *Atmospheric Chemistry and Physics* 13.6, pp. 3121–3132. ISSN: 16807324. DOI: [10.5194/acp-13-3121-2013](https://doi.org/10.5194/acp-13-3121-2013). URL: <http://www.atmos-chem-phys.net/13/3121/2013/>.
- Sindelarova, K. et al. (2014). "Global data set of biogenic VOC emissions calculated by the MEGAN model over the last 30 years". In: *Atmospheric Chemistry and Physics*

- 14.17, pp. 9317–9341. ISSN: 16807324. DOI: [10.5194/acp-14-9317-2014](https://doi.org/10.5194/acp-14-9317-2014). arXiv: [arXiv:1011.1669v3](https://arxiv.org/abs/1011.1669v3).
- Stavrakou, T et al. (2009). “Evaluating the performance of pyrogenic and biogenic emission inventories against one decade of space-based formaldehyde columns”. In: *Atmospheric Chemistry and Physics* 9.3, pp. 1037–1060. DOI: [10.5194/acp-9-1037-2009](https://doi.org/10.5194/acp-9-1037-2009). URL: <http://dx.doi.org/10.5194/acp-9-1037-2009>.
- Brinksma, E. J. et al. (2002). “Five years of observations of ozone profiles over Lauder, New Zealand”. In: *Journal of Geophysical Research* 107.D14, pp. 1–11. ISSN: 0148-0227. DOI: [10.1029/2001JD000737](https://doi.org/10.1029/2001JD000737). URL: <http://doi.wiley.com/10.1029/2001JD000737>.
- Baray, Jean-Luc et al. (2012). “One year ozonesonde measurements at Kerguelen Island (49.2S, 70.1E): Influence of stratosphere-to-troposphere exchange and long-range transport of biomass burning plumes”. In: *Journal of Geophysical Research* 117.D6. ISSN: 2156-2202. DOI: [10.1029/2011JD016717](https://doi.org/10.1029/2011JD016717). URL: <http://dx.doi.org/10.1029/2011JD016717>.
- Mintz, Y (1982). “The sensitivity of numerically simulated climates to land surface conditions”. In: *Land Surface Processes in Atmospheric General Circulation Models*, pp. 109–111.
- Chen, D. et al. (2009). “Regional CO pollution in China simulated by the high-resolution nested-grid GEOS-Chem model”. In: *Atmospheric Chemistry and Physics Discussions* 9.2, pp. 5853–5887. ISSN: 1680-7324. DOI: [10.5194/acpd-9-5853-2009](https://doi.org/10.5194/acpd-9-5853-2009). URL: <http://dx.doi.org/10.5194/acpd-9-3825-2009>.
- Giglio, Louis, James T. Randerson, and Guido R. Van Der Werf (2013). “Analysis of daily, monthly, and annual burned area using the fourth-generation global fire emissions database (GFED4)”. In: *Journal of Geophysical Research* 118.1, pp. 317–328. ISSN: 21698961. DOI: [10.1002/jgrg.20042](https://doi.org/10.1002/jgrg.20042).
- Horowitz, Larry W. et al. (1998). “Export of reactive nitrogen from North America during summertime: Sensitivity to hydrocarbon chemistry”. In: *Journal of Geophysical Research* 103.D11, pp. 13451–13476. ISSN: 0148-0227. DOI: [10.1029/97JD03142](https://doi.org/10.1029/97JD03142). URL: <http://doi.wiley.com/10.1029/97JD03142> <http://www.agu.org/pubs/crossref/1998/97JD03142.shtml>.
- Crounse, John D et al. (2011). “Peroxy radical isomerization in the oxidation of isoprene”. In: *Physical Chemistry Chemical Physics* 13.30, pp. 13607–13613. ISSN: 1463-9076. DOI: [doi:10.1039/c1cp21330j](https://doi.org/10.1039/c1cp21330j). URL: <http://dx.doi.org/10.1039/C1CP21330J>.
- Jozef, Peeters et al. (2014). “Hydroxyl Radical Recycling in Isoprene Oxidation Driven by Hydrogen Bonding and Hydrogen Tunneling: The Upgraded LIM1 Mechanism”. In: *Journal of Physical Chemistry*.
- Guenther, Alex (2016). MEGAN. URL: <http://lar.wsu.edu/megan/>.
- Pegoraro, E. et al. (2004). “Effect of drought on isoprene emission rates from leaves of *Quercus virginiana* Mill.” In: *Atmospheric Environment* 38.36, pp. 6149–6156. ISSN: 13522310. DOI: [10.1016/j.atmosenv.2004.07.028](https://doi.org/10.1016/j.atmosenv.2004.07.028). URL: <http://linkinghub.elsevier.com/retrieve/pii/S1352231004007198>.
- Dunne, Erin et al. (2017). “Comparison of VOC measurements made by PTR-MS, Adsorbent Tube/GC-FID-MS and DNPH-derivatization/HPLC during the Sydney Particle Study, 2012: a contribution to the assessment of uncertainty in current

- atmospheric VOC measurements". In: *Atmospheric Measurement Techniques Discussions*, pp. 1–24. ISSN: 1867-8610. DOI: [10.5194/amt-2016-349](https://doi.org/10.5194/amt-2016-349). URL: <https://www.atmos-meas-tech-discuss.net/amt-2016-349/>.
- Lee, Hanlim et al. (2015). "Investigations of the Diurnal Variation of Vertical HCHO Profiles Based on MAX-DOAS Measurements in Beijing: Comparisons with OMI Vertical Column Data". In: *Atmosphere*. URL: [10.3390/atmos6111816](https://doi.org/10.3390/atmos6111816).
- Schreier, Stefan F. et al. (2016). "Estimates of free-Tropospheric NO₂ and HCHO mixing ratios derived from high-Altitude mountain MAX-DOAS observations at mid-latitudes and in the tropics". In: *Atmospheric Chemistry and Physics* 16.5. ISSN: 16807324. DOI: [10.5194/acp-16-2803-2016](https://doi.org/10.5194/acp-16-2803-2016).
- Leue, C et al. (2001). "Quantitative analysis of NO x emissions from Global Ozone Monitoring Experiment satellite image sequences". In: *J. Geophys. Res.* 106.D6, p. 5493. DOI: [10.1029/2000jd900572](https://doi.org/10.1029/2000jd900572). URL: <http://dx.doi.org/10.1029/2000jd900572>.
- Stavrakou, T. et al. (2015). "How consistent are top-down hydrocarbon emissions based on formaldehyde observations from GOME-2 and OMI?" English. In: *Atmospheric Chemistry and Physics* 15.20, pp. 11861–11884. ISSN: 1680-7324. DOI: [10.5194/acp-15-11861-2015](https://doi.org/10.5194/acp-15-11861-2015). URL: <http://www.atmos-chem-phys.net/15/11861/2015/acp-15-11861-2015.html>.
- Schenkeveld, V. M. Erik et al. (2017). "In-flight performance of the Ozone Monitoring Instrument". In: *Atmospheric Measurement Techniques* 10.5, pp. 1957–1986. ISSN: 1867-8548. DOI: [10.5194/amt-10-1957-2017](https://doi.org/10.5194/amt-10-1957-2017). URL: <http://www.atmos-meas-tech-discuss.net/amt-2016-420/> <https://www.atmos-meas-tech.net/10/1957/2017/>.
- Palmer, Paul I et al. (2001). "Air mass factor formulation for spectroscopic measurements from satellites' Application to formaldehyde retrievals from the Global Ozone Monitoring Experiment". In: *Journal of Geophysical Research* 106.D13.
- Lorente, Alba et al. (2017). "Structural uncertainty in air mass factor calculation for NO₂ and HCHO satellite retrievals". In: *Atmospheric Measurement Techniques* 2, pp. 1–35. ISSN: 1867-8610. DOI: [10.5194/amt-10-759-2017](https://doi.org/10.5194/amt-10-759-2017). URL: <https://www.atmos-meas-tech.net/10/759/2017/amt-10-759-2017.html> <http://www.atmos-meas-tech-discuss.net/amt-2016-306/>.
- Eskes, H J and K F Boersma (2003). "Averaging kernels for DOAS total-column satellite retrievals". In: *Atmospheric Chemistry and Physics* 3.1, pp. 1285–1291. ISSN: 1680-7324. DOI: [10.5194/acpd-3-895-2003](https://doi.org/10.5194/acpd-3-895-2003). URL: <http://dx.doi.org/10.5194/acpd-3-895-2003>.
- Lamsal, L N et al. (2014). "Evaluation of OMI operational standard NO₂ column retrievals using in situ and surface-based NO₂ observations". In: *Atmos. Chem. Phys* 14, pp. 11587–11609. DOI: [10.5194/acp-14-11587-2014](https://doi.org/10.5194/acp-14-11587-2014). URL: www.atmos-chem-phys.net/14/11587/2014/.
- Vasilkov, A et al. (2017). "Accounting for the effects of surface BRDF on satellite cloud and trace-gas retrievals: a new approach based on geometry-dependent Lambertian equivalent reflectivity applied to OMI algorithms". In: *Atmospheric Measurement Techniques* 10.1, pp. 333–349. DOI: [10.5194/amt-10-333-2017](https://doi.org/10.5194/amt-10-333-2017). URL: <http://www.atmos-meas-tech.net/10/333/2017/>.
- Vigouroux, C. et al. (2009). "Ground-based FTIR and MAX-DOAS observations of formaldehyde at Réunion Island and comparisons with satellite and model data".

- In: *Atmospheric Chemistry and Physics Discussions* 9, pp. 15891–15957. ISSN: 1680-7316. DOI: [10.5194/acpd-9-15891-2009](https://doi.org/10.5194/acpd-9-15891-2009).
- Instrument, O M I (2002). "OMI Algorithm Theoretical Basis Document Volume I". In: I.August, pp. 1–50.
- Zhu, Lei et al. (2016). "Observing atmospheric formaldehyde (HCHO) from space: validation and intercomparison of six retrievals from four satellites (OMI, GOME2A, GOME2B, OMPS) with SEAC4RS aircraft observations over the Southeast US". In: *Atmospheric Chemistry and Physics* 0, pp. 1–24. ISSN: 1680-7375. DOI: [10.5194/acp-2016-162](https://doi.org/10.5194/acp-2016-162). URL: <http://www.atmos-chem-phys.net/16/13477/2016/acp-16-13477-2016.pdf>.
- De Smedt, I. et al. (2015). "Diurnal, seasonal and long-term variations of global formaldehyde columns inferred from combined OMI and GOME-2 observations". In: *Atmospheric Chemistry and Physics* 15.21, pp. 12519–12545. ISSN: 16807324. DOI: [10.5194/acp-15-12519-2015](https://doi.org/10.5194/acp-15-12519-2015). URL: <http://www.atmos-chem-phys-discuss.net/15/12241/2015/5Cnhttp://www.atmos-chem-phys-discuss.net/15/12241/2015/acpd-15-12241-2015.pdf>.
- Barkley, Michael P. et al. (2013). "Top-down isoprene emissions over tropical South America inferred from SCIAMACHY and OMI formaldehyde columns". In: *Journal of Geophysical Research Atmospheres* 118.12, pp. 6849–6868. ISSN: 21698996. DOI: [10.1002/jgrd.50552](https://doi.org/10.1002/jgrd.50552). URL: <http://dx.doi.org/10.1002/jgrd.50552>.
- Abad, Gonzalo González et al. (2016). "Smithsonian Astrophysical Observatory Ozone Mapping and Profiler Suite (SAO OMPS) formaldehyde retrieval". In: *Atmospheric Measurement Techniques* 9.7, pp. 2797–2812. ISSN: 18678548. DOI: [10.5194/amt-9-2797-2016](https://doi.org/10.5194/amt-9-2797-2016).
- De Smedt, I. et al. (2012). "Improved retrieval of global tropospheric formaldehyde columns from GOME-2/MetOp-A addressing noise reduction and instrumental degradation issues". In: *Atmospheric Measurement Techniques* 5.11, pp. 2933–2949. ISSN: 18671381. DOI: [10.5194/amt-5-2933-2012](https://doi.org/10.5194/amt-5-2933-2012).
- Chance, K. et al. (2000). "Satellite observations of formaldehyde over North America from GOME". In: *Geophysical Research Letters* 27.21, pp. 3461–3464. ISSN: 00948276. DOI: [10.1029/2000GL011857](https://doi.org/10.1029/2000GL011857). URL: <http://dx.doi.org/10.1029/2000gl011857>.
- Zhu, Lei et al. (2013). "Variability of HCHO over the Southeastern United States observed from space : Implications for VOC emissions". In: vol. 1.